

**PERFORMANCE OF ADMIXTURES INTENDED TO
RESIST CORROSION IN CONCRETE EXPOSED TO A
MARINE ENVIRONMENT**

Huiping Cheng

and

Ian N. Robertson



**UNIVERSITY OF HAWAII
COLLEGE OF ENGINEERING**

DEPARTMENT OF CIVIL AND ENVIRONMENTAL ENGINEERING

Research Report UHM/CEE/06-08

December 2006

**PERFORMANCE OF ADMIXTURES INTENDED TO RESIST
CORROSION IN CONCRETE EXPOSED TO A MARINE
ENVIRONMENT**

Huiping Cheng

Ian N. Robertson

Research Report UHM/CEE/06-08

December 2006

ACKNOWLEDGEMENTS

This report was prepared by Huiping Cheng under the direction of Dr. Ian Robertson in the Department of Civil and Environmental Engineering at the University of Hawaii at Manoa.

The authors are grateful to Drs. H.R. Riggs and Si-Hwan Park for reviewing this report and providing valuable suggestions. Special thanks are also extended to laboratory technicians Miles Wagner and Jeffrey Snyder for their technical assistance. Appreciation is also extended to Gaur Johnson, Justin Nishii, Williams Baega, Wa Lok Hoi and Derek Yoshimura for their help during testing in the Structures Laboratory.

The authors acknowledge the considerable contributions made by the State of Hawaii Department of Transportation (HDOT), Ameron Hawaii, and Hawaiian Cement during this project. Funding for this project was provided by the HDOT. Aggregates and other constituents for the concrete mixtures were donated by Ameron Hawaii and Hawaiian Cement. The findings and opinions in this report are those of the authors and do not necessarily reflect the opinions of the funding agency.

ABSTRACT

A study was conducted to evaluate the effects of water/cement ratios, Hawaiian aggregates and various admixtures, which are added to concrete to protect the embedded reinforcing steel from corrosion, on corrosion resistance for reinforced concrete exposed to marine environment. Concrete specimens were proportioned using corrosion-inhibiting admixtures intended to slow the corrosion process. Laboratory specimens were exposed to cyclic ponding to simulate marine conditions, while field panels were located at Pier 38 in Honolulu Harbor. The corrosion-inhibiting admixtures included in this project were categorized into two types. Type 1 intends to reduce the concrete permeability, including Xypex Admix C-2000, latex modifier, fly ash, silica fume and Kryton KIM. Type 2 admixtures intend to raise the threshold value for chloride concentration at which the reinforcement corrosion is initiated, including Darex Corrosion Inhibitor (DCI), Rheocrete CNI, Rheocrete 222+ and FerroGard 901. The focus of this study was on the performance of the field panels after about 3 years of exposure to a marine environment.

Relevant properties of the field panels are reported, including half-cell potential readings and chloride concentrations at various depths below the concrete surface. Based on chloride concentrations and half-cell measurements, it was concluded that the control panel with lower water cement ratio (0.35) performed significantly better than the panel with higher water cement ratio (0.40).

It was also concluded that concrete using Type 1 admixtures show lower chloride concentrations at various depths from the top of the panel compared with the corresponding control panels. Chloride migration rates were also lower for these panels.

Panels using Type 2 admixtures had chloride concentrations that were similar to the corresponding control specimens.

The control panel with 0.40 water cement ratio recorded half-cell readings that indicate a high probability of corrosion after 3.4 years field exposure. Panels with Type 1 admixtures recorded significantly lower half-cell potentials, with most in the less than 10% corrosion probability range. Panels with Type 2 admixtures showed varying degrees of corrosion probability.

TABLE OF CONTENTS

Abstract	iii
Table of Contents	v
List of Tables	vii
LIST OF FIGURES	viii
LIST OF FIGURES	viii
Chapter 1 introduction	1
1.1 Introduction.....	1
1.2 Objective.....	3
1.3 Scope.....	3
Chapter 2 background and literature review.....	5
2.1 Introduction.....	5
2.2 Background of the long-term project.....	5
2.3 Mechanisms of corrosion of steel in concrete	7
2.4 Initiation and propagation of corrosion	9
2.5 Corrosion-inhibiting admixtures.....	13
2.6 Testing	15
2.7 Summary	19
Chapter 3 EXPERIMENTAL PROCEDURES	21
3.1 Introduction.....	21
3.2 Laboratory test procedures (phase II)	21
3.3 Field test procedures (Phase III)	33
3.4 Summary	41
Chapter 4 Results fROm laboratory specimens	43
4.1 Introduction.....	43
4.2 Electrical tests	43
4.3 Chemical test (chloride concentrations)	50
Chapter 5 results from field panels	53
5.1 Introduction.....	53
5.2 Chloride concentration.....	54
5.3 Half-cell potential	89
Chapter 6 cONCLUSIONS.....	115

References.....	117
Appendix A.....	119
Appendix B.....	127

LIST OF TABLES

Table 2-1 Admixtures Used in The Project and Their Mechanics.....	14
Table 2-2 Corrosion Ranges for Half-cell Potential Test Results (CSE).....	17
Table 2-3 Maximum Chloride-ion Content for Corrosion Protection of Reinforcement .	18
Table 3-1 Admixtures used with each aggregate.....	23
Table 3-2 Mixture variables considered	24
Table 3-3 Main properties for each panel.....	33
Table 3-4. Distance from top of panel to MSL, MHHW, and MLLW.....	40
Table 4-1 Number of laboratory specimens for each mix design.....	43
Table 4-2 : Specimens removed from laboratory cycling prior to this study	44
Table 4-3 : Specimens removed from laboratory cycling during this study.....	45
Table 4-4 : Electrical and observational results.....	47
Table 4-5 Modified Electrical and observational results	49
Table 5-1 Locations of the holes drilled on each panel	53
Table 5-2 Change of Chloride Concentration for bottom hole at a depth of 1.0”	86
Table 5-3 Average Change of Chloride Concentration for bottom hole at a depth of 0.5”	87
Table 5-4 Average Change of Chloride Concentration for bottom hole at a depth of 1.0”	88
Table 5-5 Average Change of Chloride Concentration for bottom hole at a depth of 1.5”	88
Table 5-6 Corrosion ranges for half-cell potential test results (CSE).....	90

LIST OF FIGURES

Figure 1-1 Three Phases of the Long Term Project.....	2
Figure 2-1 Corrosion cell in reinforced concrete (Hime and Erlin 1987).....	7
Figure 2-2 Initiation and propagation periods for corrosion in a reinforced concrete structure (Tuutti's model)	10
Figure 3-1 Process of all tests	22
Figure 3-2 Picture and schematic of a typical laboratory specimen	25
Figure 3-3 An overview of all laboratory specimen placed in the structural lab at UH ...	26
Figure 3-4 Points where half-cell reading were taken (left), half-cell set up (right)	28
Figure 3-5 Test locations on top surface of laboratory specimen.....	29
Figure 3-6 Section A-A (Chloride sample method 1).....	30
Figure 3-7 Section B-B Chloride sample method 2 (Core driller).....	31
Figure 3-8 Slicing and Crushing of Concrete Samples.....	32
Figure 3-9 CL-2000 Chloride Concentration Testing Instrument	32
Figure 3-10: Location of Field Specimens at Pier 38 in Honolulu Harbor, Oahu.	34
Figure 3-11 Placement of the 25 panels at Pier 38	35
Figure 3-12 Previous Chloride Collection by Method 1 (Drilling bit).....	36
Figure 3-13 Core drilling using method 2.....	37
Figure 3-14 Current Chloride Collection by Method 2 (Core driller)	37
Figure 3-15 Half-cell Test Locations.....	39
Figure 3-16 Electrical connection to reinforcing bar	41
Figure 4-1 Acid-soluble chloride concentration vs. depth for Con3 mixture.....	51
Figure 5-1. Acid-soluble chloride concentration vs. depth for panel 1	56

Figure 5-2. Acid-soluble chloride concentration vs. depth for panel 7.	57
Figure 5-3. Acid-soluble chloride concentration vs. depth for panel 2.	58
Figure 5-4. Acid-soluble chloride concentration vs. depth for panel 3.	60
Figure 5-5. Acid-soluble chloride concentration vs. depth for panel 3A.....	60
Figure 5-6 Acid-soluble chloride concentration vs. depth for panel 4.	61
Figure 5-7 Acid-soluble chloride concentration vs. depth for panel 5	62
Figure 5-8 Acid-soluble chloride concentration vs. depth for panel 6	63
Figure 5-9. Acid-soluble chloride concentration vs. depth for panel 5A.....	64
Figure 5-10. Acid-soluble chloride concentration vs. depth for panel 15.	65
Figure 5-11. Acid-soluble chloride concentration vs. depth for panel 16.	66
Figure 5-12. Acid-soluble chloride concentration vs. depth for panel 17.	67
Figure 5-13. Acid-soluble chloride concentration vs. depth for panel 17A.....	68
Figure 5-14. Acid-soluble chloride concentration vs. depth for panel 20.	69
Figure 5-15. Acid-soluble chloride concentration vs. depth for panel 18.	70
Figure 5-16. Acid-soluble chloride concentration vs. depth for panel 19.	71
Figure 5-17. Acid-soluble chloride concentration vs. depth for panel 21.	72
Figure 5-18. Acid-soluble chloride concentration vs. depth for panel 14.	73
Figure 5-19. Acid-soluble chloride concentration vs. depth for panel 11.	74
Figure 5-20. Acid-soluble chloride concentration vs. depth for panel 12.	75
Figure 5-21. Acid-soluble chloride concentration vs. depth for panel 13.	76
Figure 5-22. Acid-soluble chloride concentration vs. depth for panel 8.	77
Figure 5-23. Acid-soluble chloride concentration vs. depth for panel 9.	78
Figure 5-24. Acid-soluble chloride concentration vs. depth for panel 10.	79

Figure 5-25. Acid-soluble chloride concentration vs. depth for panel 22	80
Figure 5-26 Chloride concentrations for bottom hole of all panels at depth of 0.5”	82
Figure 5-27 Chloride concentrations for bottom hole of all panels at depth of 1”	83
Figure 5-28 Chloride concentrations for bottom hole of all panels at depth of 1.5”	84
Figure 5-29 Comparison of resistance to chloride penetration for each admixture @ 0.5”	87
Figure 5-30 Comparison of resistance to chloride penetration for each admixture @1.0”	88
Figure 5-31 Comparison of resistance to chloride penetration for each admixture @1.5”	89
Figure 5-32 Schematic Drawing of the 18 Hall-cell testing locations on the top of each panel.....	91
Figure 5-33 3D Presentation for each half cell potential of Panel 1 at the age of 3.4 years	91
Figure 5-34 Comparison of the average half-cell at the different ages for Panel 1 (Con 1)	92
Figure 5-35 3D Presentation for each half cell potential of Panel 7 at the age of 3.4 years	93
Figure 5-36 Comparison of the average half-cell at the different ages for Panel 7 (Con 7)	93
Figure 5-37 3D Presentation for each half cell potential of Panel 2 at the age of 3.4 years	94

Figure 5-38 Comparison of the average half-cell at the different ages for Panel 2 (HCon 2)	95
Figure 5-39 Comparison of the average half-cell at the different ages for Panel 3 (DCI3)	96
Figure 5-40 Comparison of the average half-cell at the different ages for Panel 3A (DCI3A)	97
Figure 5-41 Comparison of the average half-cell at the different ages for Panel 4 (HDCI4)	98
Figure 5-42 Comparison of the average half-cell at the different ages for Panel 5 (CNI5)	99
Figure 5-43 Comparison of the average half-cell at the different ages for Panel 6 (CNI6)	100
Figure 5-44 Comparison of the average half-cell at the different ages for Panel 5A (CNI5A)	101
Figure 5-45 Comparison of the average half-cell at the different ages for Panel 15 (Rhe 15)	102
Figure 5-46 Comparison of the average half-cell at the different ages for Panel 16 (Rhe 16)	103
Figure 5-47 Comparison of the average half-cell at the different ages for Panel 17 (Rhe 17)	103
Figure 5-48 Comparison of the average half-cell at the different ages for Panel 17A (Rhe 17A)	104

Figure 5-49 Comparison of the average half-cell at the different ages for Panel 18 (Hfer 18).....	105
Figure 5-50 Comparison of the average half-cell at the different ages for Panel 19 (Hfer 19).....	105
Figure 5-51 Half-cell at 3.4 years for Panel 20 (Fer 20).....	106
Figure 5-52 Comparison of the average half-cell at the different ages for Panel 21 (Xyp 21).....	107
Figure 5-53 Comparison of the average half-cell at the different ages for Panel 14 (LA 14)	108
Figure 5-54 Comparison of the average half-cell at the different ages for Panel 11 (FA11)	109
Figure 5-55 Comparison of the average half-cell at the different ages for Panel 12 (HFA12).....	109
Figure 5-56 Comparison of the average half-cell at the different ages for Panel 13 (HFA 13).....	110
Figure 5-57 Comparison of the average half-cell at the different ages for Panel 8 (SF-Rh8)	111
Figure 5-58 Comparison of the average half-cell at the different ages for Panel 9 (SF-Rh9)	111
Figure 5-59 Comparison of the average half-cell at the different ages for Panel 10 (SF10)	112
Figure 5-60 Comparison of the average half-cell at the different ages for Panel 22 (Kry22)	113

CHAPTER 1 INTRODUCTION

1.1 Introduction

Reinforced concrete structures have been used for more than 150 years because of their strength, durability and low-cost in different applications. In most cases, these structures can perform well for decades with relatively little or no maintenance. However, when the structures are exposed to a marine environment, deterioration can occur much quicker than normal due to chloride attack.

Among the commonly used methods intended to prevent or decelerate the corrosion process, which include protective coatings, corrosion-resistant alloys, corrosion-inhibiting admixtures, engineering plastics and polymers, and cathodic and anodic protection, corrosion-inhibiting admixtures were one of the most user-friendly and cost-effective solutions. Corrosion inhibitors are chemical admixtures that are added to concrete to prevent or delay corrosion of the embedded steel bars.

Since 1999, an ongoing research project in the UH structural laboratory has been reviewing the performance of various corrosion-inhibiting admixtures in reinforced concrete made from the local aggregates available on the island of Oahu. This long-term project includes three phases, as shown below in Figure 1-1.

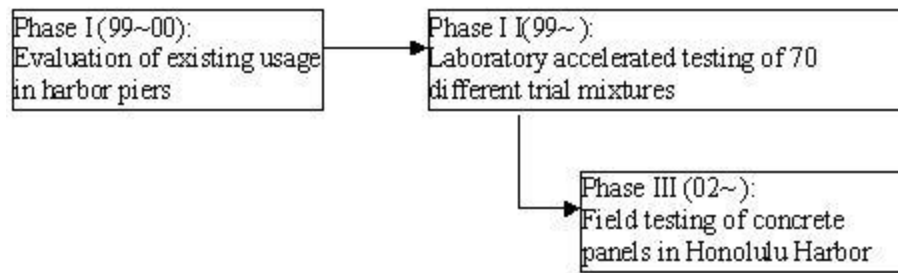


Figure 1-1 Three Phases of the Long Term Project

Phase I started in 1999 and evaluated the effectiveness of corrosion-inhibiting admixtures used in various piers at harbor facilities on the island of Oahu (Bola and Newton 2000). The admixtures chosen for the further laboratory research were determined from the Phase I results.

Phase II is an accelerated corrosion study, which involved cyclic testing of hundreds of specimens using 70 different concrete mixtures according to ASTM G 109 (Okunaga and Robertson 2005). It was to evaluate the effectiveness of proposed corrosion-inhibiting admixtures. Corrosion of more than 600 test specimens is accelerated by cyclic ponding of a 0.3% NaCl solution.

Phase III is a corrosion study in a marine environment, which involves the fabrication and deployment of twenty-five reinforced concrete field panels located at Pier 38 in Honolulu Harbor. Each field panel utilized one of the corrosion inhibiting admixtures evaluated in the Phase II study. Field tests on the panels included air permeability and half-cell potential. Laboratory tests on dust samples collected from each panel included chloride concentration and pH. The panels will be monitored

continuously for five years. Phase III was initiated 3 years after phase II, and continues in parallel with phase II at this time.

This report provides an update on the current status of Phase II and Phase III of this study.

1.2 Objective

The objective of this research was to investigate the effects of water/cement ratio, aggregates and admixtures on corrosion resistance for specimens/ panels exposed to marine conditions. The properties of the concrete that were investigated in this study include macro-cell current, half-cell potential and chloride concentration. The corrosion inhibiting admixtures used in this study were DAREX Corrosion Inhibitor (DCI), Rheocrete CNI, Rheocrete 222+, FerroGard 901, Xypex Admix C-2000, latex modifier, silica fume, fly ash, and Kryton KIM. Thirteen different mixture designs were selected for Phase III based on results of Phase II of the study (Pham and Newton 2001, Okunaga and Robertson (2005).

1.3 Scope

This report outlines the current status of Phases II and III of this study. Chapter 2 provides the background of the overall project, information on the mechanisms of chloride-induced corrosion, and a brief review of the concrete admixtures needed in the study and their methodologies for protecting the reinforcing steel from corrosion. Also described are all the tests performed in this study. Chapter 3 presents the experimental procedures of both laboratory specimens and field panels. Results from the tests

performed on the laboratory specimens and field panels are provided in Chapter 4 and Chapter 5, respectively. And finally, the preliminary conclusions drawn from the results are presented in Chapter 6.

CHAPTER 2 BACKGROUND AND LITERATURE REVIEW

2.1 Introduction

This chapter begins with a brief review of this on-going project and the results obtained thus far. Also described in this chapter are the principles and mechanisms of the chloride-induced corrosion process in reinforced concrete, and the corrosion-inhibiting admixtures used in this study and their effects on the properties of concrete. A brief synopsis of the various tests used to determine chloride concentration, pH, air permeability, and half-cell potential is presented.

2.2 Background of the long-term project

This project started in 1999 with the initiation of Phase I, a field investigation of concrete at existing piers and docks on Oahu. In 2000, Phase II was initiated in the structural laboratory at UH. Numerous concrete mixtures with various corrosion inhibiting admixtures were evaluated following the procedures of ASTM G109-92, accelerated test of corrosion in reinforced concrete. In 2002, Phase III started with the placement of 25 concrete panels in the field at Honolulu Harbor Pier 38. Currently Phase II and Phase III are on-going. The conclusions that have been drawn since 1999 are as follows.

Phase I (1999-2000):

Corrosion in reinforced concrete was identified at all piers investigated at Honolulu Harbor and Barbers Point. Based on this investigation, two conclusions were drawn regarding corrosion inhibiting measures employed at these piers. Increased DCI

dosage resulted in decreased corrosion activity, and epoxy coated reinforcing bars appeared to effectively combat corrosion. (Bola and Newton, 2000)

Phase II - Laboratory Testing (1999-present):

This laboratory testing is still on-going but interim conclusions have been reported.

According to Kakuda and Robertson (2005), most of the data that are collected so far didn't agree well with the expectations. The Chloride concentrations did not show a strong correlation with observed corrosion. PH levels did not show any correlation to the severity of corrosion while the air permeability for the majority of the specimens showed little or no correlation between the permeability and initiation of corrosion.

Phase III - Long-Term Field Monitoring (2002-present)

Some interim conclusions of this part were presented by Uno et al.. (2004).

The correlation between chloride concentration at 1.0 in. (25 mm) depth in the laboratory specimens and field panels for the control, DCI, FerroGard 901 and latex-modified mixtures, was an average of 1.2 cycles per year. This rate is also equal to 10.3 months of field exposure per laboratory ponding cycle.

The correlation between chloride concentration at 1.0 in. (25 mm) depth in the laboratory specimens and field panels for the silica fume panels was an average of 2.4 cycles per year. The rate is also equivalent to 5.1 months of field exposure per laboratory ponding cycle.

Based on the conclusions obtained from previous stages, the measurement, water/air permeability, is not used any more due to their inefficiency of predicting corrosion. The measurement of chloride concentrations is modified to improve accuracy.

2.3 Mechanisms of corrosion of steel in concrete

Corrosion is usually defined as the destruction of a metal by chemical or electrochemical reaction with its environment. The definition thus gives two types of corrosion: General corrosion (chemical) and localized (electrochemical). As for reinforced concrete, the alkaline nature of the concrete protects the steel from most chemical corrosive reactions by developing a passive protective layer on the surface of the steel. The corrosion of steel in concrete is therefore typically of the electrochemical type.

The electrochemical corrosion process creates an electrochemical corrosion cell similar to a battery. The components include an anode, a cathode, and an electrolyte, which can be seen in Figure 2-1.

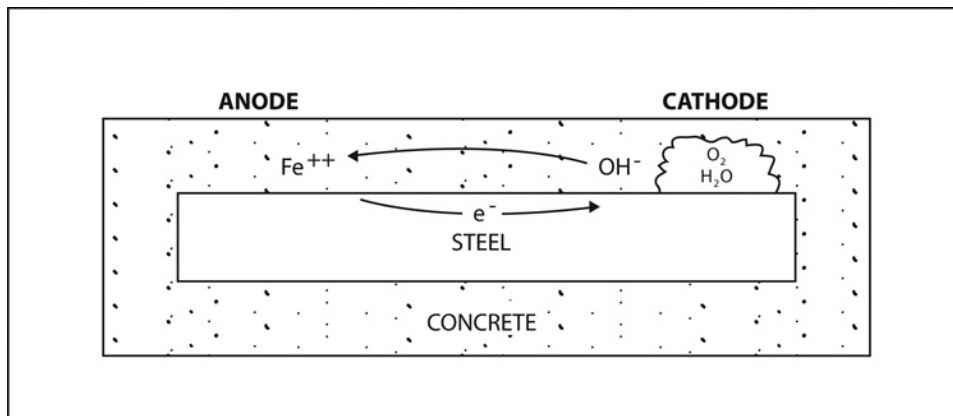


Figure 2-1 Corrosion cell in reinforced concrete (Hime and Erlin 1987)

In the case of corrosion of steel in concrete, the anode forms on an area of reinforcing steel where the passive protective layer is breached and oxidation begins to occur.



These free electrons travel along the reinforcing steel to a cathode located elsewhere on the steel. With a sufficient supply of oxygen provided by the highly alkaline concrete, the reduction occurs at the cathode as displayed in Equation 2.2.



Moisture surrounding the reinforcing steel provides a conducting environment allowing the hydroxyl ions to travel back to the anode site, where the hydroxyl ions $[(\text{OH})^-]$ combine with Fe^{2+} cations to form a fairly soluble ferrous hydroxide, $\text{Fe}(\text{OH})_2$, which is rust that possesses a whitish appearance. With sufficient oxygen, $\text{Fe}(\text{OH})_2$ is further oxidized to form $\text{Fe}(\text{OH})_3$, which is the more common form of rust that has a reddish brown appearance.

As the electrochemical process continues the corrosion products build up at the anode site. Since the corrosion products occupy more volume than the original reinforcing steel, the concrete begins to expand. The expansive stress in the reinforced concrete decreases the bond between the concrete and the steel weakening the structure, eventually cracking the concrete and causing spalling and delamination.

2.4 Initiation and propagation of corrosion

2.4.1 The natural protective layer of concrete

During hydration of cement a highly alkaline pore solution (pH between 12 and 14), principally of NaOH and KOH, develops. In this environment the thermodynamically stable compounds of iron are iron oxides and oxyhydroxides. Thus, when uncoated reinforcing steel is embedded in alkaline concrete, a thin protective oxide film, which is called the passive film, forms spontaneously on the surface of the steel. This passive film is only a few nanometers thick and is composed of more or less hydrated iron oxides with varying degree of Fe^{2+} and Fe^{3+} . This protective layer prevents the reinforcing steel from corroding. However, the thin layer can be destroyed by carbonation of concrete or by the presence of chloride ions. Once the passivating layer is compromised, the reinforcing steel is depassivated and is susceptible to corrosion.

2.4.2 Initiation of corrosion

The service life of reinforced concrete structures can be divided into two distinct phases as shown in Figure 2-2. The first phase is the initiation of corrosion, in which the reinforcement is passive but phenomena that can lead to loss of passivity, e.g. carbonation or chloride penetration in the concrete cover, take place. The second phase is propagation of corrosion that begins when the steel is depassivated and finishes when a limiting state is reached beyond which consequences of corrosion cannot be further tolerated.

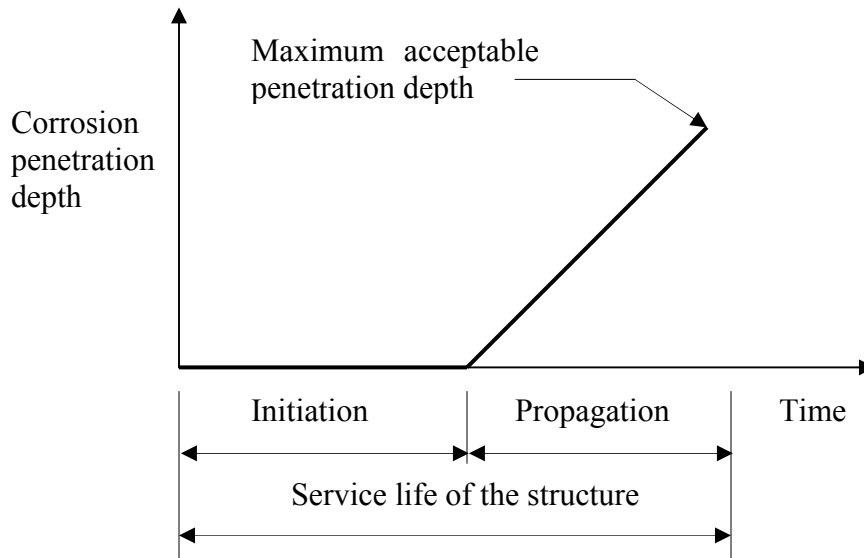


Figure 2-2 Initiation and propagation periods for corrosion in a reinforced concrete structure (Tuutti's model)

During the initiation phase two main kinds of aggressive substance, CO_2 and chlorides, can penetrate from the surface of concrete and depassivate the protective layer on the steel.

1) Carbonation:

In moist environments, carbon dioxide present in the air forms an acid aqueous solution that can penetrate through the concrete and react with the hydroxide ions in the concrete pore solution, thus neutralize the alkalinity of the concrete. As the PH drops, the natural passivation decreases and the unprotected steel begins to corrode.

Carbonation doesn't cause any damage to the concrete itself, indeed it may even lead to an increased concrete strength. But it has important effects on corrosion of the embedded steel. The first consequence is that the pH of the pore solution drops from a high alkalinity to approaching neutrality, in which the steel corrodes as if it were in

contact with water. A second consequence of carbonation is that chlorides initially bound in the form of calcium chloroaluminate hydrates may be liberated, making the pore solution even more aggressive.

2) Chloride-attack:

If an environment provides chloride ions, they can penetrate into concrete and reach the reinforcement. If the chloride concentration at the surface of the reinforcement reaches a critical level (threshold value), the protective layer may be locally destroyed.

The duration of the initiation depends on the cover depth and the penetration rate of the aggressive agents as well as on the concentration necessary to depassivate the steel. The influence of concrete cover is obvious and design codes define cover depths. The rate of ingress of the aggressive agents depends on the quality of the concrete such as porosity and permeability and on the microclimatic conditions (wetting, drying) at the concrete surface.

The corrosion of reinforced concrete in a marine environment is usually of the chloride-attack type. But the actual situation is much more complicated than in ideal theoretical analysis. What will happen to a particular metal in a particular environment cannot be completely predicted and must be learned by testing that particular metal under the particular conditions.

For the field panels in phase III of this project, some of them shown that the top to middle part, which is in the tidal zone, experienced more and quicker corrosion than the bottom part, which is fully submerged. While in the splash and tidal zones, concrete is wetted and then dried for some time. During the drying period, water that splashes

onto the concrete and the surrounding air may provide oxygen to initiate the carbonation corrosion. Thus the concrete may suffer a combination of carbonation and chloride attack, making the corrosion rate much higher than that is fully submerged.

2.4.3 Propagation of corrosion

The initiation of corrosion leads to the breakdown of the protective layer of the reinforcement but does not start the corrosion process. At the end of initiation phase when the protective layer is destroyed, corrosion will occur only if water and oxygen are present on the surface of the reinforcement. The corrosion rate determines the time it takes to reach the maximum acceptable penetration depth (the minimally acceptable state of the structure).

Carbonation of concrete leads to complete dissolution of the protective layer. Corrosion can take place on the whole surface of steel in contact with carbonated concrete.

Chloride attack leads to localized breakdown of the protective layer, unless chlorides are present in very large amounts. The corrosion is thus localized (pitting corrosion), with penetrating attacks of limited areas (pits) surrounded by non-corroded areas. Only when very high levels of chlorides are present (or the pH decreases) may the passive film be destroyed over wide areas of the reinforcement and the corrosion will be of a general nature.

2.5 Corrosion-inhibiting admixtures

Among all methods to delay corrosion, adding admixtures to the concrete is among the least expensive with good effectiveness.

There are two issues concerned to initiate the corrosion:

1) Chloride ions pass through the concrete cover and reach the surface of the embedded reinforcing steel

2) When the chloride concentration at the surface of the steel reaches a threshold value at which the natural passive layer is broke down, the steel may begin to corrode.

The threshold value depends on several parameters; however, the electrochemical potential of the reinforcement, which is related to the amount of oxygen that can reach the surface of the steel has a major influence. Relatively low levels of chlorides are sufficient to initiate corrosion in structures exposed to the atmosphere, where oxygen can easily reach the reinforcement. Much higher levels of chlorides are necessary in structures immersed in seawater or in zones where the concrete is water saturated, so that oxygen supply is hindered and thus the potential for corrosion of the reinforcement is rather low.

In order to improve the ability of reinforced concrete to resist chloride-induced corrosion, corrosion inhibiting admixtures added to the concrete mixture are designed to affect either or both of the following:

1) to reduce the concrete permeability, thus reducing the speed of chloride ingress

2) to raise the threshold value for chloride concentration at which the corrosion is initiated, thus increasing the difficulty of initiation of corrosion.

For simplicity, the admixtures will be referred to here as Type 1 or Type 2 based on their approach to reducing corrosion.

The admixtures DAREX Corrosion Inhibitor (DCI), Rheocrete CNI, Rheocrete 222+, FerroGard 901, Xypex Admix C-2000, latex, fly ash, silica fume, and Kryton KIM were added to the concrete mixtures for this study. Their functions are described in Table 2-1.

Table 2-1 Admixtures Used in The Project and Their Mechanics

	Admixture	Report abbreviation	Function
1	DAREX Corrosion Inhibitor	DCI	Forming a protective layer (Fe_2O_3) on the anode steel (Type 2)
2	Rheocrete CNI	CNI	
3	Rheocrete 222+	Rhe	Forming a protective physical layer on both anode and cathode (Type 2) and lining the pores with chemical compounds that impart hydrophobic properties to the concrete (Type 1)
4	Ferrogard 901	Fer	Forming a physical layer on both anode and cathode (Type 2)
5	Xypex Admix C-2000	Xyp	Forming a crystalline formation throughout the pores and capillary tracts of the concrete (Type 1)
6	Fly Ash	FA	Filling voids in concrete (Type 1)
7	Silica Fume (from Master Builders)		
8	Silica Fume (from W.R. Grace)	SF	Filling voids in concrete (Type 1)
9	Pro-Crylic latex modifier	LA	Type 1
10	Kryton KIM	Kry	Type 1

More detailed information about all admixtures used in this report are provided by Uno and Robertson (2004).

From the table, Type 1 admixture includes Xypex, fly ash, silica fume, latex modifier and kryton. Type 2 admixture include CNI, DCI, FerroGard. Rheocrete 222+ has both functions and is categorized into Type 2.

Concretes using type 1 admixtures are expected to have reduced air permeability. Concretes using Type 2 admixtures are expected to have a higher chloride concentration threshold value.

2.6 Testing

Various tests were performed during the Phase II and Phase III of this project to determine the mechanical, chemical, and electrical properties of hardened concrete and the reinforcing steel. The mechanical tests performed in the study were used to evaluate the properties of concrete including compressive strength, elastic modulus, and Poisson's ratio (Pham and Newtonson 2000). The chemical tests were used to assess the corrosion-resistance properties of the concrete which include chloride concentration and pH values. Electrical tests include macro-cell and half-cell potential to evaluate the inhibiting properties of the various admixtures. Only those related to this report are described here.

2.6.1 Electrical tests

The electrical tests used in this study include macrocell current and half-cell potential. These tests are described briefly below.

2.6.1.1 Macrocell Current

Macrocell corrosion current is created between two layers of reinforcing steel. It was used as the primary measurement for the laboratory specimens in Phase II.

The current measurement provides an indication of the amount of reinforcing steel that is consumed by the corrosion process. The test measures the coupled current formed by the top layer of steel being exposed to a chloride rich environment, while the bottom reinforcement is exposed to a low chloride environment. The top steel acts as the anode, and the bottom steel is the cathode. A resistor connects the top and bottom layers of steel, and voltage is measured across the resistor (ASTM G 109-92; Civjan et al., 2003). According to ASTM 109-92 guidelines, when the macrocell current reaches 1 μA , corrosion is initiated.

The macrocell current method is a low-cost, simple, and reliable test method. Studies have found a good correlation between macrocell corrosion measured in a slab and the corresponding corrosion found on the anodic reinforcing steel after removal (Civjan et al., 2004). Other studies have noticed that the macrocell technique appears to underestimate the corrosion rate, at times by an order of magnitude (Berke et al., 1990).

2.6.1.2 Half-Cell Potential

In this technique, the corrosion potential of the reinforcing steel is measured with respect to a standard reference electrode such as a saturated calomel electrode, copper/copper-sulfate electrode, silver-silver chloride electrode etc. (Srinivasan et al., 1994). The half-cell test was used for both laboratory specimens and field panels during phases II and III.

This test is described in ASTM C876, “Standard Test Method for Half-Cell Potential of Reinforcing Steel in Concrete.” Test results indicate the likelihood of corrosion on the reinforcing steel within the concrete. One drawback of the half cell

potential test is the need to access the reinforcing steel. Once the potential measurements using a copper sulfate electrode (CSE) are obtained, they can be interpreted using Table 2-2.

Table 2-2 Corrosion Ranges for Half-cell Potential Test Results (CSE)

Measured Potential (mV)	Statistical risk of corrosion occurring
< -350	90%
Between -350 and -200	50%
> -200	10%

SCE (Saturated Calomel Electrode) was used in this study and therefore all the original readings have to be converted to results using a copper sulfate electrode (CSE) by adding 77 mV.

The half-cell potential test has many advantages. It is inexpensive due to the simple equipment used, large structures can be easily and quickly surveyed, and data obtained from the test are straight forward and simple to interpret. According to some studies of corrosion in marine areas, there are some disadvantages as well. Potential measurement alone cannot give an absolute indication of the condition of reinforcing embedded in concrete (Srinivasan et al.. 1994). In a study of corrosion in marine areas, Sharp et al.. (1988) used both electropotential and resistivity measurements. The measurements were confirmed by physical examination of the embedded steel. The study concluded that the correlation between test results and actual corrosion was moderate, suggesting that more investigation into the accuracy of these test methods is required (Sharp et al.. 1988).

2.6.2 Chemical Test – Chloride Concentration Test

The chemical test performed on the concrete specimens during this report is chloride concentration test.

Among the two methods available to measure chloride concentrations, the total-chloride (acid-soluble) concentration method is used in this project because of its ease of use. Concrete powder is mixed into an extraction liquid such as nitric acid, and a testing meter is placed in the solution to determine the level of acid-soluble chloride concentration. Results are then compared to recommended safe limits of chloride content from ACI 318. These limits are presented in Table 2-3.

Table 2-3 Maximum Chloride-ion Content for Corrosion Protection of Reinforcement

Type of member	Maximum water-soluble chloride ion content, percent by mass of cement
Prestressed concrete	0.06
Reinforced concrete exposed to chloride	0.25
Reinforced concrete that will be dry or protected from moisture in service	1.00
Other reinforced concrete construction	0.30

(Taken from Table 4.4.1 in ACI 318)

It is important to notice that the table specifies a maximum water-soluble chloride ion content instead of the total (acid-soluble) chloride ion content which is the measure used in this study. So it is necessary to convert the threshold value of water-soluble to acid-soluble.

Only the water-soluble chloride ions are available to participate in the corrosion of embedded steel. Studies have shown that up to about 50% of the total chloride ions in concrete can be “tied up” by the cement matrix, which is not water-soluble (Technical

Bulletin TB-0105, W.R. Grace & Co.-Com). Therefore, it is safe to use an acid-soluble threshold value two times as the water-soluble value shown in the ACI table. For the concrete exposed to marine environment, the water-soluble chloride concentration limit is 0.25 percent by weight of cement, and thus yields the total (acid-soluble) value of 0.50 percent by weight of cement.

All the chloride concentrations used after in this report are meant the acid-soluble chloride concentration.

2.7 Summary

This chapter presented a literature review of the principles and mechanisms of corrosion, the different admixtures that were added to concrete in this study to protect the reinforcing steel from corrosion and the principles of the macro-cell potential, half-cell potential and chloride concentration tests.

CHAPTER 3 EXPERIMENTAL PROCEDURES

3.1 Introduction

This chapter presents the test procedures that are used during this study.

During Phase I, half-cell potential and resistivity tests were performed on cone at the Harbor piers. Results of these tests are reported by Bola and Newton (2000).

Physical and mechanical tests that represent the properties of the concrete mixtures with different admixtures and materials were performed. They include slump test, air content test, compressive strength test, elastic modulus and Poisson's ratio tests. These test procedures and the results are presented by Pham and Newton (2000) and are not repeated in this report.

During Phase II, chemical and electrical tests plus the air permeability test were used to monitor the corrosion specimens. They include the macrocell current test, half-cell test, chloride concentration test, pH test and air permeability test. (Kakuda et al., 2005; Okunaga et al., 2005). During Phase III, half-cell potential, pH, chloride concentration and air permeability tests were performed (Uno et al., 2004).

3.2 Laboratory test procedures (phase II)

After cast and cured, the specimens are put under ponding cycles while the macrocell current are taken until the value reaches the critical point such that corrosion is thought initiated. Then the specimens are removed from cycling. Half-cell current, chloride concentration and air permeability measurements are taken. Thereafter the specimens are broken up and the pH testing samples are taken underneath the top layer rebar. The whole procedure is represented below in Figure 3-1.

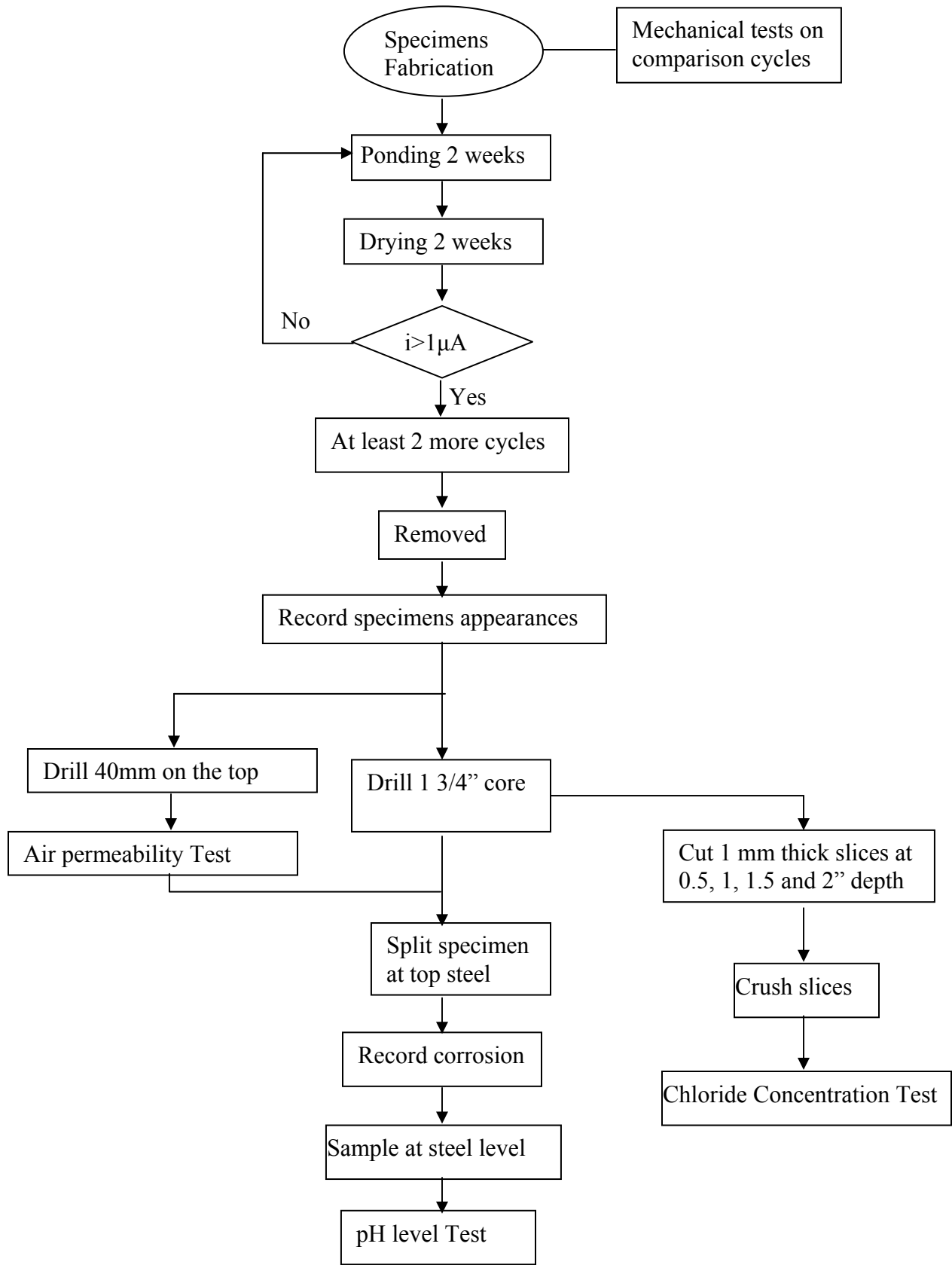


Figure 3-1 Process of all tests

3.2.1 Specimen preparation

All of the specimens were made at the UH structures laboratory in 1999 and 2000.

Aggregates from two main quarries on the island of Oahu were used in the concrete mixtures, namely Kapaa quarry and Halawa quarry. Eight types of corrosion inhibiting admixtures were used namely DCI, CNI, Rheocrete 222+, FerroGard 901, Xypex, Latex, Fly Ash, Silica Fume from Master Builder Inc. and W.R. Grace Inc. Table 3-1 lists the various admixtures used with each of the aggregate source.

Table 3-1 Admixtures used with each aggregate

Admixture	Aggregate Source	
	Kapaa	Halawa
None (Control)	x	x
DCI	x	
CNI	x	x
Rheocrete	x	x
FerrGuard	x	
Xypex	x	
Latex	x	
SF (W.R. Grace)	x	x
SF-Rh (Master Builder)		x
Fly Ash	x	x

In addition to the corrosion inhibiting admixtures, other basic properties of concrete mixture are also varied in the laboratory specimens as shown in Table 3-2.

Table 3-2 Mixture variables considered

Aggregate	Admixture	w/c	Paste content	Pozzolan content	Admixture Dosage	Latex Content
Kapaa	None(control)	3 levels	2 levels	--		--
	DCI	2 levels	2 levels	--	3 levels	--
	CNI	2 levels	2 levels	--	3 levels	--
	Rheocrete	3 levels	2 levels	--	1 level	--
	Xypex	3 levels	2 levels	--	1 level	--
	Latex	2 levels	--	--	--	3 levels
	FA	2 levels	2 levels	3 levels	--	--
	SF (W.R.)	2 levels	2 levels	3 levels	--	--
Halawa	None(control)	3 levels	2 levels	--	--	--
	CNI	2 levels	2 levels	--	3 levels	--
	Rheocrete	3 levels	2 levels	--	--	--
	FA	2 levels	2 levels	3 levels	--	--
	SF(W.R.)	2 levels	2 levels	3 levels	--	--
	SF(M.B.)	2 levels	2 levels	3 levels	--	--

The particular properties of all the specimens were presented by Okunaga and Robertson (2005).

The laboratory specimens were prepared according to ASTM G 109-92 but modified slightly by installing an additional top reinforcing bar. Each specimen is 11×6×4.5 inches as shown in Figure 3-2 and Figure 3-3.

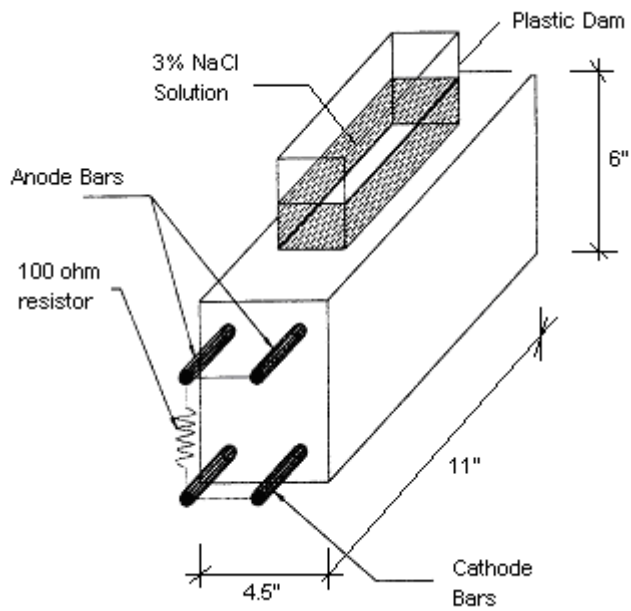


Figure 3-2 Picture and schematic of a typical laboratory specimen



Figure 3-3 An overview of all laboratory specimen placed in the structural lab at UH

All the specimens were stored in the basement of the structures laboratory in Holmes Hall at UH, which provides a laboratory environment with a relatively constant temperature of 73°F (27.8°C) and humidity of around 54%. The specimens were subjected to an accelerated ponding cycle using a 3% NaCl solution. Each cycle is 4 weeks long. A 400mL volume of the NaCl solution is added to the plastic dam on the top of the specimen. Two weeks later the solution is removed and then the specimen is allowed to dry for two weeks, which completes one cycle. The voltage potential is monitored in the middle of wetting, i.e. one week after the NaCl solution is added. The macrocell current can be calculated from the voltage potential. The cycle is repeated until the macrocell current is equal to or greater than 10 μA , at which point corrosion is presumed to have initiated according to ASTM109. The specimen is subjected to at least two more ponding cycles to ensure that the macrocell reading remains above 10 μA . It is then removed from cycling.

3.2.2 Macrocell Current Test

The macrocell current is calculated based on the voltage potential measured during each ponding cycle. In the accelerated corrosion process, the top layer of reinforcing steel is exposed to a chloride rich environment, while the bottom steel is exposed to a low chloride environment. A current is formed between the top bar, which acts as anode, and the bottom bar as cathode, through the connecting 100 ohm resistor. A Fluke 45 Dual Display Multimeter is used to measure the voltage across the resistor. The current is then determined from:

$$\text{Current} = \text{Potential} / \text{Resistance.}$$

The macrocell readings presented in this report are only those of specimens that have exceeded the 10 μA current. The full readings are kept as a record for further use.

3.2.3 Half-cell Current Test

The half-cell current tests in this report were only performed after the specimens reach failure and were removed from cycling. A calomel reference electrode was used to take the half-cell measurements. Three readings were taken over each of the top reinforcing bars at approximately 3 in., 5.5in., and 8 in. from the end of the specimen.

See Figure 3-4.

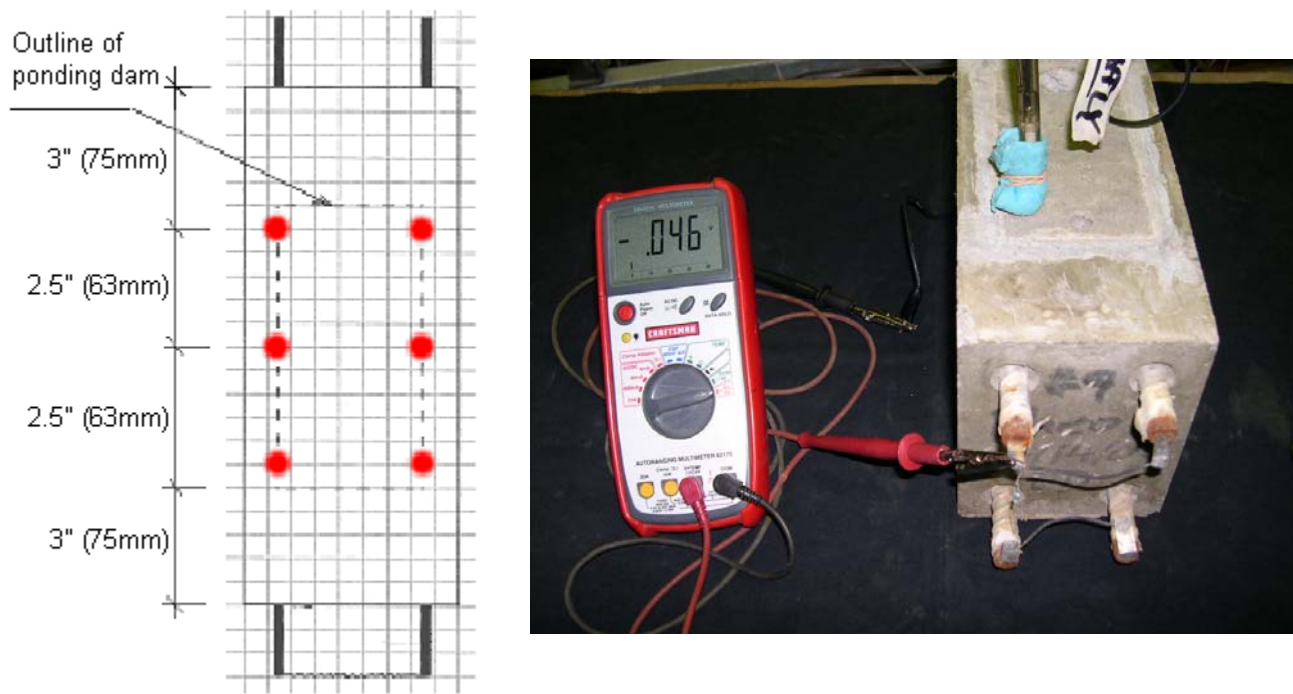


Figure 3-4 Points where half-cell reading were taken (left), half-cell set up (right)

3.2.4 Chloride Concentration Test

A Chloride Test System, CL-2000 (James Instruments, Inc.), was used for the chloride concentration test. A 3 gram (0.106 oz.) crushed concrete sample is dissolved in 20ml (0.676 fl.oz.) of extraction liquid. The CL-2000 instrument can then measure the chloride concentration as a percentage of the concrete. Based on the content of the particular mixture, the chloride concentration is converted to a percentage by weight of cement. To collect the samples, two methods are used for the specimens involved in this report. In both methods, crushed concrete samples were recovered from depths of 0.5", 1.0" and 1.5" below the top surface. In the second method, a sample was also collected at a depth of 2". The first method was used for specimens that were removed from ponding before

June, 2005. To get at least 3 grams (0.106 oz.) sample of concrete powder at the depth of 1" from the top surface of the specimen, for example, a 0.75 in. (19mm) diameter hole was drilled between the top two reinforcing bars to a depth of 0.75" and then the dust was blown out. Then the powder between 0.75 in. and 1.25 in. depth was collected as the sample. Since the collected powder covers a range of 0.25 in. above and below the depth desired, this method provides an approximate result. In addition, the small drill bit size (0.75" diameter) increases the likelihood of a sample with predominantly aggregate or paste. This method is shown as below in Figure 3-5 and Figure 3-6. Figure 3-5 shows the top surface of a typical specimen.

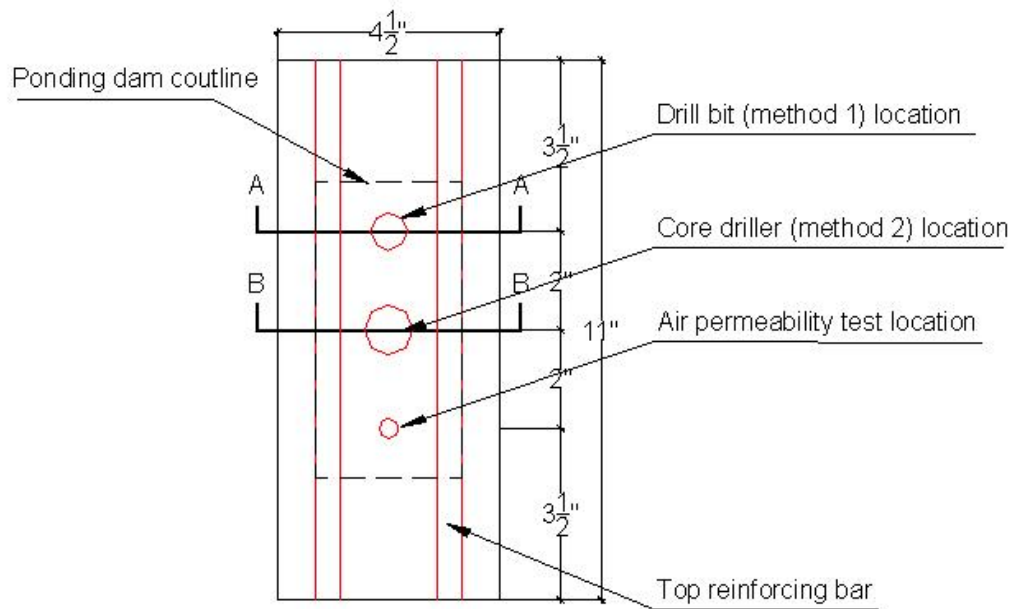


Figure 3-5 Test locations on top surface of laboratory specimen

Figure 3-6 shows how the concrete samples were obtained using method 1.

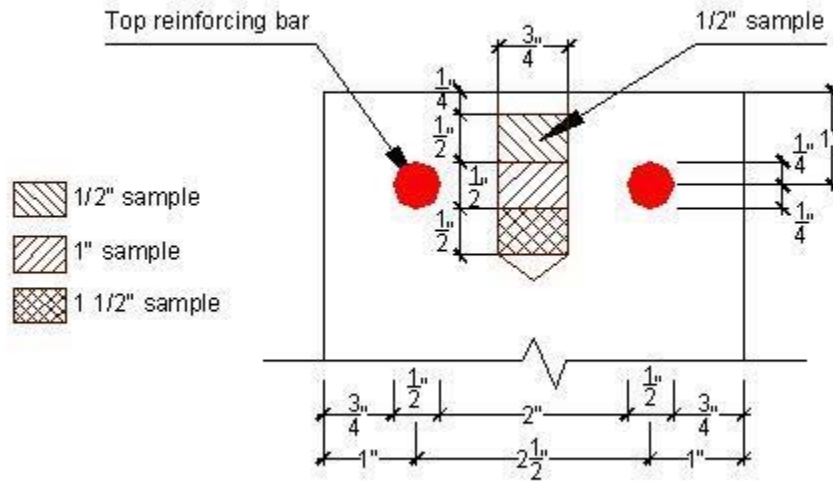


Figure 3-6 Section A-A (Chloride sample method 1)

For tests performed after June 2005, a core driller was used to extract a core sample of 1.5" diameter and 3" length. Four slices of concrete were cut at depths of 0.5", 1.0", 1.5", and 2.0" respectively using a concrete saw. Each slice was approximately 1 mm thick and 1.5" diameter, thus providing a more representative concrete sample at the exact depth desired. This method is shown below in Figure 3-7.

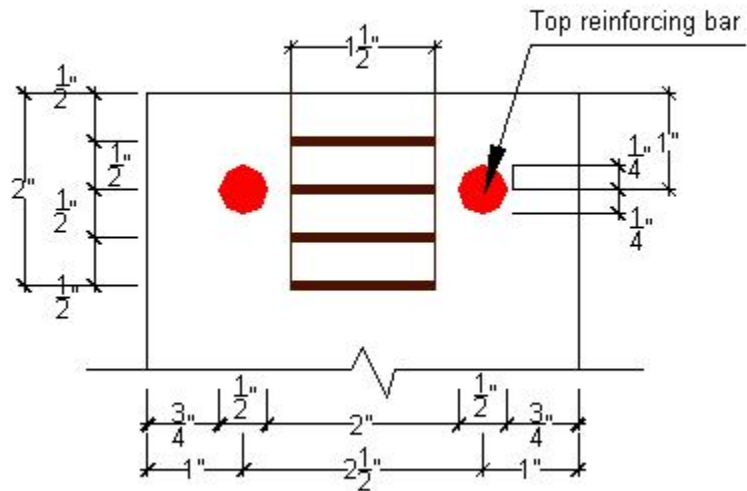


Figure 3-7 Section B-B Chloride sample method 2 (Core driller)

Each concrete slice was then crushed into a coarse powder using a hammer. To get the fine powder required for the chemical test, a steel rolling pin was used to crush the coarse powder into fine powder. Then the chemical test was performed to obtain the chloride concentration in percentage of weight of concrete. The slices and the coarse and fine powder samples are shown in Figure 3-8.

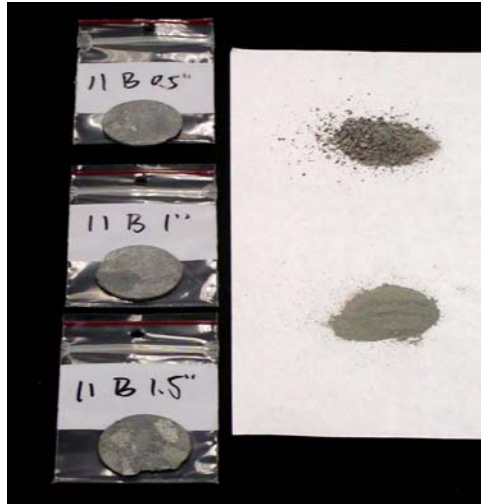


Figure 3-8 Slicing and Crushing of Concrete Samples

The dust samples were dissolved in a 20 ml (0.67 fl. Oz.) of extraction liquid provided by James Instruments Inc, as shown in Figure 3-9. The concrete dust and liquid were shaken for one minute to allow reaction time before taking the measurement. Chloride concentrations were measured in percentage by weight of concrete and converted to percentage by weight of cement using the cement content from the mixture proportions.



Figure 3-9 CL-2000 Chloride Concentration Testing Instrument

3.3 Field test procedures (Phase III)

The twenty-five field panels were fabricated in 2002 and placed at Pier 38 in Honolulu harbor seven days after casting. The panels are located such that the bottom of each panel is always below sea level, and the top of each panel is always above sea level. The middle of the panels is therefore in the tidal/wave zone.

Table 3-3 Main properties for each panel

Panel			w/c	Dosage of admixture	
Aggregate	No.	Admixture			
Kapaa	1	Control	0.40	-	
	7	Control	0.35	-	
	3	DCI	0.40	2 gal/cu. yd.	
	3A	DCI	0.40	4 gal/cu. yd.	
	5	CNI	0.40	2 gal/cu. yd.	
	6	CNI	0.40	2 gal/cu. yd.	
	5A	CNI	0.40	4 gal/cu. yd.	
	15	Rhe	0.40	1 gal/cu. yd.	
	16	Rhe	0.40	1 gal/cu. yd.	
	20	Ferr	0.40	3 gal/cu. yd.	
	21	Xyp	0.40	2% cement replacement	
	14	LA	0.40	5% cement replacement	
	11	FA	0.36(w/c+p)	15% cement replacement	
	8	SF-Rh	0.40	5% cement replacement	
	9	SF-Rh	0.40	5% cement replacement	
	10	SF	0.40	5% cement replacement	
	22	Kry	0.40	13.5 lb/cu. yd.	
	Halawa	2	HControl	0.40	-
		4	HDCI	0.40	2 gal/cu. yd.
		17	HRhe	0.40	1 gal/cu. yd.
		17A	HRhe	0.40	1 gal/cu. yd.
		18	HFerr	0.40	3 gal/cu. yd.
19		HFerr	0.40	3 gal/cu. yd.	
12		HFA	0.36(w/c+p)	15% cement replacement	
13		HFA	0.36(w/c+p)	15% cement replacement	

The 25 panels were placed at Pier 38. Figure 3-10 shows the panel locations at Pier 38.



Figure 3-10: Location of Field Specimens at Pier 38 in Honolulu Harbor, Oahu.

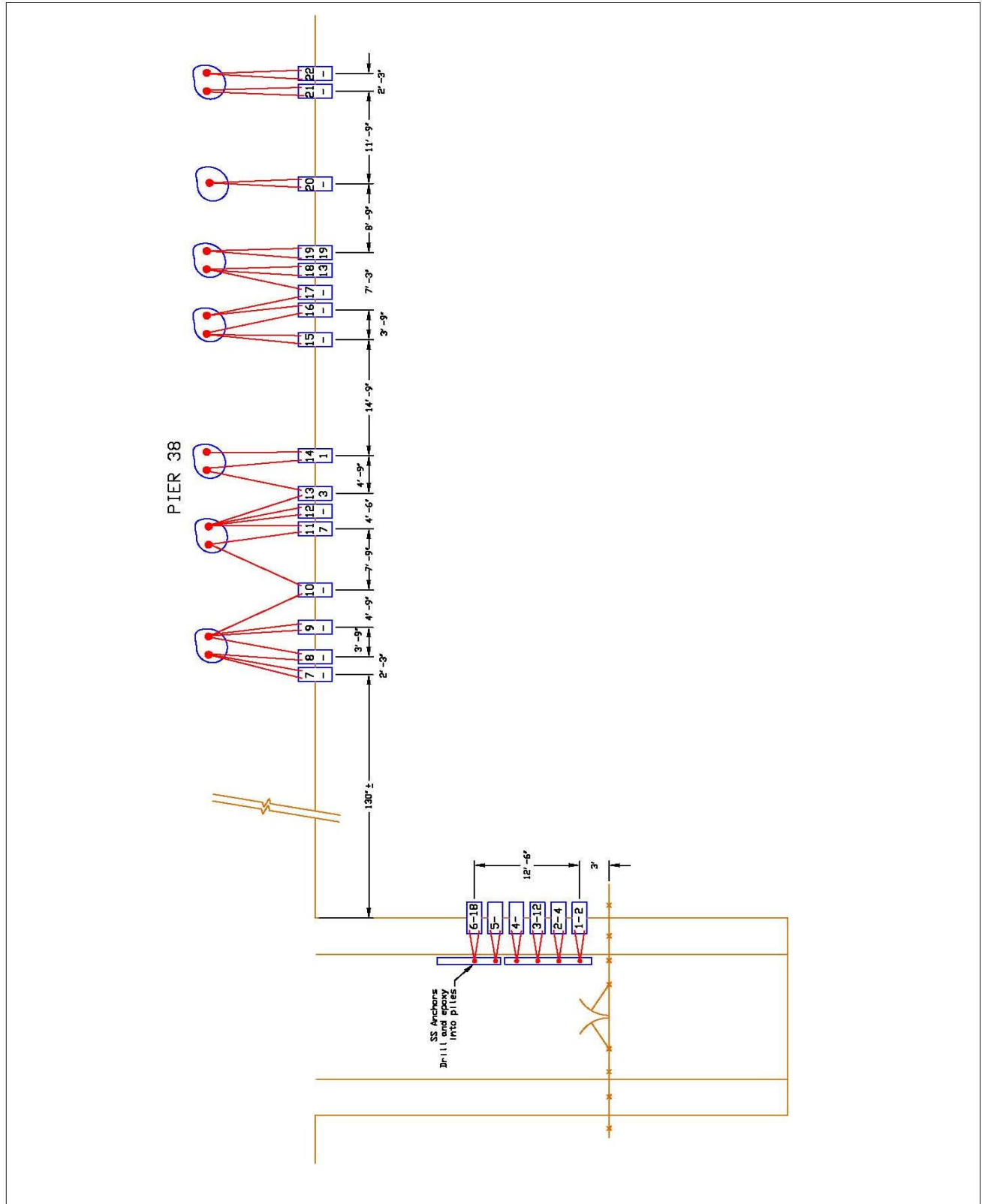


Figure 3-11 Placement of the 25 panels at Pier 38

3.3.1 Chloride concentration

Chloride concentrations were determined using the CL-2000 Chloride Field Test System by James Instruments, Inc.

To collect the concrete dust samples, method 1 (drilling bit) was used by John Uno without removing panels from the seawater, as shown in Figure 3-12

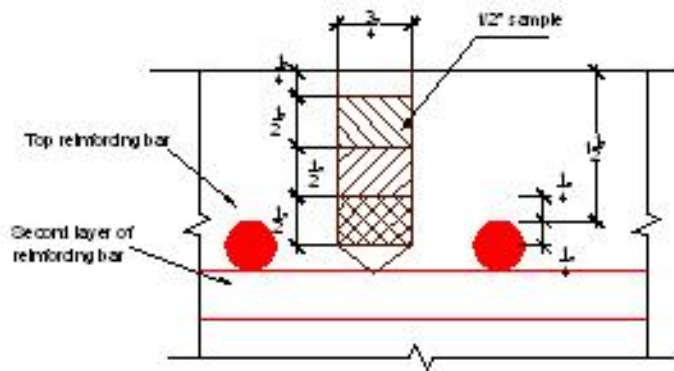


Figure 3-12 Previous Chloride Collection by Method 1 (Drilling bit)

Method 2 (core driller, shown in Figure 3-13 and Figure 3-14) was used in this report. The panels were firstly removed from the seawater. Then three cores were drilled at three different locations on each panel, i.e., top, middle and bottom using a core driller.



Figure 3-13 Core drilling using method 2

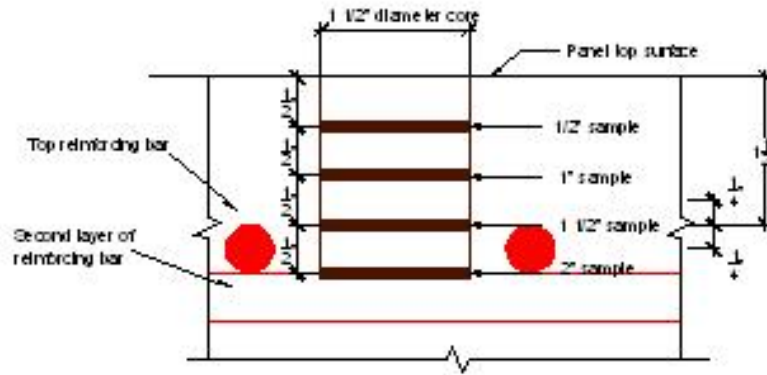


Figure 3-14 Current Chloride Collection by Method 2 (Core driller)

The top samples are always above the tide thus dry. The middle samples were from the tidal zone while the bottom samples are always wet. The actual locations of the drilled and cored holes are shown in the Chapter 5 afterwards.

Each core was cut into four slices at depths of 1/2", 1", 1 1/2" and 2" from the top surface of the panel as shown in Figure 3-14. The first test hole is located in an area in

the upper half of the tidal zone. The second is in an area that is in the tidal zone. And the third test hole is located in the lower half of the tidal zone.

The core slices were crushed and tested following the same procedure as described previously for the laboratory specimens samples.

The first set of measurements of chloride concentration was taken in 2003, at the approximate age of 1 to 1.5 years after placement of the panels. The second set of data was taken in December 2005.

3.3.2 Half-cell potential test

The calomel reference electrode used for the laboratory specimens was also used to take half-cell measurements on the top surface of the field panels. To establish the electrical connection between the reference electrode and the reinforcing bars embedded in the panel, an access hole located at the top end of each concrete panel was formed during panel fabrication. A steel screw with attached electrical wire was then drilled into the end of the exposed steel bar to establish an electrical connection. After measurement, the hole was covered with plexiglass epoxied to the concrete to prevent exposed bar and screw from corroding.

The first set of measurements of half-cell potential was taken in 2003. The half-cell potential tests were conducted at ten locations on the front face of each panel, labeled 1 to 10 in Figure 3-15. When the second set of measurements was performed in December 2005, eight more locations, labeled as 3a, 4a, 7a, 8a, 11 and 12, were adopted in order to get a more accurate average as shown in Figure 3-15 too.

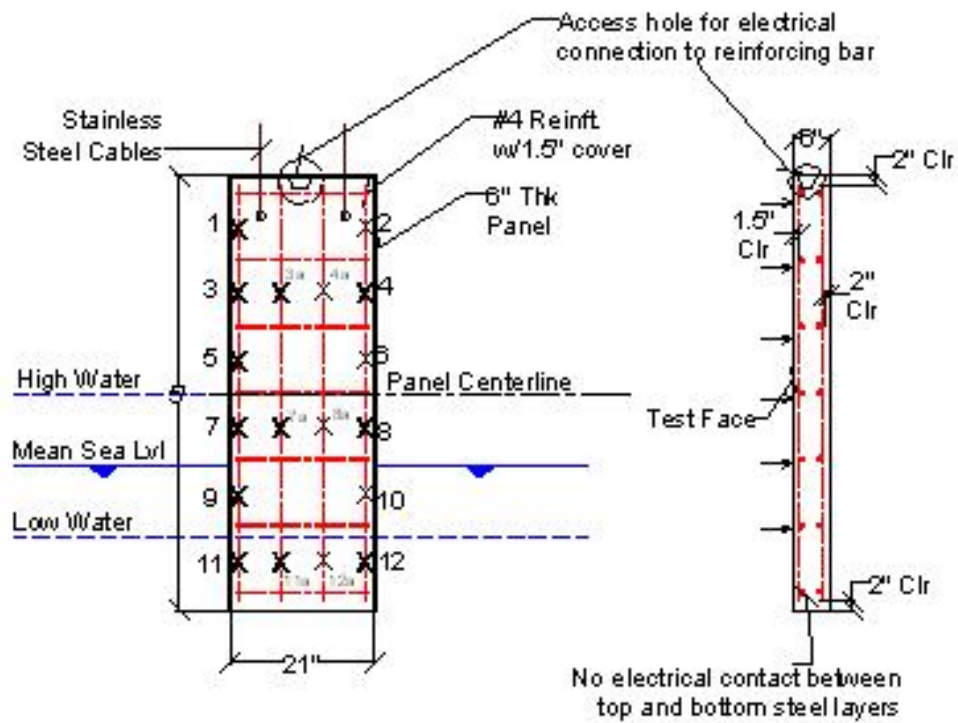


Figure 3-15 Half-cell Test Locations

The tide levels shown in this figure are approximate tidal range. It varies for each specimen. The distances from the top of each panel to mean sea level (MSL), mean higher high water (MHHW), and mean lower low water (MLLW) are presented in Table 3-4.

Table 3-4. Distance from top of panel to MSL, MHHW, and MLLW.

Specimen	MSL		MHHW		MLLW	
	in.	(mm)	in.	(mm)	in.	(mm)
Control panel 1	42.1	(1069)	29.1	(740)	52.0	(1320)
Control panel 2	40.7	(1035)	27.8	(706)	50.6	(1286)
Control panel 7	42.1	(1069)	29.1	(740)	52.0	(1320)
DCI panel 3	46.7	(1186)	33.7	(857)	56.6	(1437)
DCI panel 3A	40.0	(1015)	27.0	(686)	49.8	(1266)
DCI panel 4	32.5	(825)	19.5	(496)	42.4	(1076)
Rheocrete CNI panel 5	47.2	(1199)	34.3	(870)	57.1	(1450)
Rheocrete CNI panel 5A	46.6	(1183)	33.6	(854)	56.4	(1434)
Rheocrete CNI panel 6	39.9	(1013)	26.9	(684)	49.8	(1264)
Rheocrete 222+ panel 15	43.3	(1099)	30.3	(770)	53.1	(1350)
Rheocrete 222+ panel 16	42.4	(1078)	29.5	(749)	52.3	(1329)
Rheocrete 222+ panel 17	56.6	(1438)	43.7	(1109)	66.5	(1689)
Rheocrete 222+ panel 17A	37.9	(964)	25.0	(635)	47.8	(1215)
FerroGard 901 panel 18	39.8	(1010)	26.8	(681)	49.6	(1261)
FerroGard 901 panel 19	41.4	(1053)	28.5	(724)	51.3	(1304)
FerroGard 901 panel 20	39.3	(998)	26.3	(669)	49.2	(1249)
Xypex Admix C-2000 panel 21	42.2	(1072)	29.3	(743)	52.1	(1323)
Latex panel 14	33.9	(862)	21.0	(533)	43.8	(1113)
Fly ash panel 11	42.4	(1076)	29.4	(747)	52.2	(1327)
Fly ash panel 12	47.4	(1205)	34.5	(876)	57.3	(1456)
Fly ash panel 13	42.3	(1073)	29.3	(744)	52.1	(1324)
M.B. Silica fume panel 8	44.8	(1138)	31.9	(809)	54.7	(1389)
M.B. Silica fume panel 9	43.7	(1110)	30.8	(781)	53.6	(1361)
Grace Silica fume panel 10	37.4	(951)	24.5	(622)	47.3	(1202)
Kryton KIM panel 22	47.5	(1206)	34.5	(877)	57.4	(1457)

The electrical connection for the half-cell test was obtained by drilling a hole at the top end of the panel as shown in Figure 3-16. After the readings were taken, the hole was covered by a piece of plastic and sealed by epoxy firmly.

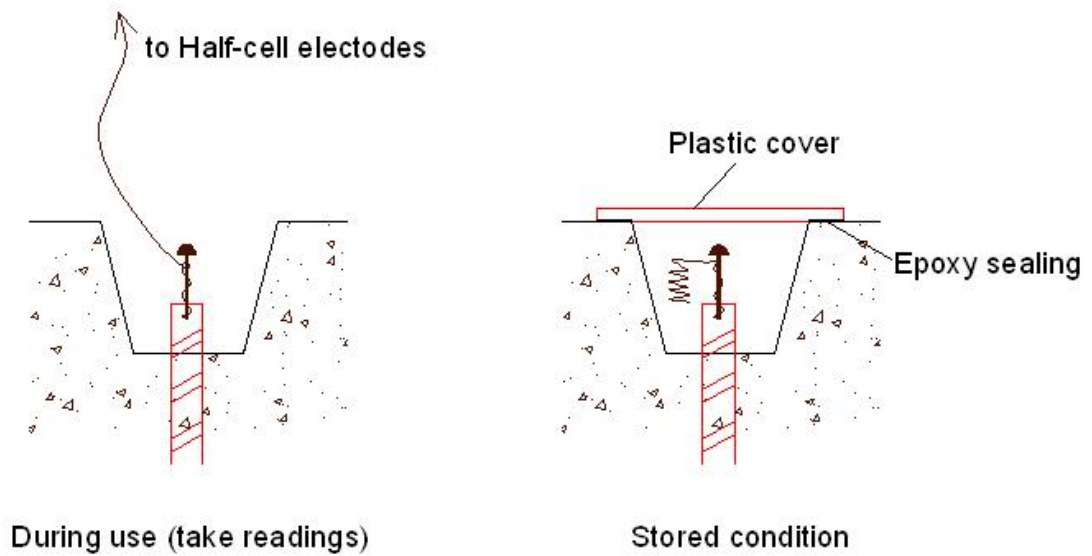


Figure 3-16 Electrical connection to reinforcing bar

3.4 Summary

This chapter presents the experimental procedures for all the tests performed in this study. The tests include macro-cell potential, half-cell potential and chloride concentration tests.

CHAPTER 4 RESULTS FROM LABORATORY SPECIMENS

4.1 Introduction

This chapter presents a discussion of the results from electrical and chemical tests performed on the laboratory specimens. Results from each of the electrical tests were evaluated to determine whether or not corrosion would be expected in the specimen. These results were then compared with the visual inspections to assess the validity of the test method. The chloride concentration test results were also compared to the visual inspections to identify any trends or threshold values.

4.2 Electrical tests

As previously presented, all the laboratory specimens were made from two types of aggregates and eight types of corrosion inhibiting admixtures. Eight specimens were made for every mix design, as shown in Table 4-1.

Table 4-1 Number of laboratory specimens for each mix design

Agg.	Mix No.	1	2	3	4	5	6	7	8	9	10	11	Total
Kapaa	Control	8	8	8	8	8	8						48
	DCI	8	8	8	8	8	8						48
	CNI	8	8	8	8	8	8						48
	Rheocrete	8	8	8	8	8	8						48
	FerroGard	8	8	8	8	8	8						48
	Xypex	8	8	8	8	8	8						48
	Latex	8	8	8	8	8	8						48
	Fly Ash	8	8	8	8	8	8	8	8	8	8	8	8
Silica Fume	8	8	8	8	8	8	8	8	8	8	8	8	88
Halawa	Hcontrol	4	4	4	4	4	4						24
	HCNI	4	4	4	4	4	4						24
	HRheo	4	4	4	4	4	4						24
	HFA		4	4	4	4	4	4	4				28
	HSF	4	4	4	4	4	4						24
	HSF-MB		4	4		4	4	4					20
													656

Some specimens were removed from laboratory cycling prior to this study and used for the previous stage of research. These removed specimens are shown in Table 4-2.

Table 4-2 : Specimens removed from laboratory cycling prior to this study

Uno and Robertson (2004)

Agg.	Mix No.	1	2	3	4	5	6	7	8	9	10	11	Total
Kapaa	Control	5	5	2	6								18
	DCI	3	2	1	1	1	1						9
	CNI												
	Rheocrete	1	1	1	1	1	1						6
	FerroGard	1	2	1	1	5	1						11
	Xypex	4	4		4	4							16
	Latex	7	1	2		1	1						12
	Fly Ash					4	1			1	1		7
	Silica Fume	1	2	1	1	3	2	2					12
Halawa	Hcontrol	4	4		1	4							13
	HCNI												0
	HRheo				4	4							8
	HFA					4							4
	HSF												
	HSF-Rh												
												116	

The specimens removed from laboratory cycling during this study are shown in Table 4-3, which are totally 41 specimens.

Table 4-3 : Specimens removed from laboratory cycling during this study

Agg.	Mix No.	1	2	3	4	5	6	7	8	9	10	11	Total
Kapaa	Control			2									2
	DCI	5			1								6
	CNI												0
	Rheocrete				1								1
	FerroGard		1		5								6
	Xypex						4						4
	Latex			2									2
	Fly Ash						3				10* 3		6
Silica Fume	2				5		2					9	
Halawa	Hcontrol				3								3
	HCNI	1			1								2
	HRheo												0
	HFA												0
	HSF												0
	HSF-Rh												0
													41

Two electrical tests were performed on each specimen listed in Table 4-3. The macrocell current between the top and bottom reinforcing bars was measured according to the ASTM standard G 109-92. If this current exceeds $10 \mu A$, it is anticipated that corrosion has been initiated at the top bars. The second measurement was the half cell potential on the specimen's top surface, using a calomel reference electrode. The potential was measured at six locations on each specimen; three measurements over each top reinforcement bar. The measured negative value with the largest magnitude was the value used in the evaluation of each specimen.

Table 4-4 presents the electrical results along with the results of visual inspection of the concrete specimen and top steel reinforcing bars. The table lists the specimens, the number of cycles until when the specimen was removed from cycling, final macrocell current readings, half cell potential result, and observations of the top reinforcing bars

and outside of the specimen. The macrocell current measurements were separated into categories: values above $10 \mu A$, values between $2 \mu A$ and $10 \mu A$, and values below $2 \mu A$.

For half cell readings, any value that was below -350 mV indicates a 90% probability of corrosion; any value that fell between -350 mV and -200 mV was considered uncertain for corrosion; if the value was greater than -200 mV then there was less than 10% probability of corrosion.

The observations of the inside of the specimens were identified with a similar color coding. If the reinforcing bars exhibit substantial overall corrosion or major pitting corrosion, the bars were considered moderately to substantially corroded. If small areas of corrosion or less severe pitting were observed, the specimen was categorized as “minor” corrosion. If the bars were completely clear of corrosion or had negligible corrosion, they were designated as uncorroded.

Table 4-4 : Electrical and observational results

Specimen	Cycles	Macro Cell	Half Cell	Reinforcement Corrosion	Visual Inspection
Con3 #2	53	$i > 10 \mu a$	10%	mod to substantial	Outside in good condition
Con3 #7	53	$i > 10 \mu a$	10%	mod to substantial	Some discoloration
DCI1 #1	55	$2 < i < 10 \mu a$	10%	minor	Outside in good condition
DCI1 #3	55	$i < 2 \mu a$	10%	minor	Outside in good condition
DCI1 #4	55	$i > 10 \mu a$	10%	mod to substantial	Outside in good condition
DCI1 #5	55	$i > 10 \mu a$	10%	mod to substantial	Outside in good condition
DCI1 #7	55	$i > 10 \mu a$	10%	minor	Outside in good condition
DCI4 #4	53	$i > 10 \mu a$	10%	mod to substantial	Outside in good condition
Rheo4 #7	42	$i > 10 \mu a$	10%	mod to substantial	Some voids
Ferr2 #1	42	$i > 10 \mu a$	10%	mod to substantial	Outside in good condition
Ferr4 #3	38	$i > 10 \mu a$	UN	mod to substantial	A void on top
Ferr4 #4	38	$i > 10 \mu a$	90%	mod to substantial	Cracks and voids on top
Ferr4 #5	38	$i < 2 \mu a$	10%	uncorroded	Outside in good condition
Ferr4 #6	38	$i < 2 \mu a$	10%	minor	A void on top
Ferr4 #7	38	$i > 10 \mu a$	90%	mod to substantial	A void on top
Xyp6 #1	37	$2 < i < 10 \mu a$	10%	minor	Outside in good condition
Xyp6 #2	37	$i > 10 \mu a$	10%	mod to substantial	Outside in good condition
Xyp6 #3	37	$i > 10 \mu a$	10%	mod to substantial	A tiny crack on top
Xyp6 #4	37	$i > 10 \mu a$	10%	minor	Some voids and discoloration on top
LA3 #1	45	$i > 10 \mu a$	UN	mod to substantial	Outside in good condition
LA3 #6	45	$i > 10 \mu a$	UN	mod to substantial	Lots of small holes on top
FA6 #1	50	$2 < i < 10 \mu a$	10%	minor	Outside in good condition
FA6 #2	50	$i > 10 \mu a$	90%	mod to substantial	A small crack on top
FA6 #4	50	$i < 2 \mu a$	10%	minor	Outside in good condition
FA10* #1	43	$i > 10 \mu a$	90%	mod to substantial	A void and brown spots
FA10* #3	43	$2 < i < 10 \mu a$	UN	mod to substantial	A tiny crack on the top
FA10* #4	43	$i < 2 \mu a$	10%	minor	Some discoloration
SF1 #1	52	$i > 10 \mu a$	10%	minor	Outside in good condition
SF1 #6	52	$i > 10 \mu a$	UN	mod to substantial	A tiny void
SF5 #1	52	$2 < i < 10 \mu a$	10%	uncorroded	Outside in good condition
SF5 #2	52	$i > 10 \mu a$	10%	mod to substantial	Some discoloration

SF5 #3	52	2 < i < 10 μ a	UN	minor	Outside in good condition
SF5 #4	52	2 < i < 10 μ a	10%	mod to substantial	A void and discoloration
SF5 #6	52	2 < i < 10 μ a	10%	minor	Outside in good condition
SF7 #1	52	i > 10 μ a	90%	mod to substantial	Some discoloration
SF7 #2	52	i > 10 μ a	10%	mod to substantial	Outside in good condition
Hcon4 #2	35	i > 10 μ a	90%	mod to substantial	Outside in good condition
Hcon4 #3	35	i > 10 μ a	UN	mod to substantial	A void on top
Hcon4 #4	35	2 < i < 10 μ a	10%	minor	Some cracks and voids on top
HCN12 #4	48	i > 10 μ a	10%	mod to substantial	Lots brow spots on top
HCN14 #1	27	i > 10 μ a	90%	mod to substantial	Cracks on top & right side

It can be seen from Table 4-4 that the macro-cell results have more accurate anticipation than half-cell results. This agrees with the conclusion drawn by Kakuda and Robertson (2005), which says the macrocell measurements predict well while the halfcell measurements underestimate the amount of corrosion.

Kakuda and Robertson concluded that the half-cell readings should be shifted for concretes using Hawaiian aggregates, i.e. the limits of -200mv and -350 mv are shifted to -100mv and -200mv respectively, than the table will look like the following Table 4-5.

Table 4-5 Modified Electrical and observational results

Specimen	Cycles	Macro-cell	Half Cell	Reinforcement Corrosion	Visual Inspection
Con3 #2	53	$i > 10 \mu a$	10%	mod to substantial	Outside in good condition
Con3 #7	53	$i > 10 \mu a$	10%	mod to substantial	Some discoloration
DCI1 #1	55	$2 < i < 10 \mu a$	UN	minor	Outside in good condition
DCI1 #3	55	$i < 2 \mu a$	UN	minor	Outside in good condition
DCI1 #4	55	$i > 10 \mu a$	10%	mod to substantial	Outside in good condition
DCI1 #5	55	$i > 10 \mu a$	10%	mod to substantial	Outside in good condition
DCI1 #7	55	$i > 10 \mu a$	10%	minor	Outside in good condition
DCI4 #4	53	$i > 10 \mu a$	10%	mod to substantial	Outside in good condition
Rheo4 #7	42	$i > 10 \mu a$	UN	mod to substantial	Some voids
Ferr2 #1	42	$i > 10 \mu a$	UN	mod to substantial	Outside in good condition
Ferr4 #3	38	$i > 10 \mu a$	90%	mod to substantial	A void on top
Ferr4 #4	38	$i > 10 \mu a$	90%	mod to substantial	Cracks and voids on top
Ferr4 #5	38	$i < 2 \mu a$	10%	uncorroded	Outside in good condition
Ferr4 #6	38	$i < 2 \mu a$	10%	minor	A void on top
Ferr4 #7	38	$i > 10 \mu a$	90%	mod to substantial	A void on top
Xyp6 #1	37	$2 < i < 10 \mu a$	10%	minor	Outside in good condition
Xyp6 #2	37	$i > 10 \mu a$	10%	mod to substantial	Outside in good condition
Xyp6 #3	37	$i > 10 \mu a$	10%	mod to substantial	A tiny crack on top
Xyp6 #4	37	$i > 10 \mu a$	10%	minor	Some voids and discoloration on top
LA3 #1	45	$i > 10 \mu a$	90%	mod to substantial	Outside in good condition
LA3 #6	45	$i > 10 \mu a$	90%	mod to substantial	Lots of small holes on top
FA6 #1	50	$2 < i < 10 \mu a$	UN	minor	Outside in good condition
FA6 #2	50	$i > 10 \mu a$	90%	mod to substantial d	A small crack on top
FA6 #4	50	$i < 2 \mu a$	10%	minor	Outside in good condition
FA10* #1	43	$i > 10 \mu a$	90%	mod to substantial	A void and brown spots
FA10* #3	43	$2 < i < 10 \mu a$	90%	mod to substantial	A tiny crack on the top
FA10* #4	43	$i < 2 \mu a$	10%	minor	Some discoloration
SF1 #1	52	$i > 10 \mu a$	UN	minor	Outside in good condition
SF1 #6	52	$i > 10 \mu a$	90%	mod to substantial	A tiny void
SF5 #1	52	$2 < i < 10 \mu a$	UN	uncorroded	Outside in good condition
SF5 #2	52	$i > 10 \mu a$	UN	mod to substantial	Some discoloration

SF5 #3	52	$2 < i < 10 \mu a$	90%	minor	Outside in good condition
SF5 #4	52	$2 < i < 10 \mu a$	10%	mod to substantial	A void and discoloration
SF5 #6	52	$2 < i < 10 \mu a$	UN	minor	Outside in good condition
SF7 #1	52	$i > 10 \mu a$	90%	mod to substantial	Some discoloration
SF7 #2	52	$i > 10 \mu a$	10%	mod to substantial	Outside in good condition
Hcon4 #2	35	$i > 10 \mu a$	90%	mod to substantial	Outside in good condition
Hcon4 #3	35	$i > 10 \mu a$	90%	mod to substantial	A void on top
Hcon4 #4	35	$2 < i < 10 \mu a$	UN	minor	Some cracks and voids on top
HCON2 #4	48	$i > 10 \mu a$	10%	mod to substantial	Lots brow spots on top
HCON4 #1	27	$i > 10 \mu a$	90%	mod to substantial	Cracks on top & right side

Now the prediction of macrocell and half-cell are more closely in agreement.

Among the 27 specimens which macro-cell current exceed $10 \mu a$, 24 were moderate to substantially corroded, which gives a 89% accuracy. The modified half-cell limits indicate that 12 specimens were moderate to substantially corroded among the 14 with the half-cell readings indicating 90% probability of corrosion, which gives a 86% accuracy. When the modified half-cell indicated less than 10% probability of corrosion, 9 of 16 specimens (56%) had signs of mod-substantial corrosion.

4.3 Chemical test (chloride concentrations)

4.3.1 Control mixtures

The chloride concentration data presented in this report are only of those removed from the ponding cycling. Figure 4-1 and Figure 4-2 present Control 3 and HCon4, respectively. The chloride concentrations decrease at increasing depths for Con3. This is

typical for all specimens because the chloride ions from the outside environment have to migrate from the surface of the concrete. The chloride concentrations of both Con # 3 and Con #7 specimens at a depth of 1.0” were between 1.5-2.5%, which are above the 0.50% modified threshold. It indicates the corrosion may occur at the steel level. The observations of the interior steel bars were also shown in the figure. The steel bars of both Con#3 and 7 were moderate to substantially corroded.

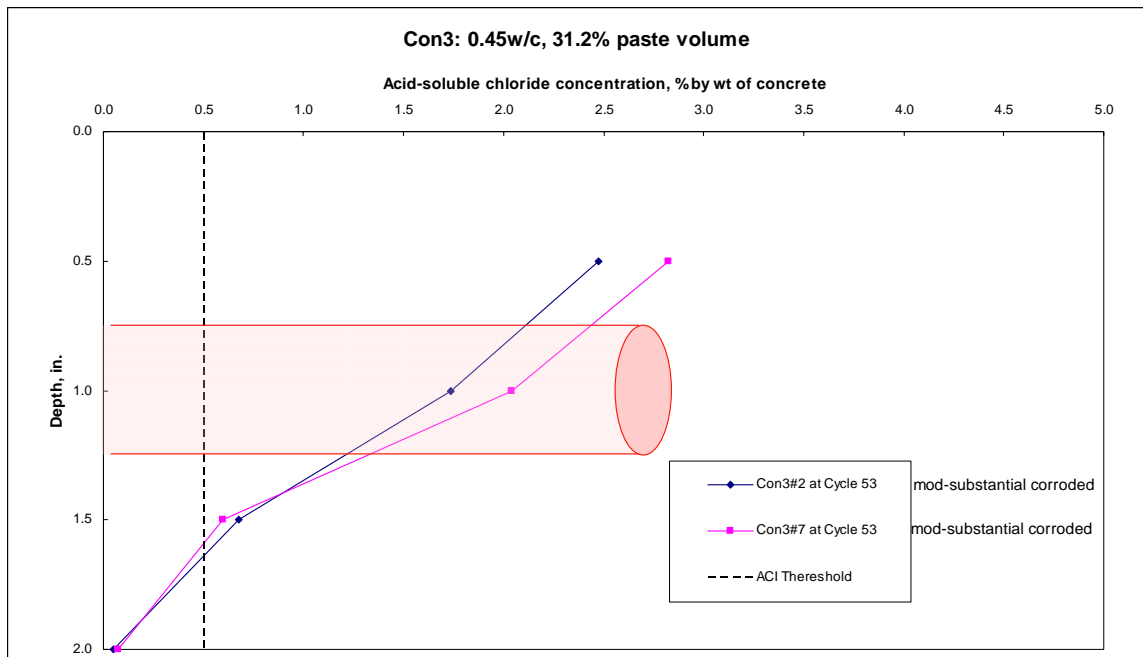


Figure 4-1 Acid-soluble chloride concentration vs. depth for Con3 mixture

Chloride concentrations for HCon4 were similar to Con3. The chloride concentrations of all HCon4 # 2, #3 and #4 specimens at a depth of 1.0” were less than the 0.50% modified threshold. It indicates the corrosion may not occur at the steel level. The interior steel bars of HCon4 #2 specimen were observed as moderate to substantial corroded while those of HCon4 #3 and #4 were of minor corrosion.

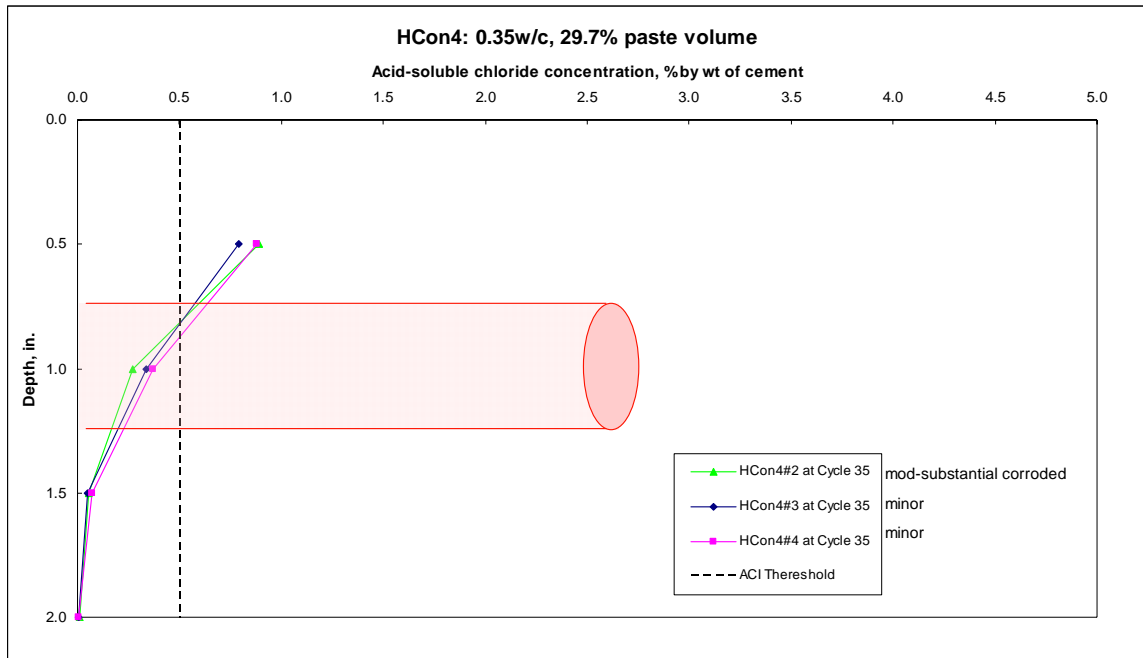


Figure 4-2 Acid-soluble chloride concentration vs. depth for HCon4 mixture

Similar figures for the other specimens are given in Appendix A for further study. It can be seen from these plots that almost all specimens observed as mod-substantially corroded have a chloride concentration between 1.5 to 2.5%, including control and both Type 1 and Type 2 admixture mixtures.

The mixtures with Type 2 admixtures, DCI, CNI, Rheo and Ferr, were expected to have higher chloride concentrations to initiate corrosion, but this is not clear from the plots generated during this study. These figures represent only 41 specimens out of the entire 650 specimens, so conclusions cannot be made at this time. This will be the scope of a future study.

CHAPTER 5 RESULTS FROM FIELD PANELS

5.1 Introduction

This chapter describes the results from tests performed on field panels. It includes the results for chemical test (chloride concentrations) and half-cell potential test.

5.1.1 Test hole locations

During each measuring, three test holes are located down the center of each panel designated as top, middle, and bottom. The location of each test hole for the two measurements is presented in Table 5-1 as the distance from the top of the panel measured along the front face of the panel.

Table 5-1 Locations of the holes drilled on each panel

Distance from top edge of panel (in.)

Panel Number	First measurement (2003) ¹			Second measurement (2005) ²		
	Top ¹	Middle ¹	Bottom ¹	Top ²	Middle ²	Bottom ²
1	16.8	27.4	37.7	7.3	33.0	52.5
2	15.2	25.8	37.5	7.5	34.0	52.5
3	17.0	27.6	37.3	7.5	33.5	52.0
3A	16.3	24.7	36.4	7.5	34.5	52.5
4	17.3	27.9	37.8	8.0	35.0	52.5
5	17.2	28.2	37.3	7.8	24.5	52.0
5A	6.8	26.2	37.1	15.5	34.3	51.5
6	15.0	26.4	38.0	8	34.5	52.5
7	16.8	27.3	37.5	16.0	27.5	37.5
8	7.6	26.3	37.6	17.0	34.0	52.5
9	14.4	25.5	36.3	7.5	33.0	52.0
10	15.9	27.1	43.7	7.3	34.0	52.5
11	16.4	26.9	37.8	8.0	34.0	52.5
12	15.2	26.4	38.4	8.0	34.0	51.5
13	15.8	27.0	38.0	7.8	34.3	51.8
14	7.5	28.0	38.0	16.0	32.5	51.5

15	7.8	25.3	36.5	16.5	33.5	52.8
16	15.8	27.2	37.3	7.5	33.8	52.5
17	7.8	25.8	37.6	15.3	33.3	52.0
17A	15.4	25.9	36.9	7.5	33.0	52.5
18	14.8	27.4	37.8	8.0	34.0	52.0
19	15.1	26.3	37.8	7.0	33.5	52.0
20	17.0	28.5	38.3	7.0	34.3	51.8
21	16.3	28.0	37.3	7.5	33.3	51.3
22	16.3	27.4	43.3	16.5	27.5	43.5

1. Using drilled hole to collect dust samples;
2. Using cored hole to collect 1" $\Phi \times 2.5$ " long core.

5.2 Chloride concentration

The acid-soluble chloride concentration value is a very important parameter to measure the chloride-induced corrosion in reinforced concrete. The data is collected about once per 1~1.5 years. The first set of data was presented by Uno and Robertson (2004). At that time an electric driller was used to collect the concrete dust samples. The sample collected at a depth of 0.5", for example, represents concrete dust from a depth of 0.5" to 1.0". The second set of data included in this report was obtained by slicing a 1" diameter core, and is therefore more accurate. It also provides an extra location at 2.0" depth which was not included in the first investigation. Since the first layer of reinforcing steel is located between the depth of 1.5 in and 2.0 in, these additional data provide chloride concentrations at the level of the bottom of the steel bars. Both sets of data are shown in the following figures for comparison. The first data are in dashed lines with hollow markers while the second are solid lines with solid markers. For ease of reading, the color for each test location is the same. For example, the dashed deep-blue line represents the first data for the top test hole while the solid deep-blue line represents the second data for the top test hole. The duration of exposure, in years, of each individual

sample is reported in each figure. Results of the chloride concentration tests were converted from percentage by mass of concrete to percentage by mass of cement using the cement content from the mixture proportions which can be found in the report by Pham and Newtonson (2000). The 0.50% threshold reported in each figure represents the modified threshold for acid-soluble chloride concentration.

5.2.1 Control mixtures

The results of the chloride concentration tests for the control panels are provided in Figure 5-1, Figure 5-2 and Figure 5-3. The chloride concentrations decrease at increasing depths for Panel 1(Con1). This is typical for all panels because the chloride ions from the outside environment have to migrate from the surface of the concrete. Chloride concentrations at all depths increase with time. At the age of 1.5 years, the top test hole had the highest concentrations at each depth, but is exceeded by the bottom test hole at the age of 3.4 years. The middle test hole always has the lowest chloride concentration though. At the age of 3.4 years, concentrations of both top and bottom holes at a depth of 1.5” were above the 0.50% modified threshold.

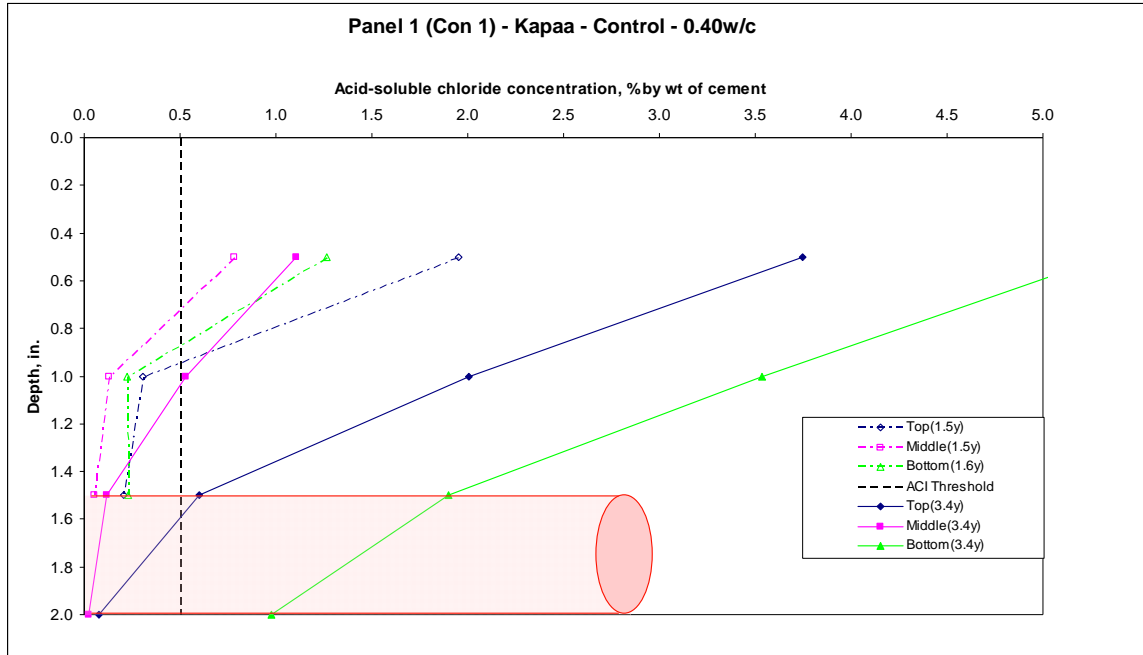


Figure 5-1. Acid-soluble chloride concentration vs. depth for panel 1

Chloride concentrations for panel 7(Con 7) were much lower than panel 1. The only difference between the two panels is the water/cement ratio. Panel 7 has a w/c ratio of 0.35 while Panel 1 has a w/c ratio of 0.40. It would appear that lower w/c ratio mixtures are less permeable to chloride migration. The bottom test hole had the highest concentrations at each depth at 1.5 years and 3.4 years. After 3.4 years, the chloride concentrations at depth of 1.5” were less than the 0.50% modified threshold.

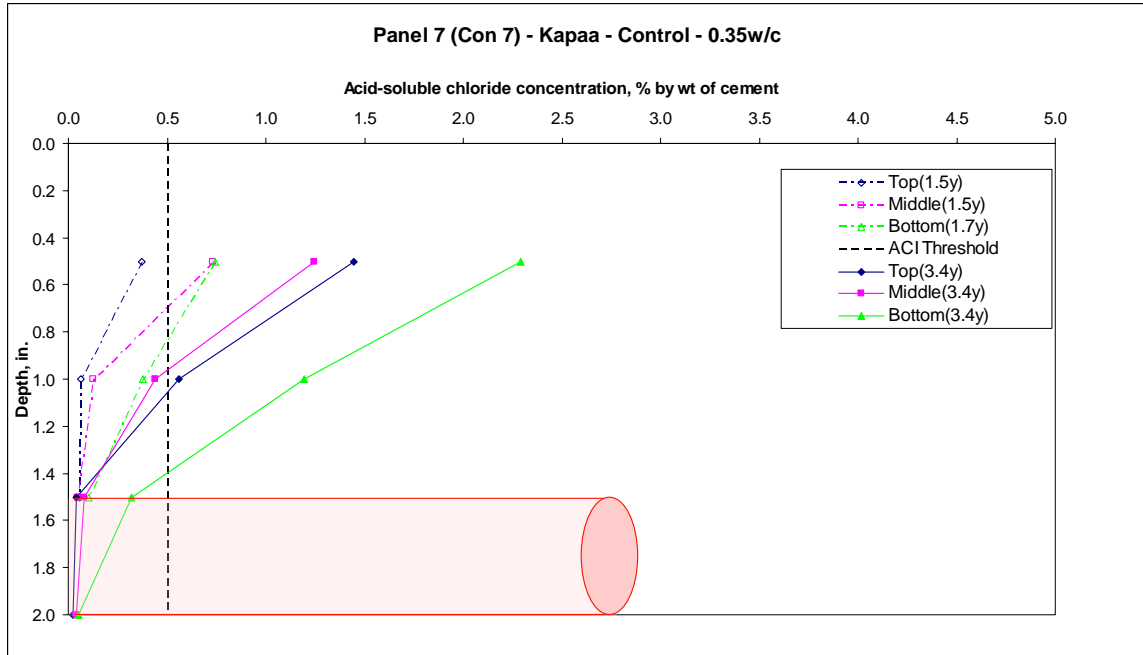


Figure 5-2. Acid-soluble chloride concentration vs. depth for panel 7.

Panel 2 (HCon 2) is the Halawa control mixture with a w/c ratio of 0.40, similar to the Kapaa control Panel 1. Chloride concentrations for panel 2 were generally lower than Panel 1 but higher than Panel 7. At the age of 1.4 years, the top test hole had the highest concentrations at each depth, but at 3.4 years, the bottom test hole had the highest values. After 3.4 years, the chloride concentrations at depth of 1.5” were less than the 0.50% modified threshold.

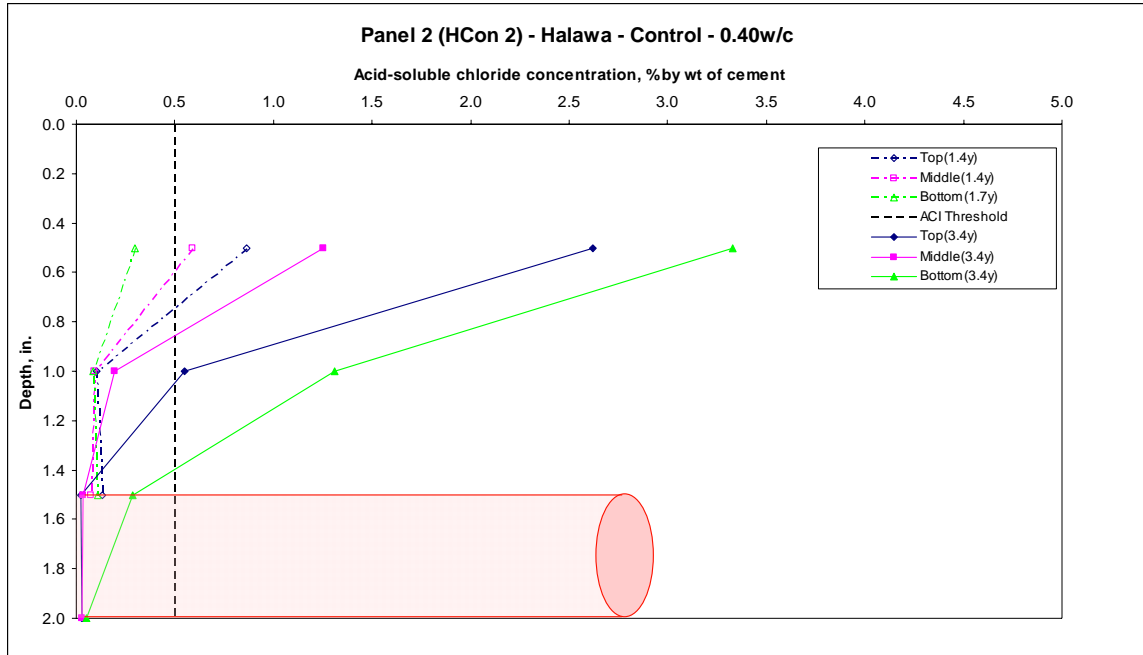


Figure 5-3. Acid-soluble chloride concentration vs. depth for panel 2.

5.2.2 DCI mixtures

Chloride concentration results for the DCI panels are presented in, Figure 5-4, Figure 5-5, and Figure 5-6. For the two panels with Kapaa aggregates (Panel 3 and 3A), the bottom hole consistently recorded the highest overall concentrations, followed by the top hole and the middle hole. Up to age 3.4 years, the concentrations for top and middle holes between depths of 1.5 in. and 2.0 in. were below the 0.50% modified threshold but the concentrations for bottom hole were significantly higher than the threshold value. This may indicate that corrosion is occurring at the level of the steel for the bottom portion of these panels.

Chloride concentrations for Panel 3A are very similar to those for Panel 3. The only difference between the two is that Panel 3A had twice the amount of DCI as Panel 3. DCI is not expected to affect the chloride permeability of the concrete, and so should not affect the chloride concentrations. It should be noted that the chloride concentration readings for Panel 3 were taken at 1.7 and 3.4 years age while the data for Panel 3A were taken at 0.7 and 2.5 years. Therefore the data are not directly comparable.

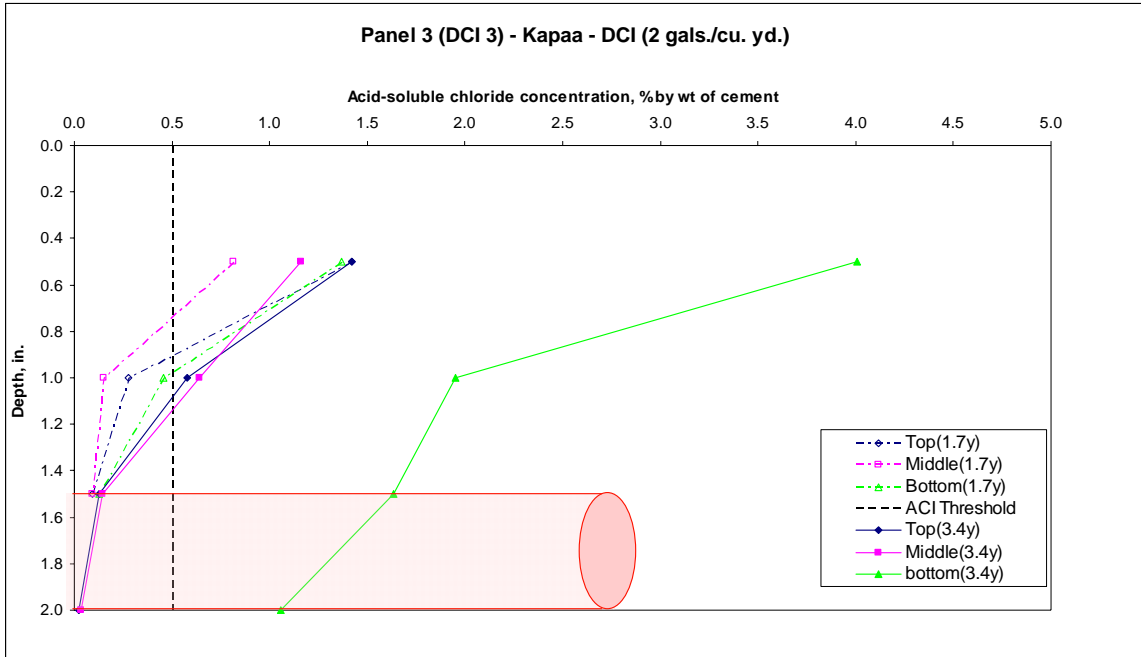


Figure 5-4. Acid-soluble chloride concentration vs. depth for panel 3.

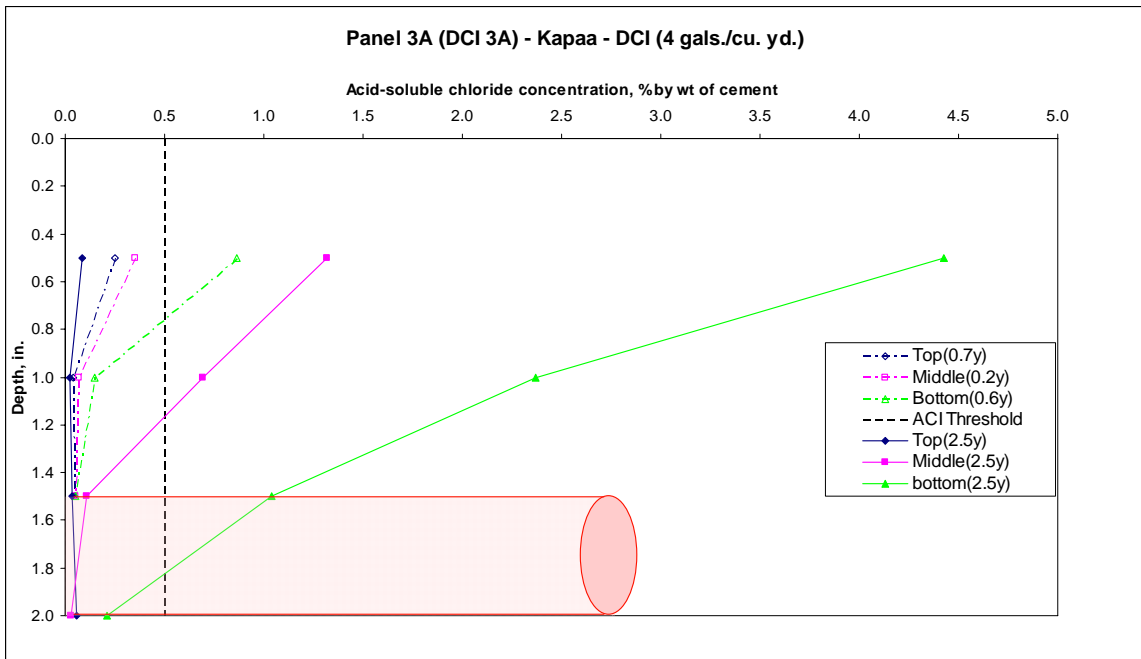


Figure 5-5. Acid-soluble chloride concentration vs. depth for panel 3A.

Chloride concentrations for Panel 4 were somewhat lower than for Panel 3 and 3A. The only difference between Panel 4 and Panel 3 is that Panel 4 contains Halawa

aggregates instead of the Kapaa aggregates used in Panel 3. At 3.4 years exposure, the concentrations for all three holes are similar.

Up to the age of 3.4 years, the concentrations between depth 1.5 in. and 2.2 in. for all three test holes were below the 0.50% modified threshold. It is unlikely that corrosion has initiated in the steel.

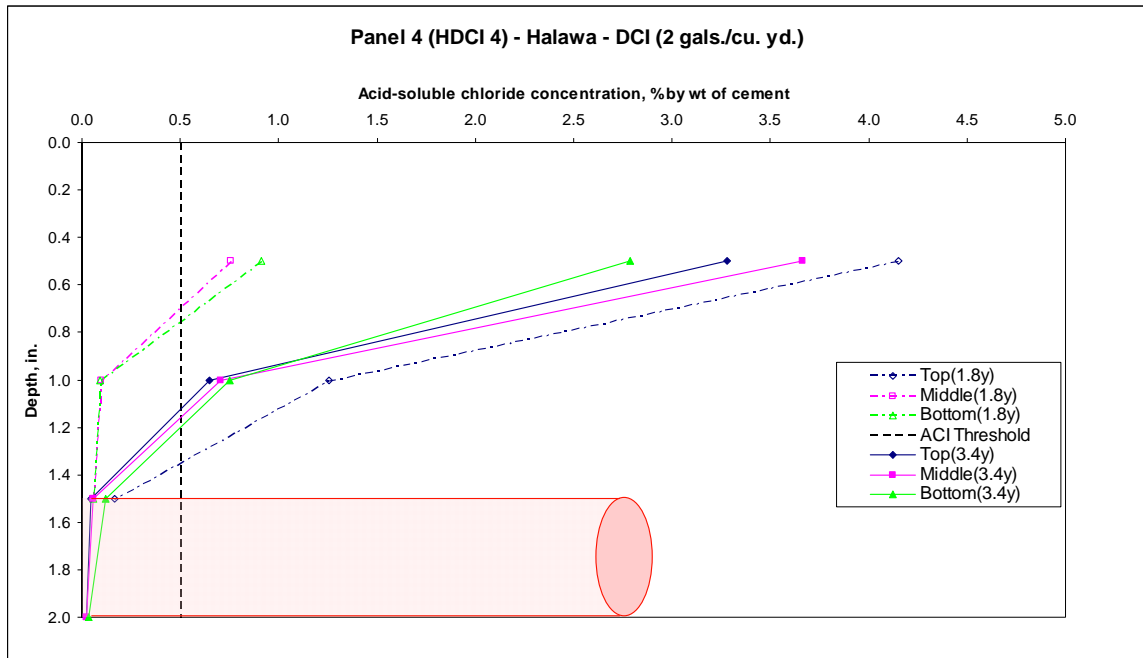


Figure 5-6 Acid-soluble chloride concentration vs. depth for panel 4.

5.2.3 Rheocrete CNI mixtures

The results of the chloride concentration tests for the Rheocrete CNI panels are provided in Figure 5-7, Figure 5-8, and Figure 5-9. Panel 5 and 6 have exactly the same mix properties while 8 and 5A has twice as much CNI as the other panels. Chloride concentrations for the bottom test hole were the highest at all ages. Unexpectedly, the chloride concentrations for both bottom and top holes of panel 5 at 3.3 years age were

smaller than at 1.7 years age, which might be due to measuring mistakes. Up to the age of 3.3 years, the concentrations between depth 1.0 in. and 1.5 in. for all three test holes were below the 0.50% modified threshold. It is unlikely that corrosion has initiated in the steel.

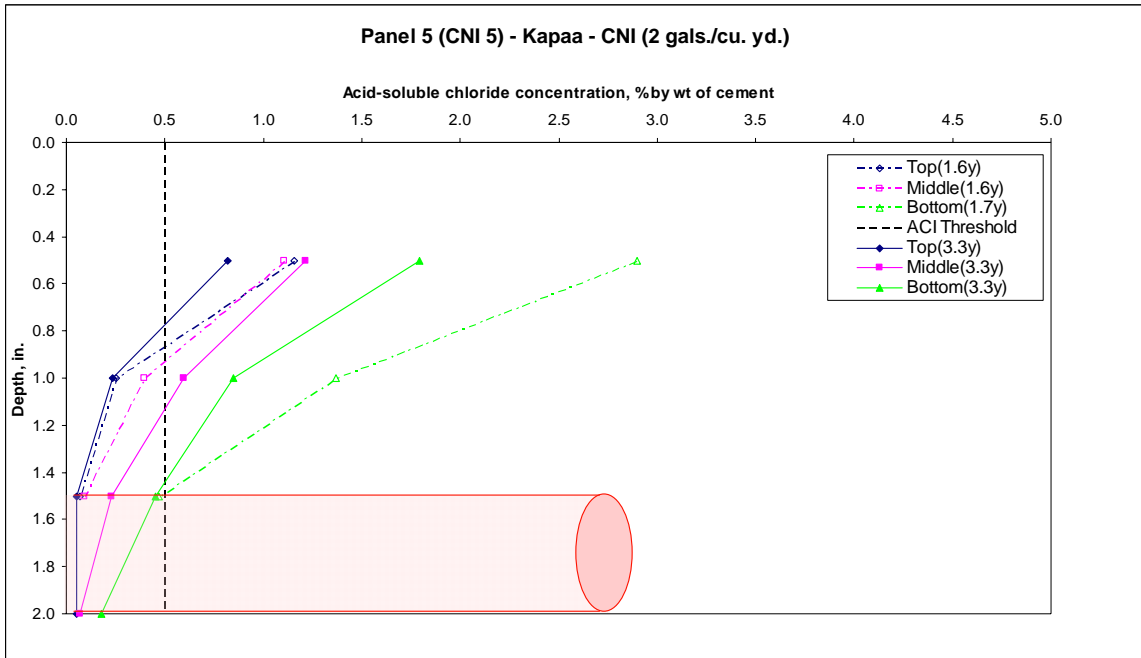


Figure 5-7 Acid-soluble chloride concentration vs. depth for panel 5

Chloride concentrations for Panel 6 are similar to those for the equivalent content and DCI specimens. The bottom test hole remained the highest concentrations at each depth, followed by the top and middle hole at all ages. At the 3.3 years age, the concentrations between depths of 1.5 in. and 2.0 in. for top and middle holes were below the 0.50% modified threshold, while they were higher than the threshold for the bottom hole. This indicates that the bottom section of the panel may have started corroding.

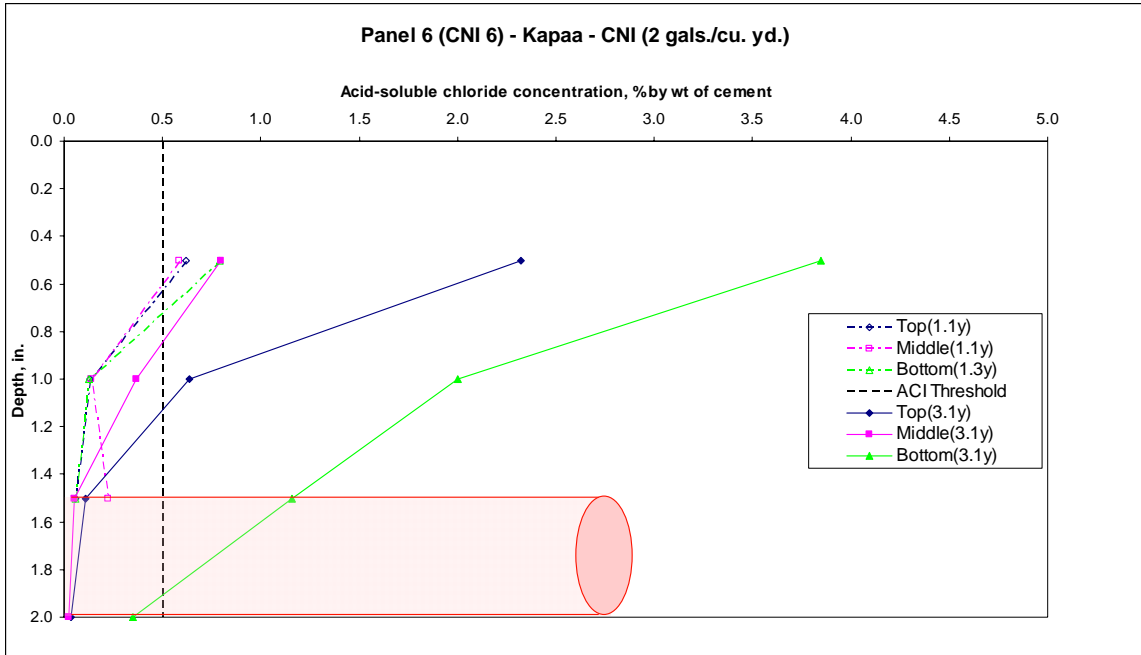


Figure 5-8 Acid-soluble chloride concentration vs. depth for panel 6

Overall, the distribution of chloride concentrations for panel 5A was similar to Panel 6 except that the top hole, instead of middle hole, has the smallest concentrations. Similar to Panel 6, the chloride concentrations between depths of 1.5 in. and 2.0 in. for the bottom hole were higher than the 0.50% modified threshold, which indicates the bottom section of the panel may be corroding.

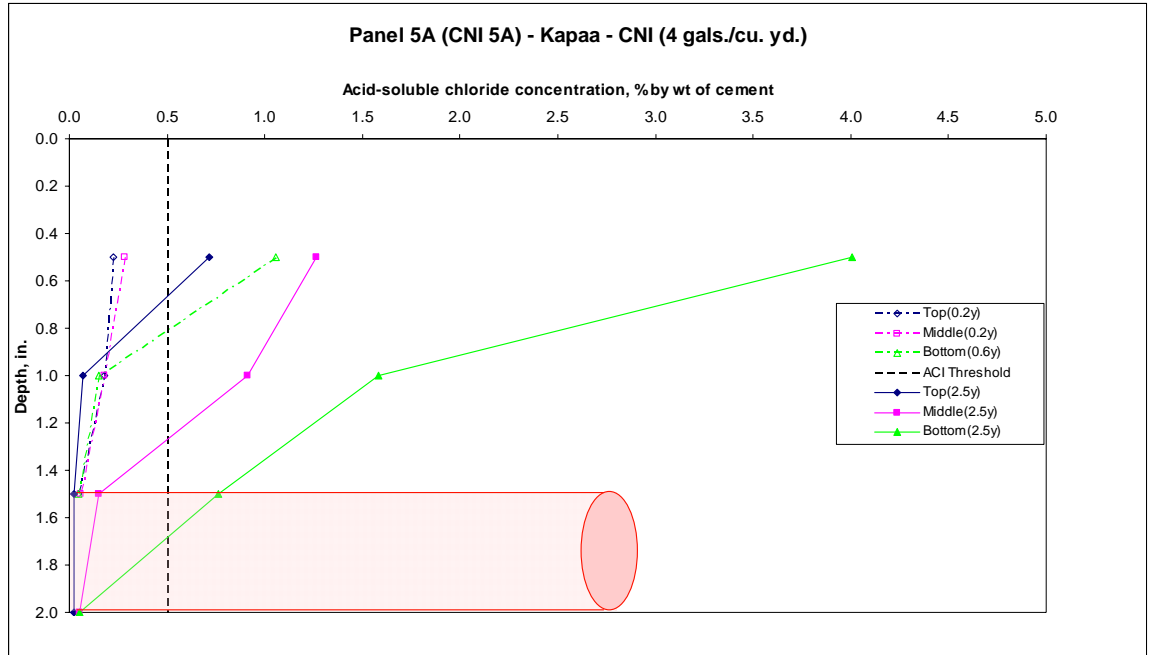


Figure 5-9. Acid-soluble chloride concentration vs. depth for panel 5A.

5.2.4 Rheocrete 222+ mixtures

Chloride concentration results for the Rheocrete 222+ panels are presented in Figure 5-10, Figure 5-11, Figure 5-12, and Figure 5-13. Panel 15 and Panel 16 were designed using the same concrete mixture, but the results are slightly different. The chloride concentration for Panel 15 reached the highest value for the bottom hole. The middle hole changed little with age while the bottom and top holes changed a lot. Up to age of 3.3 years, the concentrations between depths of 1.5 in. and 2.0 in. are below the 0.50% modified threshold for middle and top holes, but higher than threshold for the bottom hole.

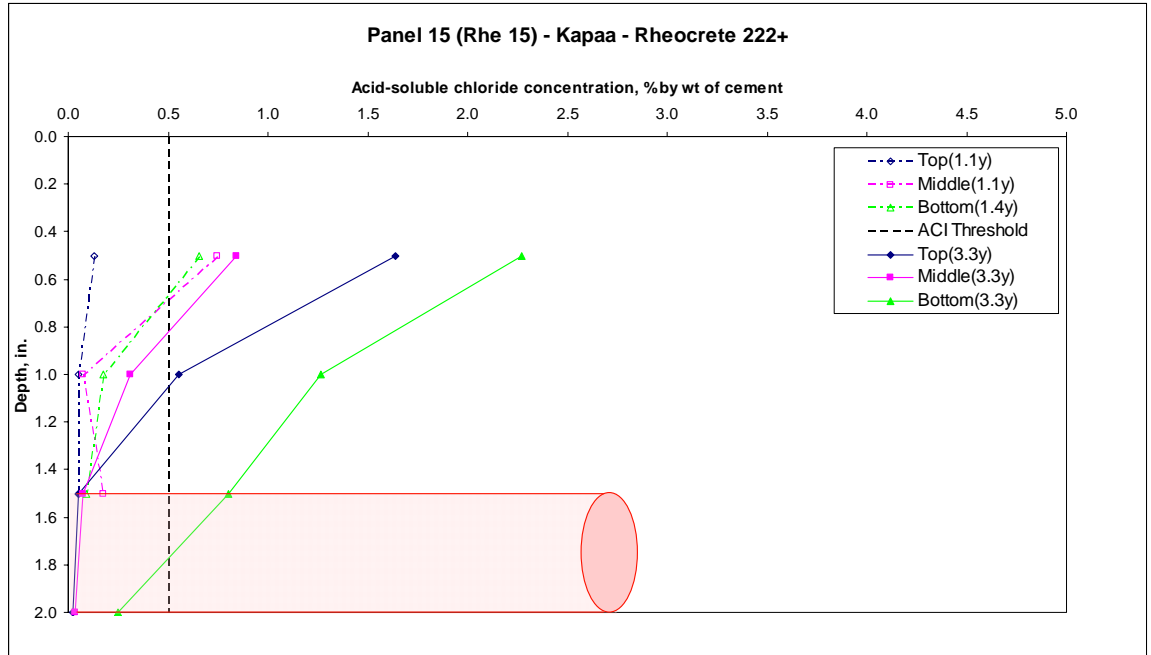


Figure 5-10. Acid-soluble chloride concentration vs. depth for panel 15.

Chloride concentrations for panel 16 are generally higher than panel 15. The concentrations for the bottom hole decreased with ages, while the concentrations for middle and top holes increased such that the middle hole has the highest concentration at 3.3 years. At 3.3 years, all holes have concentrations near or below the 0.50% modified threshold at the steel level.

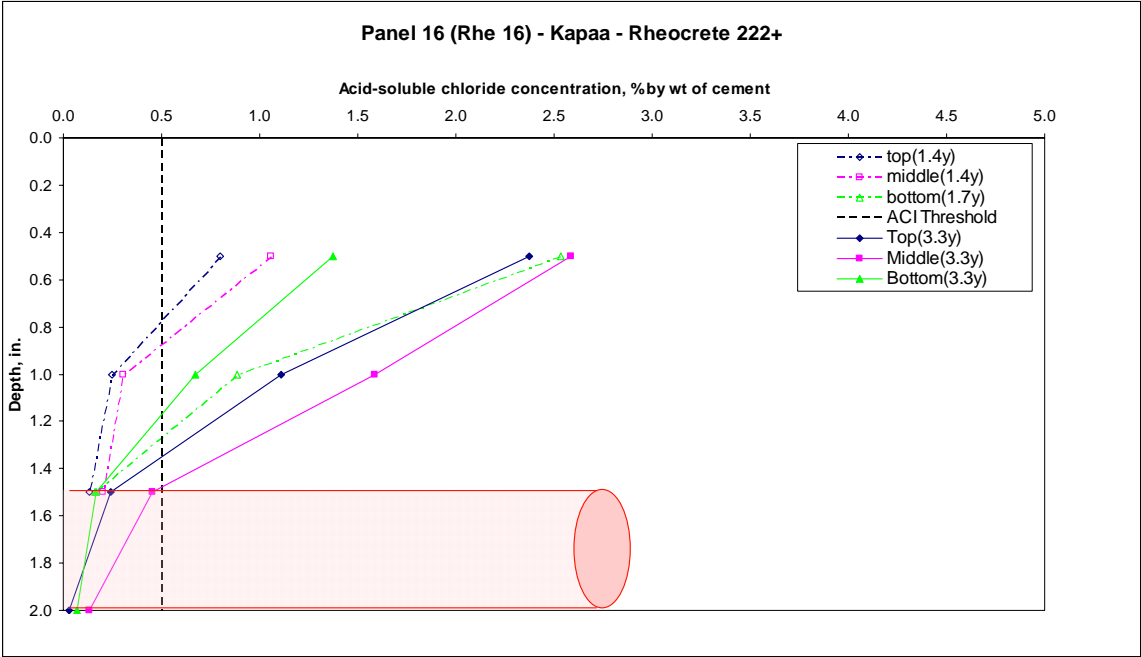


Figure 5-11. Acid-soluble chloride concentration vs. depth for panel 16.

Panel 17 and 17A were fabricated using the same mixtures as panels 15 and 16, but with Halawa aggregates. Chloride concentrations for panel 17 are all fairly small except for the bottom hole at 3.3 years. It is unclear why the bottom hole concentrations are as high as they are, but if they are representative of the entire bottom section of the panel, it is likely that corrosion would have initiated.

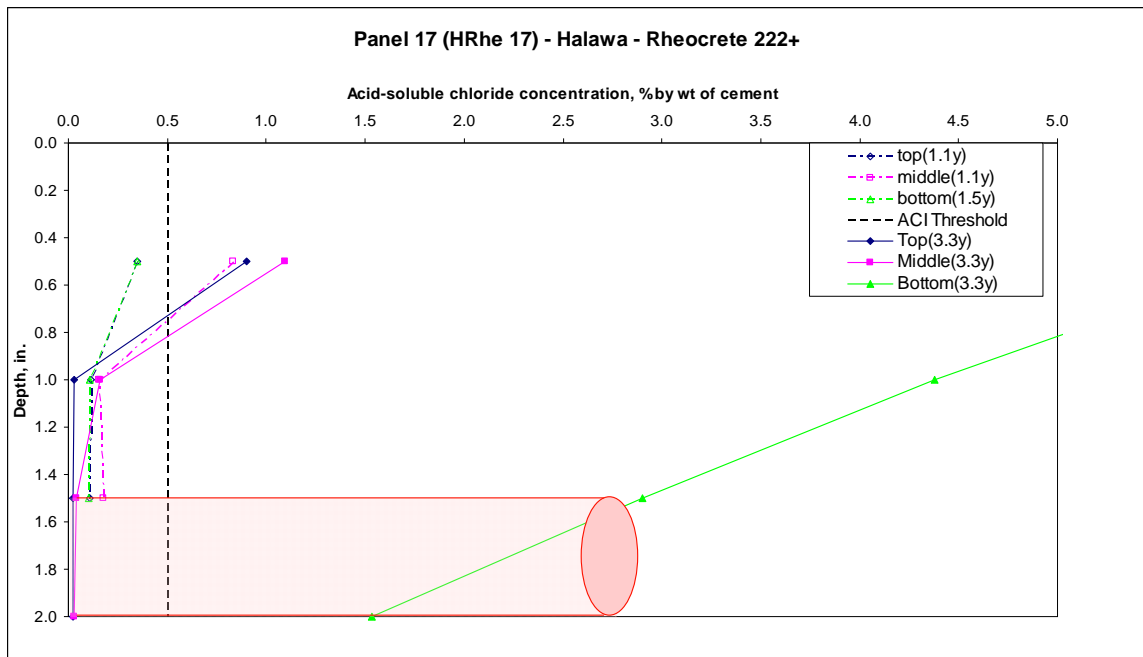


Figure 5-12. Acid-soluble chloride concentration vs. depth for panel 17.

The chloride concentrations for the bottom holes of Panel 17A are also high at 0.5 and 1.0 in depths. However, at 2.5 years, it is still below the 0.50% modified threshold, thus no corrosion is anticipated at the level of the steel for Panel 17A.

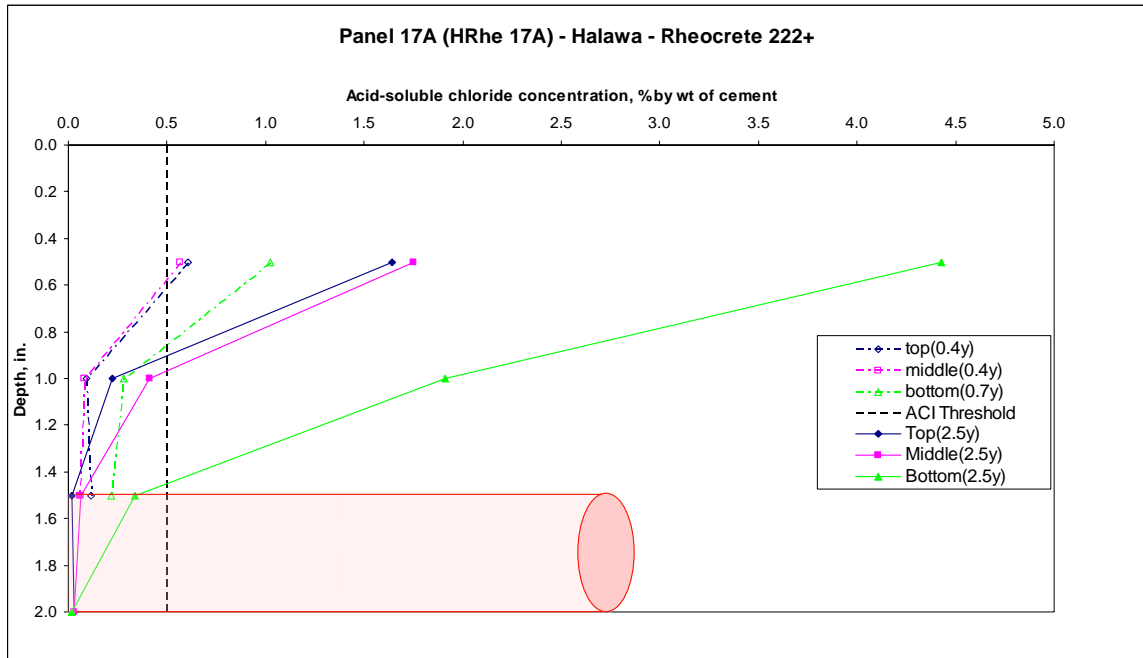


Figure 5-13. Acid-soluble chloride concentration vs. depth for panel 17A.

5.2.5 FerroGard 901 mixtures

The results of the chloride concentration tests for the FerroGard 901 panels are provided in Figure 5-14, Figure 5-15, and Figure 5-16. Panel 20 uses Kapaa aggregates while Panels 18 and 19 use Halawa aggregates. All three panels contain the same amount of Ferr Gard 901. Overall, the distributions of chloride concentrations for the three panels are quite similar.

Chloride concentrations for Panel 20 (Fer 20) are shown in Figure 5-14. At 1.2 years age, the middle hole had the highest concentration while the bottom has the lowest. At 2.9 years, the bottom hole concentrations have increased significantly such that the concentrations between depths of 1.5 in. and 2.0 in. are well above the 0.5% threshold. It indicates that corrosion may have initiated in the bottom section of the panel.

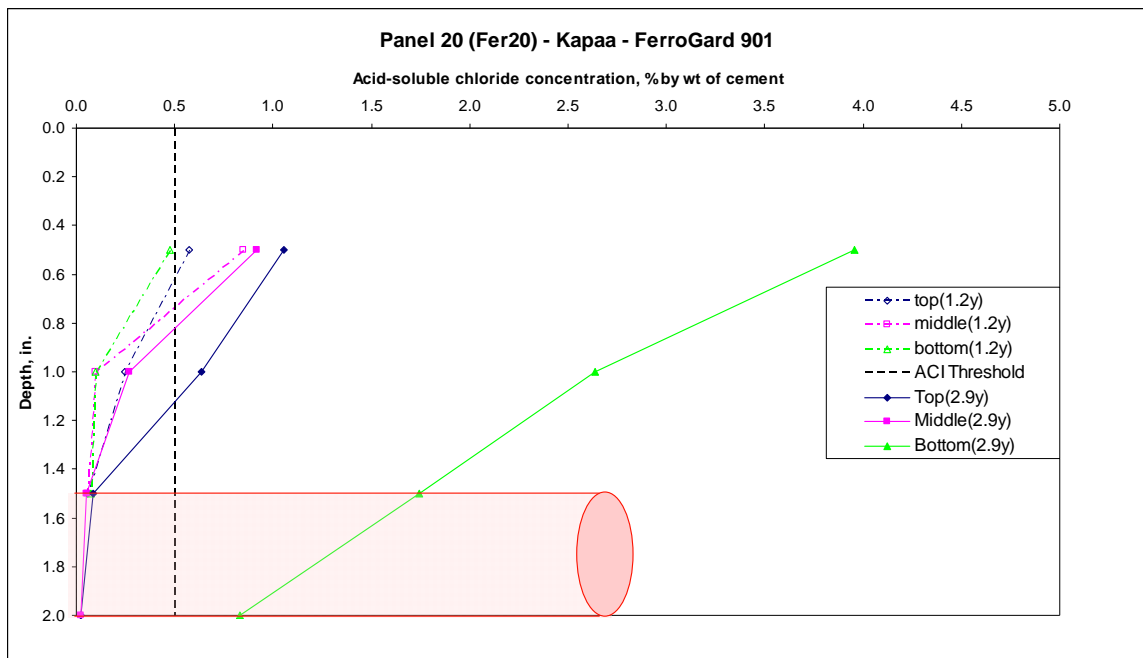


Figure 5-14. Acid-soluble chloride concentration vs. depth for panel 20.

The chloride concentrations for Panel 18 (Hfer 18) are similar to Panel 20 (Fer 20). The concentrations for top hole are greater than for Panel 20, but the bottom hole is again significantly above the 0.5% threshold at the age of 3.4 years, which indicates the corrosion has probably initiated at the bottom of the panel.

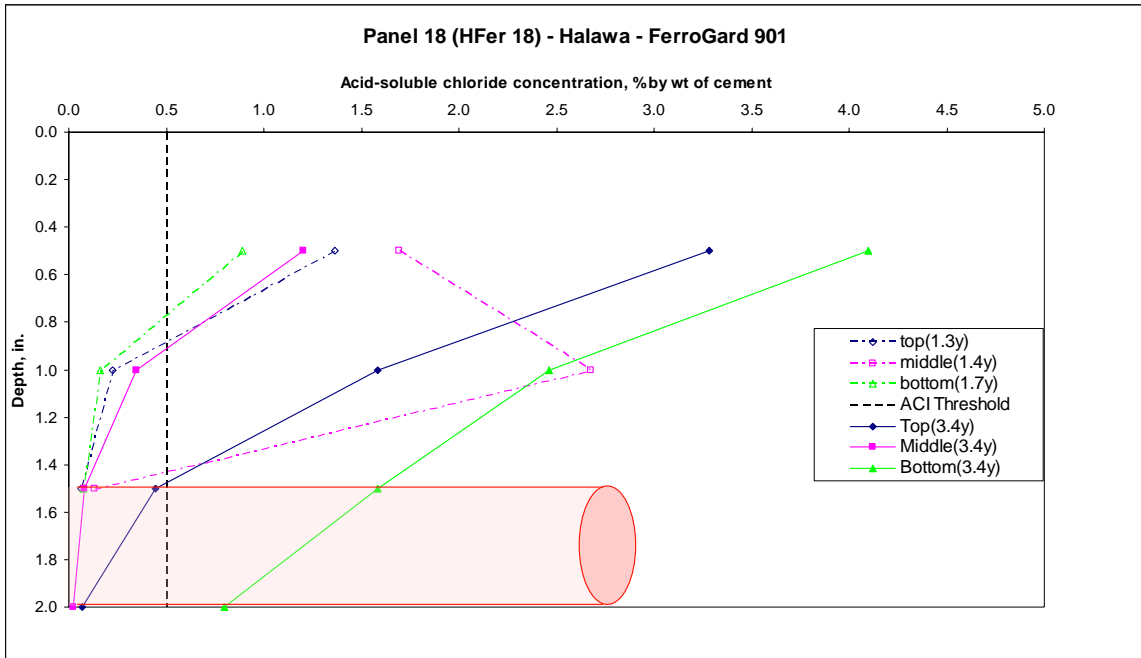


Figure 5-15. Acid-soluble chloride concentration vs. depth for panel 18.

Panel 19 (Hfer 19) was designed exactly the same as Panel 18. Chloride concentrations for Panel 19 are collectively lower than panel 18. But the concentrations for the bottom hole are again high. At the age of 3.4 years, the chloride concentration for the bottom hole at 1.5 in. depth is much higher than the 0.50% threshold, which indicates the corrosion is possible.

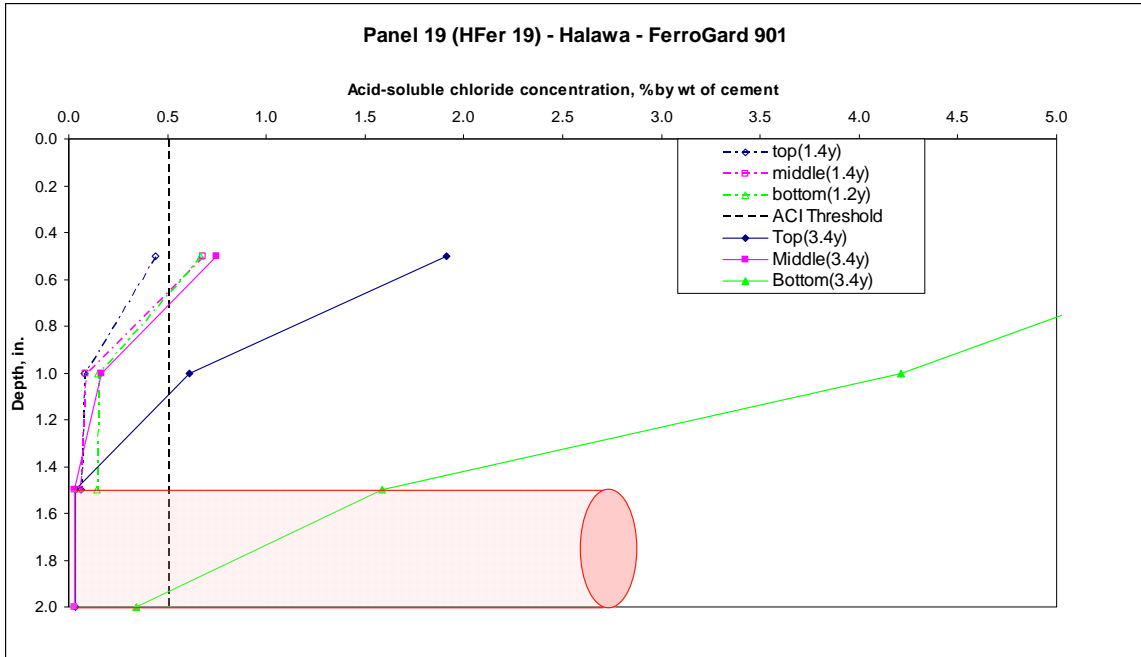


Figure 5-16. Acid-soluble chloride concentration vs. depth for panel 19.

5.2.6 Xypex C-2000 mixture

The results of the chloride concentration tests for the Xypex C-2000 panel are presented in Figure 5-17. After 3.1 years exposure, all these holes have similar concentrations. At 1.5 in. and 2.0 in. depths, all concentrations are below the 0.50% threshold, which indicates that corrosion probably is not occurring at the level of the steel.

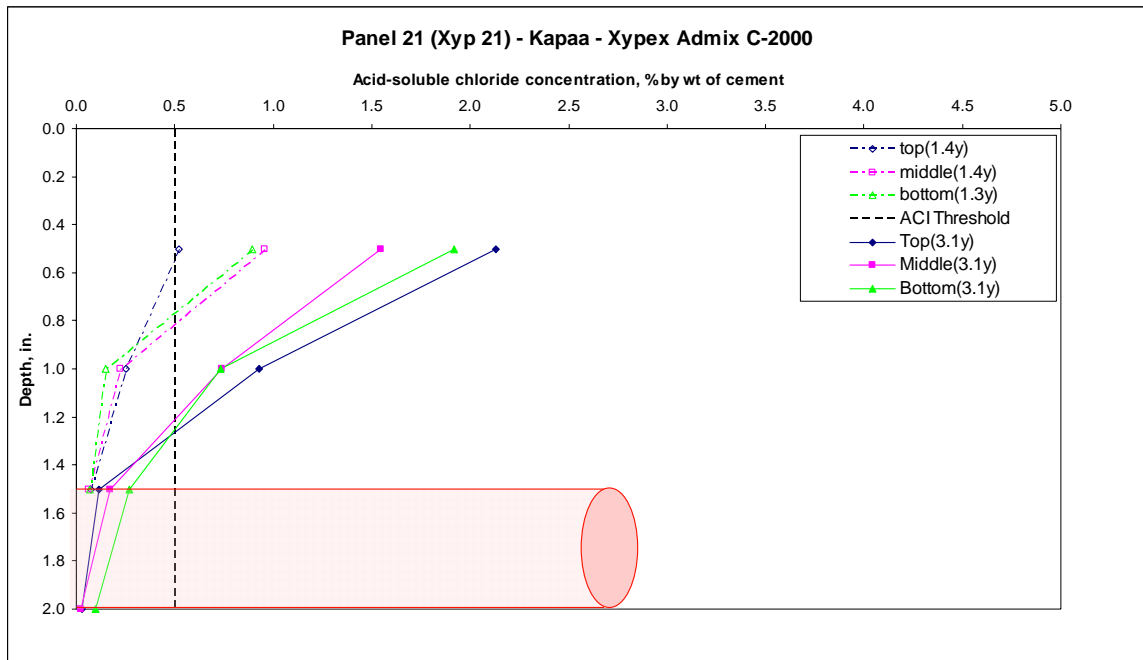


Figure 5-17. Acid-soluble chloride concentration vs. depth for panel 21.

5.2.7 Latex-modified mixture

The results of the chloride concentration tests for the latex-modified panel are provided in Figure 5-18. The concentrations for all three holes between depths of 1.5 in.

and 2.0 in. are under the 0.50% threshold, which indicates that corrosion probably is not taking place at the depth of the steel.

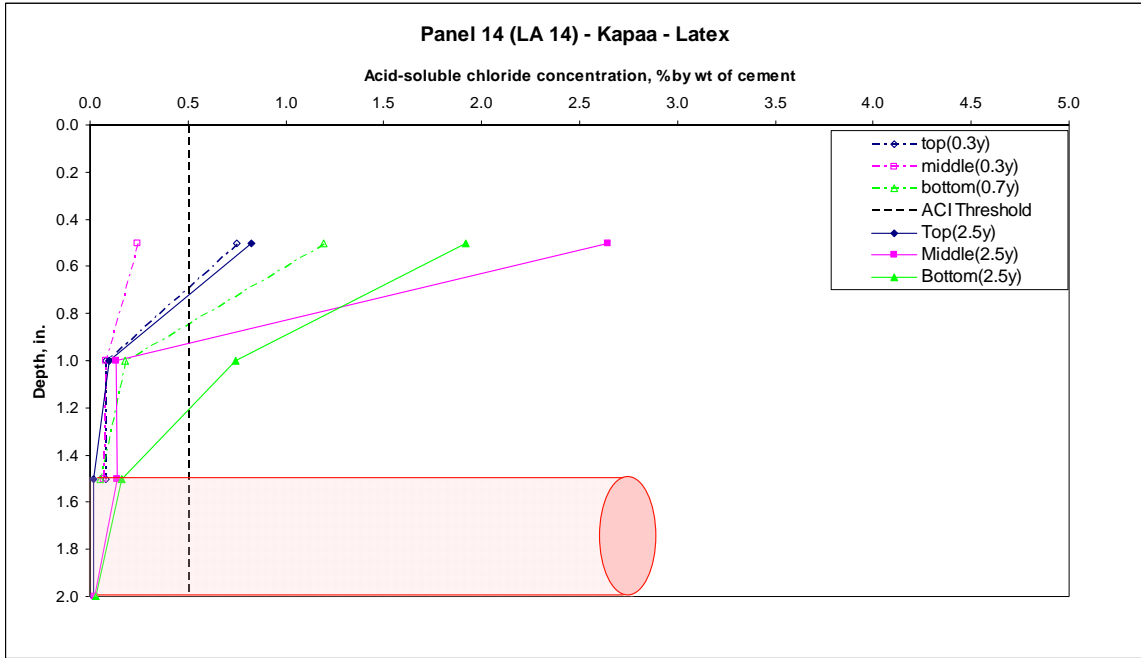


Figure 5-18. Acid-soluble chloride concentration vs. depth for panel 14.

5.2.8 Fly ash mixtures

The results of the chloride concentration tests for the Fly Ash panels are provided in Figure 5-19, Figure 5-20, and Figure 5-21. The panel 11 (FA 11) is a Kapaa mixture while Panel 12 (HFA 12) and Panel 13 (HFA 13) are Halawa mixtures. All concentrations are significantly lower than the equivalent content specimens except at 0.5 in. depth. Concentrations at depths between 1.0 in. and 2.0 in. are below the 0.50% modified threshold for all three test holes, which indicates that corrosion probably is not occurring at the level of the steel for panel 11.

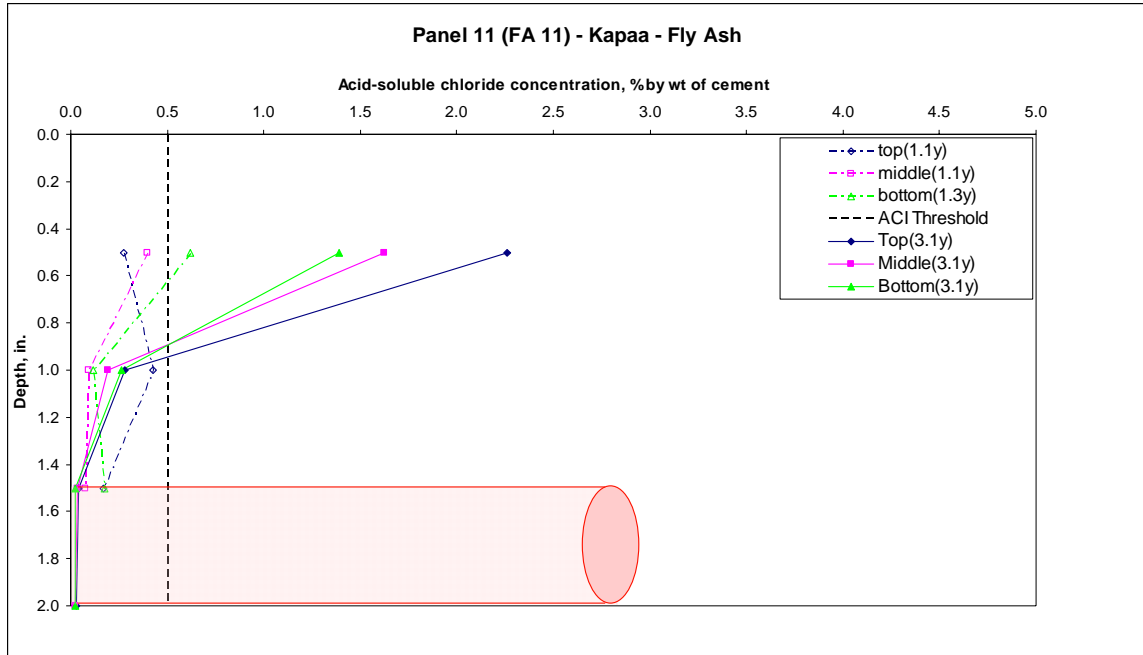


Figure 5-19. Acid-soluble chloride concentration vs. depth for panel 11.

Chloride concentrations for panel 12 are very similar to those for panel 11 at the late age. After 3.4 years exposure, concentrations at depths of 1.0 in. (25 mm) and 1.5 in. (38 mm) for all the test holes are below the 0.50% modified threshold, which suggests that corrosion probably is not taking place at the level of the steel.

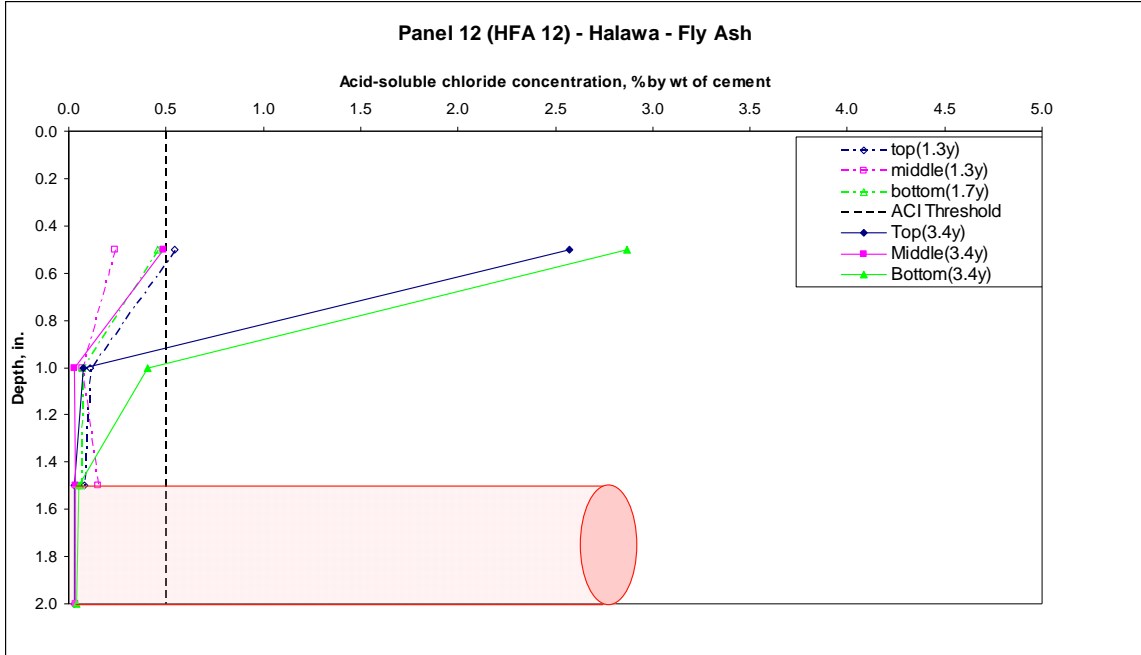


Figure 5-20. Acid-soluble chloride concentration vs. depth for panel 12.

Panel 13 was designed using the same mixture as Panel 12. Chloride concentrations for panel 13 are similar to panel 12, except for higher values in the bottom hole. Between the depths of 1.5 in. and 2.0 in., all three test holes have concentrations lower than the 0.50% modified threshold, which shows that corrosion probably is not occurring at the level of the steel.

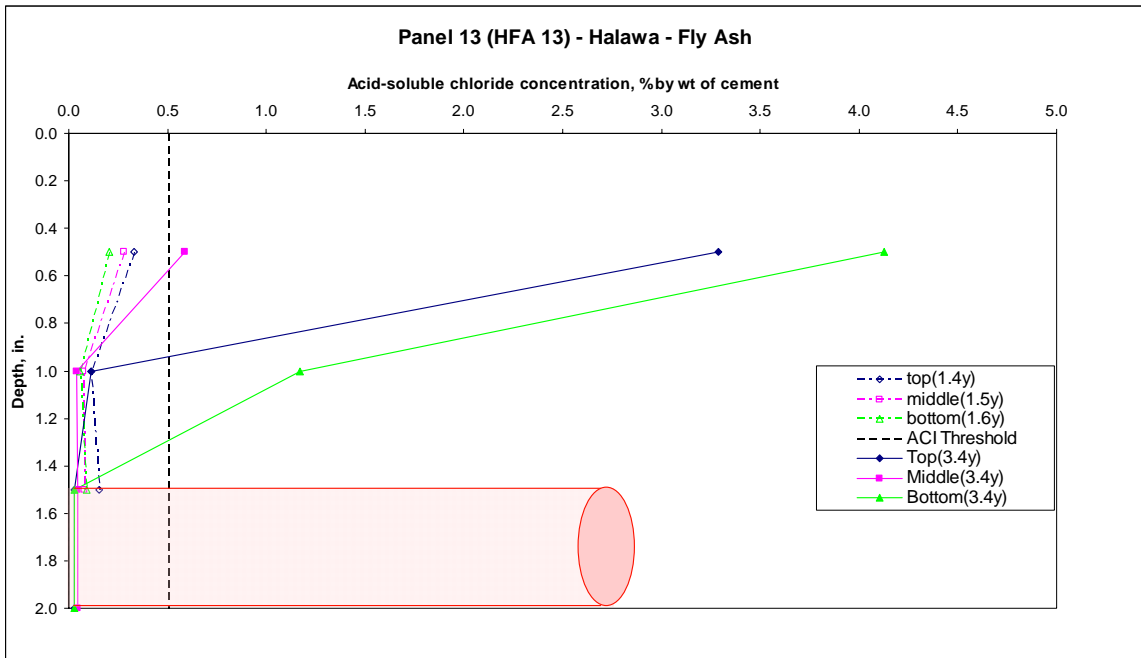


Figure 5-21. Acid-soluble chloride concentration vs. depth for panel 13.

5.2.9 Silica fume mixtures

The results of the chloride concentration tests for the panels proportioned with silica fume are presented in Figure 5-22, Figure 5-23, and Figure 5-24. All the three panels, 8 to 10, use Kapaa aggregates but with two different Silica Fume admixtures. Panel 8 (SF-Rh 8) and Panel 9 (SF-Rh 9) contain Rheomac SF100 made by Master Builders Inc., while Panel 10 (SF 10) contains Force 10,000D SF made by W.R. Grace company.

At the 0.7 years age, it was noted that the chloride concentration of the middle hole for Panel 8 at 1.5 in. depth is higher than that at 1.0 and 0.5 depths. This unusual situation might be due to measuring mistake. Up to the 2.9 years age, chloride concentrations between 1.5 in. to 2.0 in. depths are all below the 0.50% threshold. It indicates that corrosion probably has not reached the level of the steel.

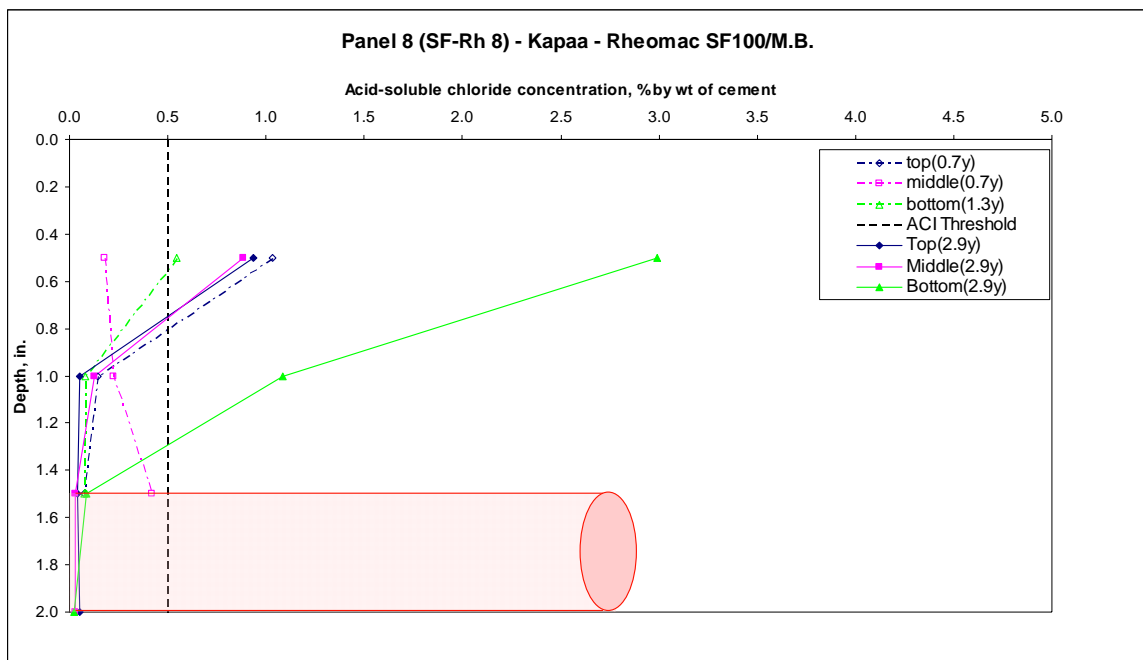


Figure 5-22. Acid-soluble chloride concentration vs. depth for panel 8.

Chloride concentrations for Panel 9 are very similar to those for Panel 8. After 2.5 years exposure, the chloride concentrations for all holes between depths of 1.5 in. to 2.0 in. are below the 0.50% threshold, which indicates that corrosion probably has not reached the level of the steel.

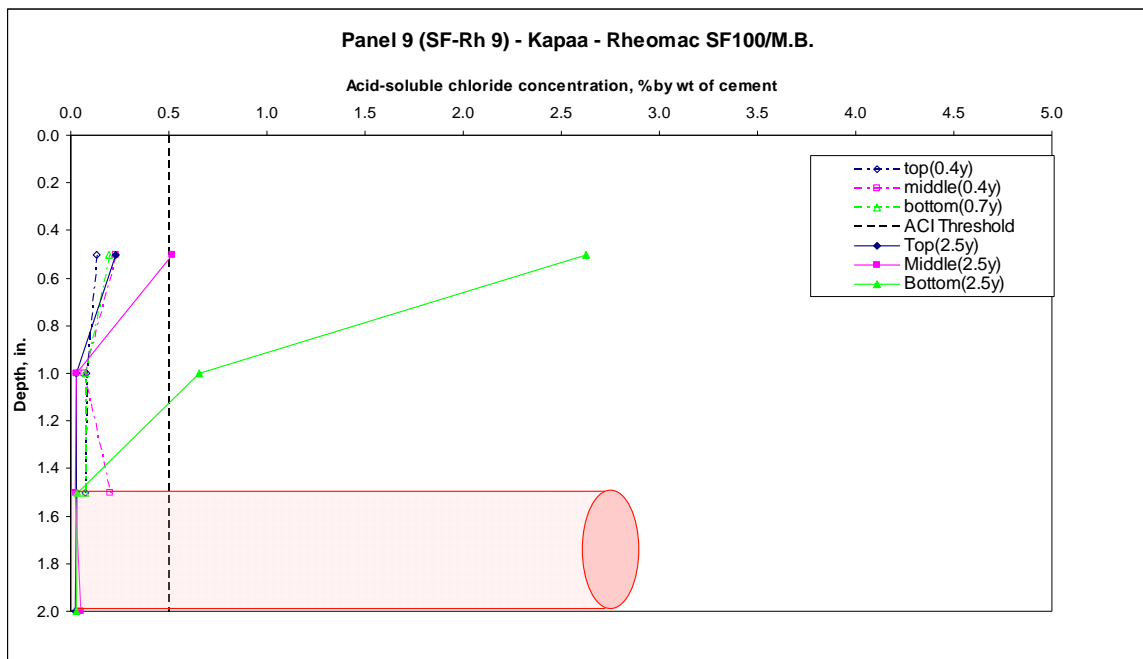


Figure 5-23. Acid-soluble chloride concentration vs. depth for panel 9.

Chloride concentrations for Panel 10 are also very similar to those for Panels 8 and 9. After 2.9 years exposure, the chloride concentrations for all holes between depths of 1.5 in. to 2.0 in. are below the 0.50% threshold, which indicates that corrosion probably is not occurring at the level of the steel.

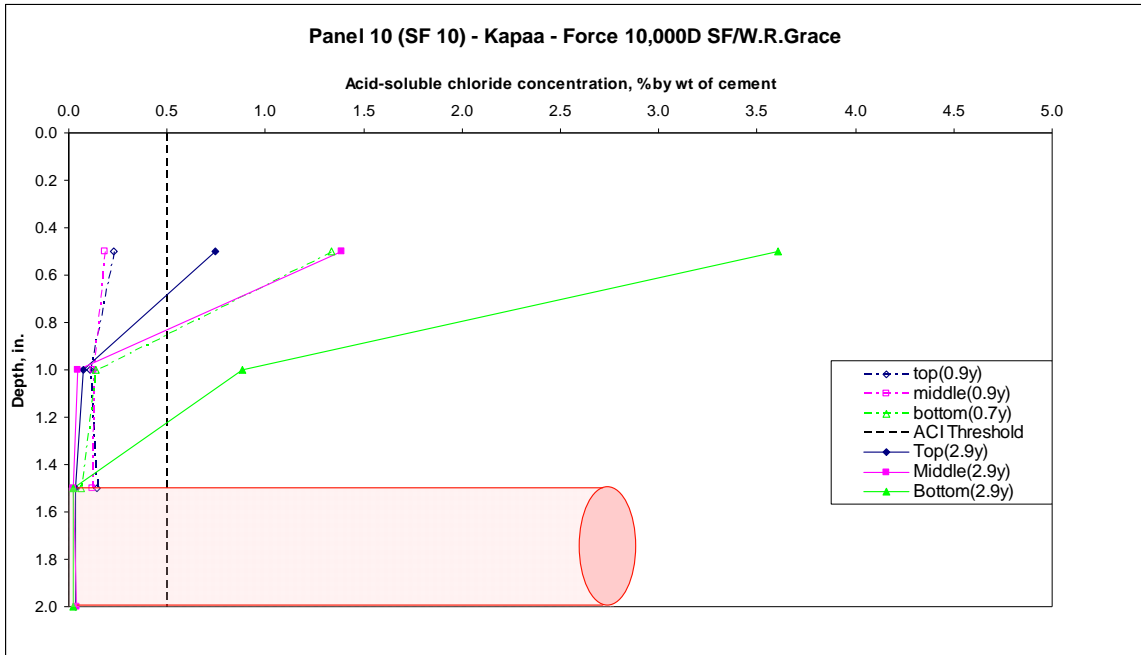


Figure 5-24. Acid-soluble chloride concentration vs. depth for panel 10.

5.2.10 Kryton KIM mixture

The results of the chloride concentration tests for the Kryton KIM panel are provided in Figure 5-25. At the 2.5 years age, all chloride concentrations between depths of 1.5 in. and 2.0 in. are below than the 0.50% modified threshold. It indicates that corrosion probably has not occur at the bottom section of the panel.

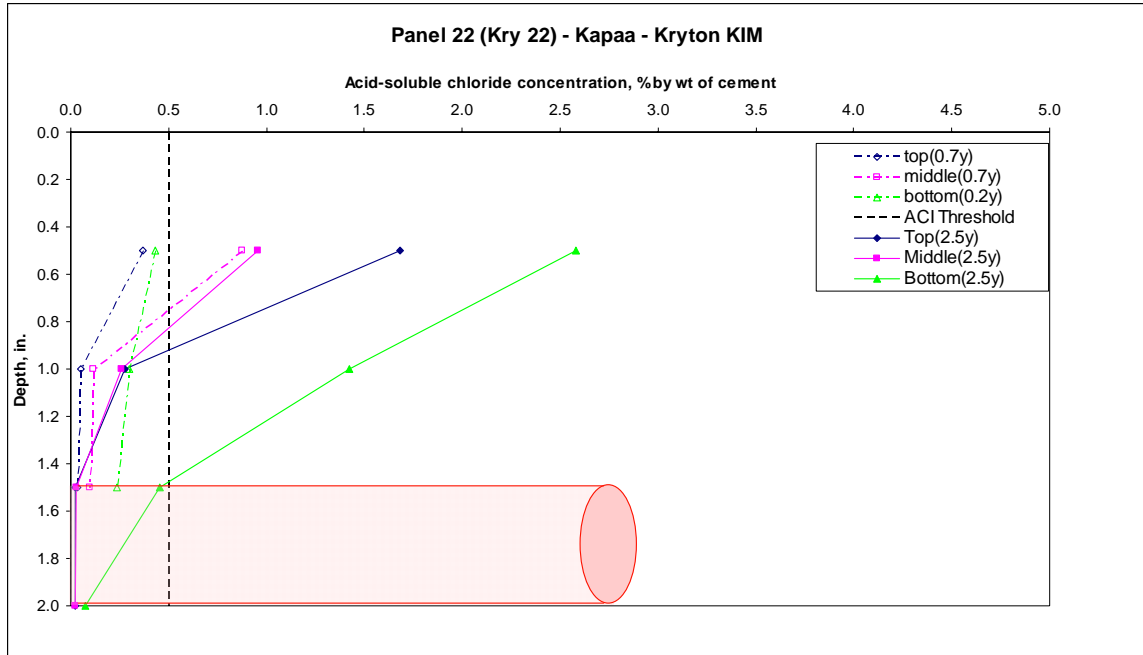


Figure 5-25. Acid-soluble chloride concentration vs. depth for panel 22

5.2.11 Comparison of all the panels

As discussed earlier, all the admixtures used in this project were divided into two categories, namely Type 1 and Type 2. Type 1 admixtures including Xypex, Fly Ash, Silica Fume and Latex modifier are intended to reduce the concrete permeability. Type 2 admixtures including DCI, CNI and FerroGard are intended to raise the chloride threshold required to initiate corrosion. Rheocrete 222+ can be considered as both Type 1 and Type 2.

The previous figures show that the chloride concentrations vary at different locations (top, middle and bottom) and at different depths (0.5in, 1.0in, 1.5in and 2.0in). In order to compare different panels, the results from the bottom test holes, which are

always under sea level, and generally show the highest chloride concentrations, are used in Figure 5-26 to Figure 5-31.

The chloride concentrations for the bottom holes of all panels at different depths are shown in Figure 5-26 to Figure 5-28. Chloride concentrations decrease with the depth below the wetted surface for all panels. Type 1 admixtures are supposed to reduce the penetration of chloride ions through the concrete cover. At the 0.5 inch depth, there is not a significant difference in performance between the Type 1, Type 2 and control panels. However, at 1 inch and 1.5 inch depth (at the level of the reinforcing steel) mixtures with Type 1 admixture have lower chloride concentrations compared with the corresponding control panels. Type 2 admixtures do not appear to affect the chloride concentrations when compared with the corresponding control panels.

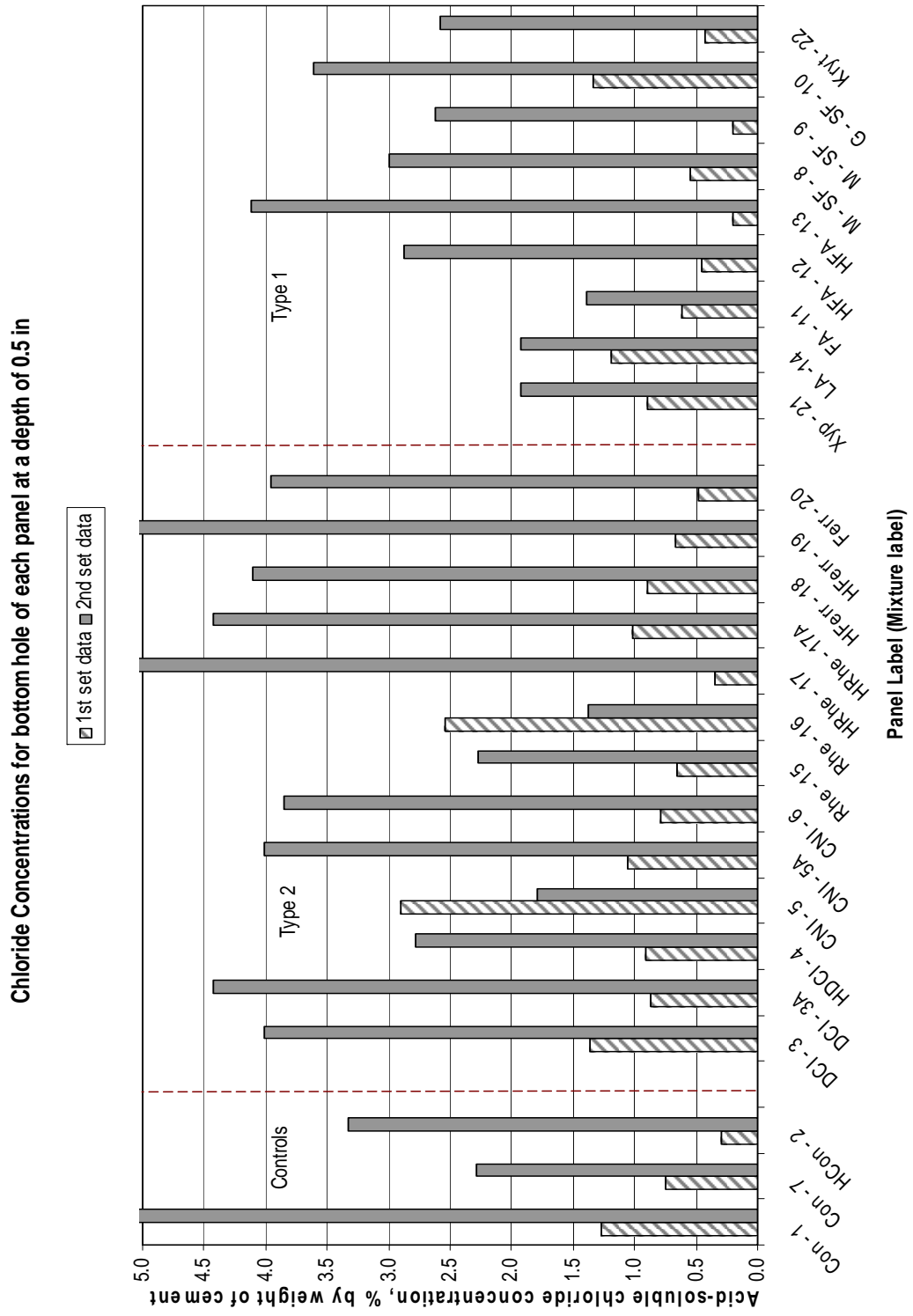


Figure 5-26 Chloride concentrations for bottom hole of all panels at depth of 0.5”

Chloride Concentrations for bottom hole of each panel at a depth of 1 in

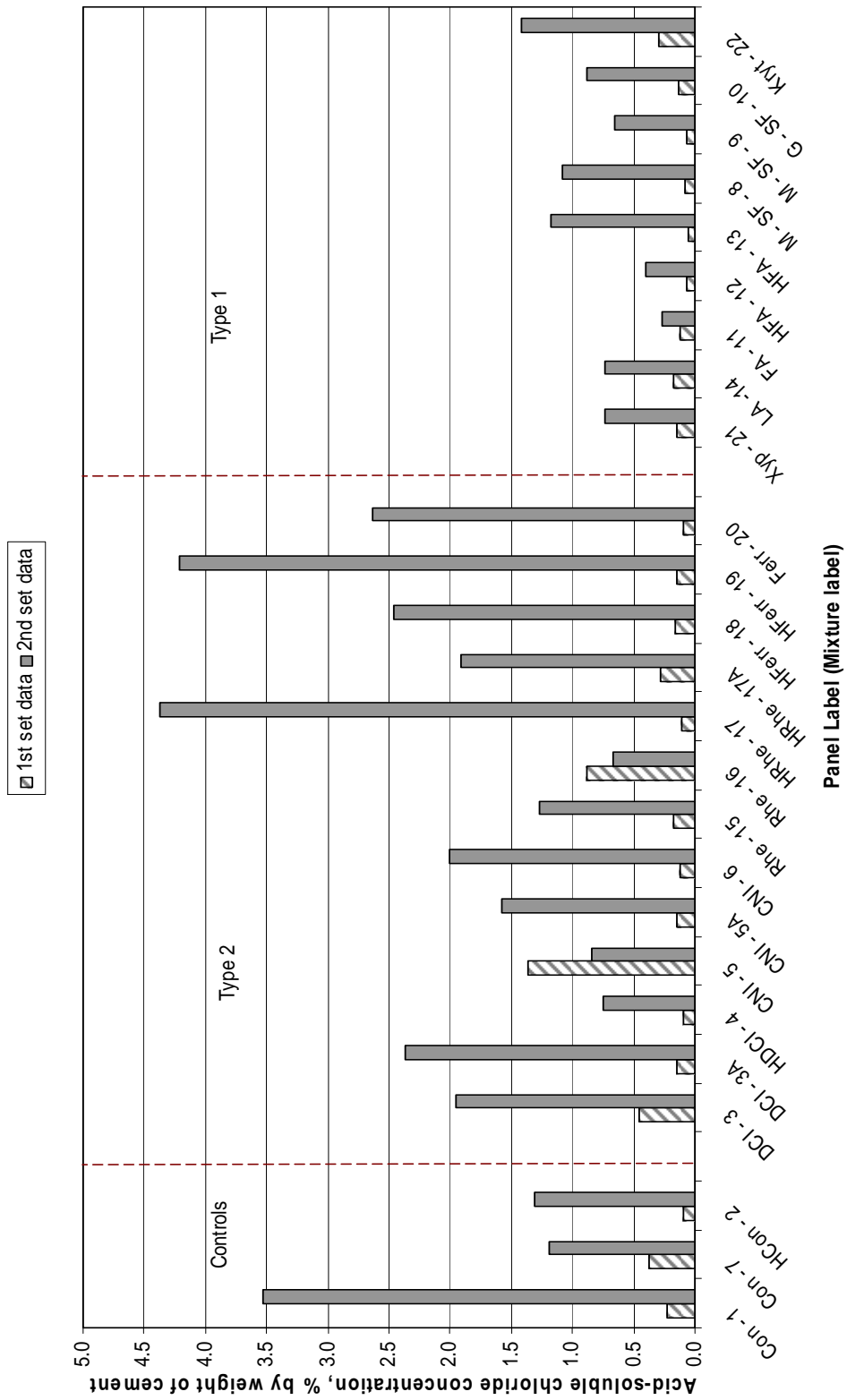


Figure 5-27 Chloride concentrations for bottom hole of all panels at depth of 1”

Chloride Concentrations for bottom hole of each panel at a depth of 1.5 in

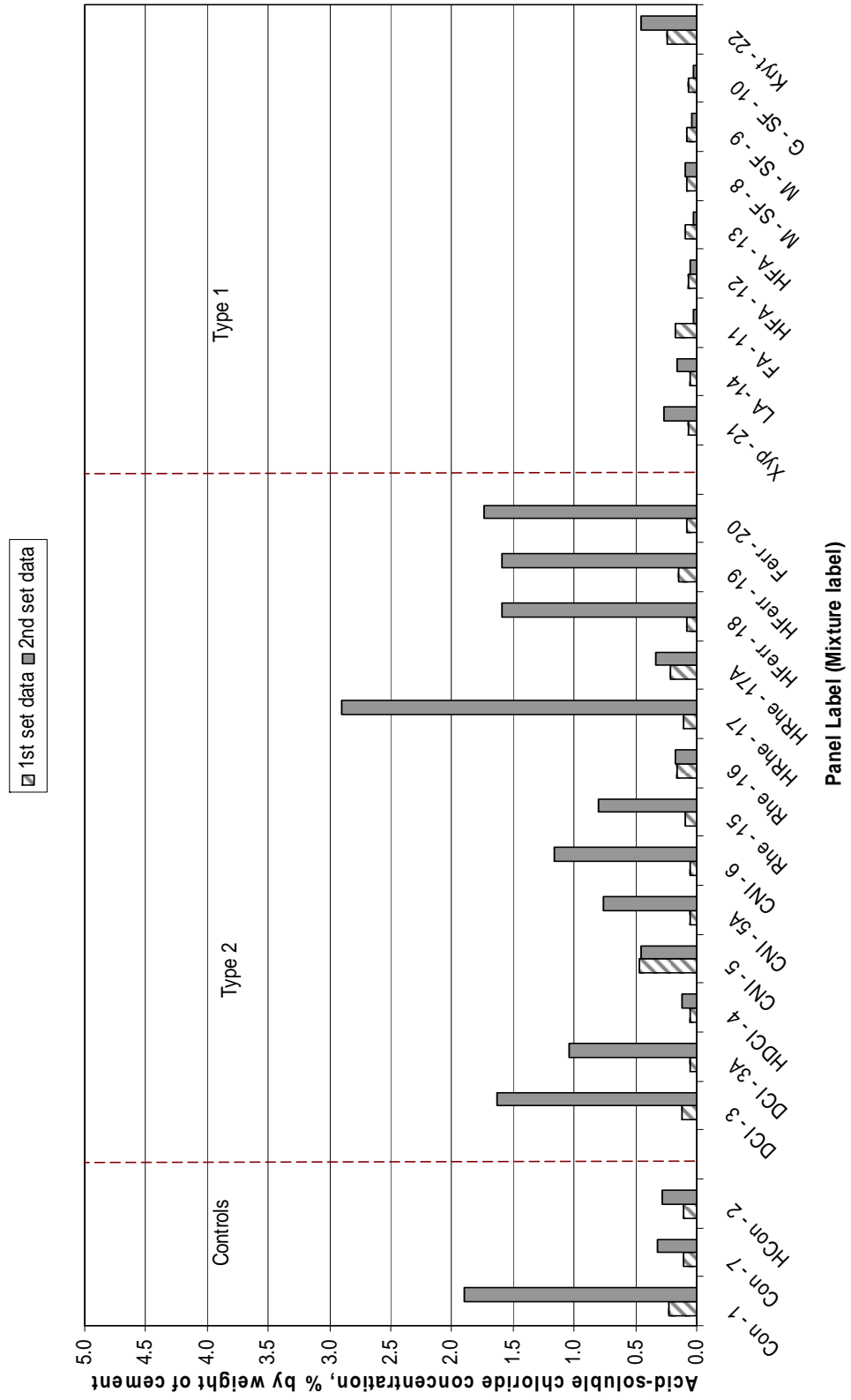


Figure 5-28 Chloride concentrations for bottom hole of all panels at depth of 1.5”

Panels with Type 1 admixtures are expected to have smaller migration speeds of chloride ions. This condition is complicated because the speed of chloride migration is a non-linear variable. Therefore it is difficult to make an accurate comparison. The following section attempts to compare chloride migration speeds based on two sets of chloride concentration readings.

The calculated results for the changes of chloride concentration of bottom holes at depth of 1.0 in. for each panel are shown in Table 5.2. For example, at the depth of 1.0 in. of the bottom hole of panel 1, the chloride concentrations at age of 1.6 years and 3.4 years are 0.222% and 3.534% by weight of cement, respectively. The calculated change of chloride concentration per year is therefore $(3.534-0.222)/(3.4-1.6) = 1.840$ percent by weight of cement per year.

Table 5-2 Change of Chloride Concentration for bottom hole at a depth of 1.0”

% by weight of cement/year

Panel		Chloride concent. % by wt of cement		Time taken	Change of chloride conc./y	average	
		First measure	Second measure				
Kapaa	Con - 1	0.222	3.534	1.8	1.840		
	Con - 7	0.378	1.195	1.7	0.480		
	DCI - 3	0.458	1.949	1.7	0.877		
	DCI - 3A	0.148	2.371	1.9	1.170		
	CNI - 5	1.370	0.848	1.6	-0.326	0.358	
	CNI - 6	0.127	2.003	1.8	1.043		
	CNI - 5A	0.153	1.581	1.9	0.752		
	Rheo - 15	0.174	1.268	1.9	0.576	0.220	
	Rheo - 16	0.887	0.671	1.6	-0.135		
	Ferr - 20	0.095	2.639	1.7	1.496		
	Xyp - 21	0.149	0.731	1.8	0.323		
	LA - 14	0.176	0.742	1.8	0.314		
	FA - 11	0.116	0.261	1.8	0.081		
	SF-Rh - 8	0.082	1.082	1.6	0.625	0.474	
	SF-Rh - 9	0.072	0.654	1.8	0.323		
	SF - 10	0.139	0.881	2.2	0.337		
	Kry - 22	0.300	1.421	2.3	0.487		
	Halawa	HCon - 2	0.087	1.310	1.7	0.719	
		HDCI - 4	0.093	0.749	1.6	0.410	
		HRhe - 17	0.109	4.376	1.8	2.371	1.639
HRhe - 17A		0.279	1.914	1.8	0.908		
HFerr - 18		0.164	2.460	1.7	1.351	1.599	
HFerr - 19		0.148	4.210	2.2	1.847		
HFA - 12		0.072	0.406	1.7	0.197	0.407	
HFA - 13		0.060	1.172	1.8	0.618		

The change of chloride concentration can be used to compare the resistance to chloride penetration for each admixture and aggregate. The bigger the change, the lower resistance to chloride penetration. For comparison, only one number is used for each combination of admixture and aggregate. For example, for the combination of Kapaa aggregate and DCI admixture, panel 3 (DCI-3) is chosen for comparison because it

contains the typical amount of admixture dosage. Some of panels with different labels are actually nominally the same, in which case the average value is used for comparison. The values used for comparison are highlighted in light blue in Table 5.2. Similar calculations were performed for the changes of chloride concentration of bottom holes at depths of 0.5” and 1.5”. These comparisons are shown in Tables 5.3, 5.4, 5.5 and Figures 5.26, 5.27, 5.28. The comparison for the depth of 2.0 in. can not be made because of the absence of the first data.

Table 5-3 Average Change of Chloride Concentration for bottom hole at a depth of 0.5”

% by weight of cement/year

	Con	DCI	CNI	Rheo	Ferr	Xyp	LA	FA	SF	SF-Rh	Kry
Kapaa	2.256	1.550	0.504	0.062	2.049	0.569	0.403	0.429	1.032	1.439	0.934
Halawa	1.785	1.171	-	2.536	2.122	-	-	1.798	-	-	-

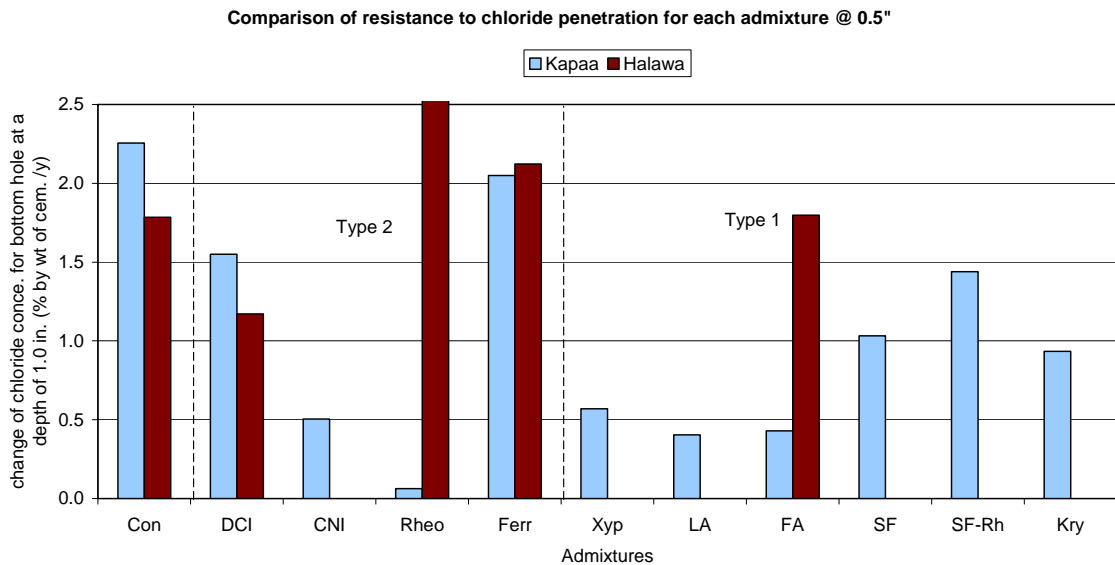


Figure 5-29 Comparison of resistance to chloride penetration for each admixture @ 0.5”

Table 5-4 Average Change of Chloride Concentration for bottom hole at a depth of 1.0”

% by weight of cement/year

	Con	DCI	CNI	Rheo	Ferr	Xyp	LA	FA	SF	SF-Rh	Kry
Kapaa	1.840	1.550	0.504	0.220	1.496	0.323	0.314	0.081	0.337	0.474	0.487
Halawa	0.719	0.410	-	1.639	1.599	-	-	0.407	-	-	-

Comparison of resistance to chloride penetration for each admixture @ 1”

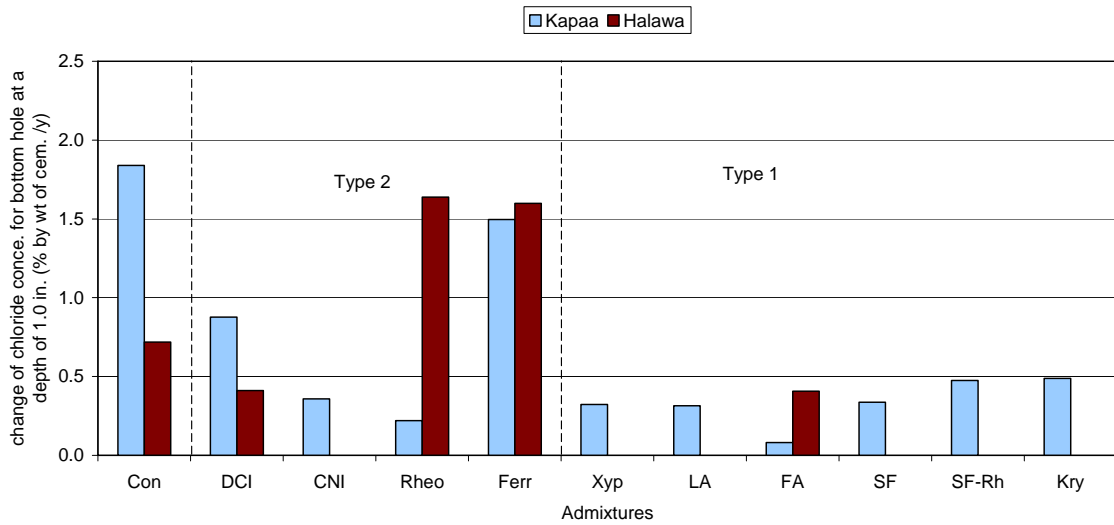


Figure 5-30 Comparison of resistance to chloride penetration for each admixture @1.0”

Table 5-5 Average Change of Chloride Concentration for bottom hole at a depth of 1.5”

% by weight of cement/year

	Con	DCI	CNI	Rheo	Ferr	Xyp	LA	FA	SF	SF-Rh	Kry
Kapaa	0.926	0.886	0.301	0.189	0.981	0.113	0.061	0	0	0	0.096
Halawa	0.103	0.041	-	0.810	0.772	-	-	0	-	-	-

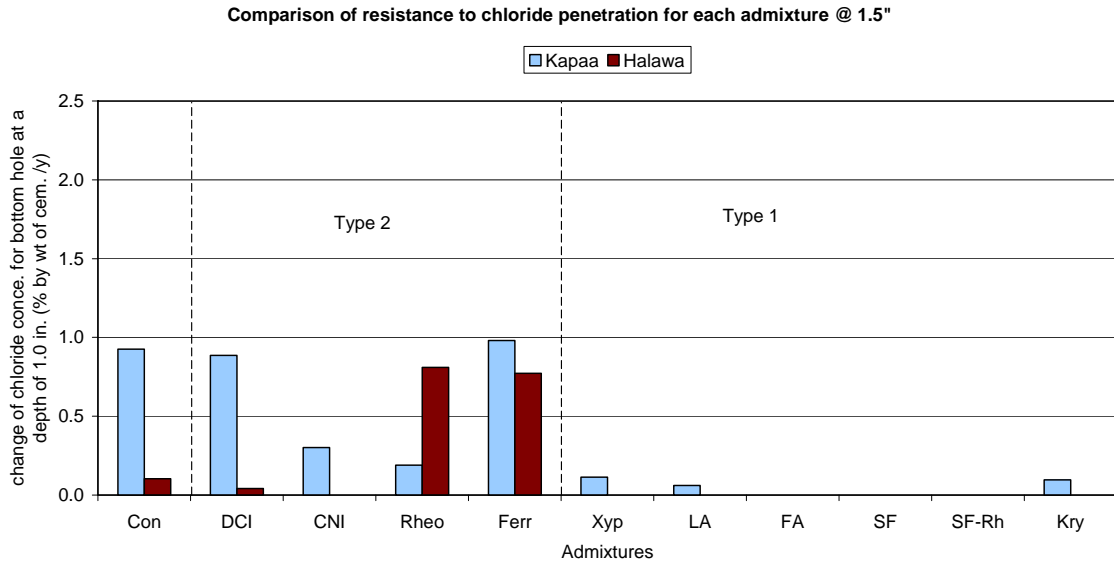


Figure 5-31 Comparison of resistance to chloride penetration for each admixture @1.5"

Previous research on the field and laboratory specimens (Uno et al., 2005, Kakuda et al., 2005) concluded that concretes made using Kapaa aggregates perform better than those using Halawa aggregates. These panels were therefore expected to have smaller changes in chloride concentration. From the above figures, this conclusion holds true for all specimens except the Control and DCI mixtures.

In the above figures, Type 1 and 2 admixtures are separated by a dashed line. Panels with Type 1 admixtures show reduced chloride migration rates through the concrete cover.

5.3 Half-cell potential

The half-cell potential test determines the probability of corrosion occurring in the field panels. The ranges for the probabilities of corrosion using a copper sulfate electrode (CSE) are represented in Table 5.6.

Table 5-6 Corrosion ranges for half-cell potential test results (CSE)

Measured Potential (mV)	Statistical risk of corrosion occurring
< -350	90%
Between -350 and -200	50%
> -200	10%

All the original data in SCE (Saturated Calomel Electrode) was converted into results using a copper sulfate electrode (CSE) by adding 77 mV.

For more accuracy, the second set of half-cell data were taken at 18 locations.

5.3.1 Control mixtures

Half-cell potential measurements for the control panels (Panel 1, 2 and 7) are presented in Figure 5-33 to Figure 5-34. Figure 5-33 shows data taken at 3.4 years as a 3-D plot. It shows how the half-cell potentials distribute across the panel. The 18 columns present the 18 locations where the half-cell potential was taken. Figure 5-34 gives a comparison of the 3.4 years Half-cell readings with the earlier readings (Uno and Robertson 2004). The average value for each row is presented. All other figures in this section have the same meaning.

Panel 1, the Kapaa control panel with 0.40 w/c ration, had a low risk of corrosion occurring at 2 years. At 3.4 years, the risk becomes much higher (Figure 5-34). The top half of panel 1 has a 50% risk of corrosion while the bottom half falls into the 90% probability of corrosion range.

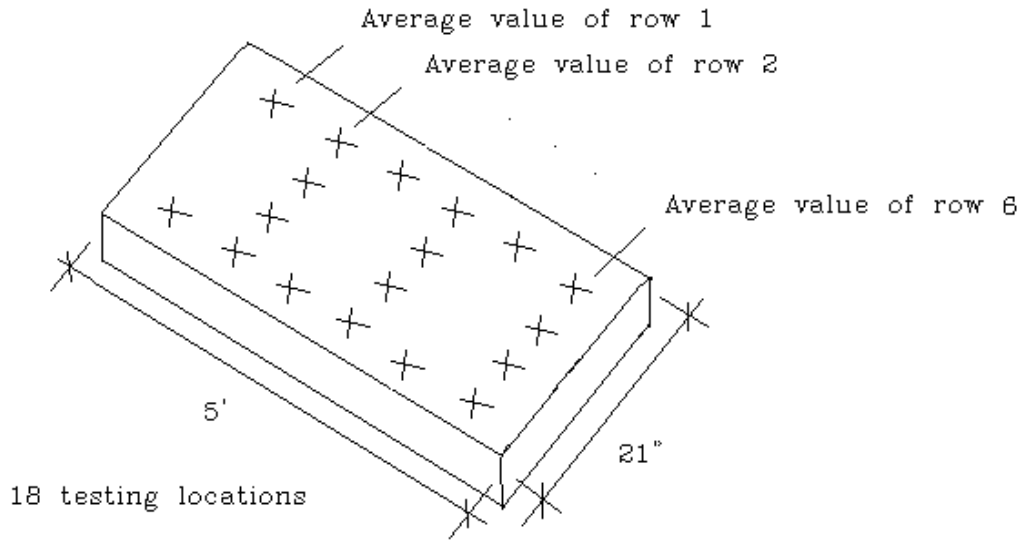


Figure 5-32 Schematic Drawing of the 18 Hall-cell testing locations on the top of each panel

Panel 1 (Con 1): Half-Cell Potentials for each location at the age of 3.4 years

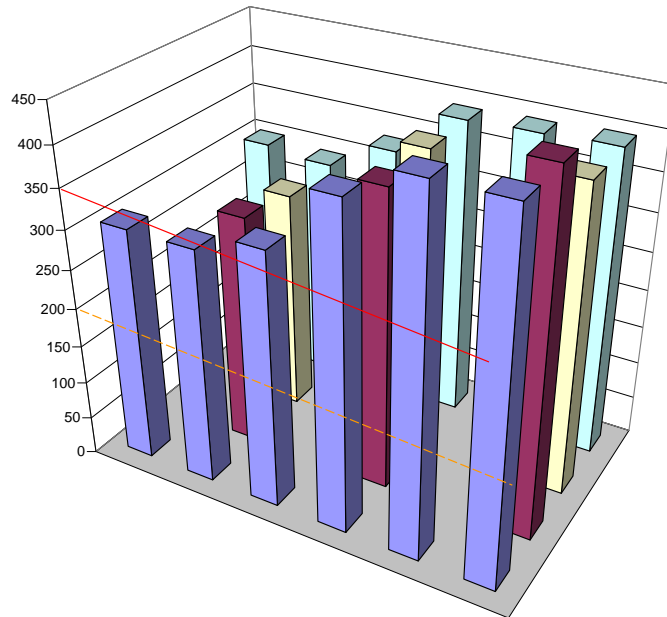


Figure 5-33 3D Presentation for each half cell potential of Panel 1 at the age of 3.4 years

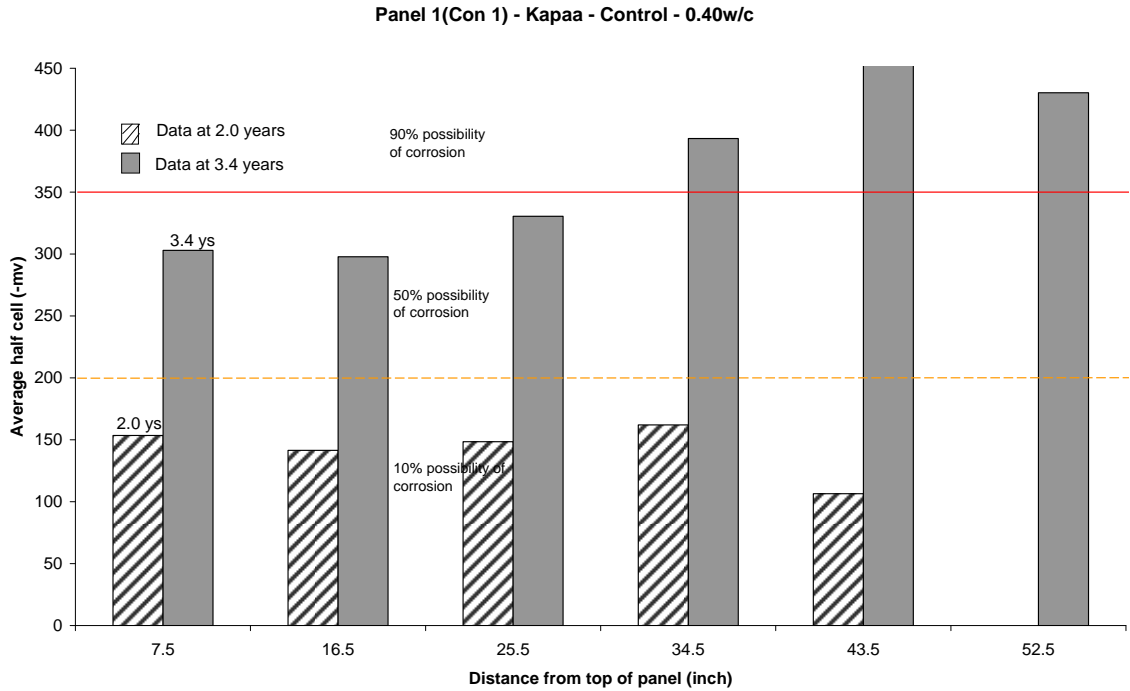


Figure 5-34 Comparison of the average half-cell at the different ages for Panel 1 (Con 1)

Figure 5-35 and Figure 5-36 present the Half-cell data for Panel 7, kapaa control panel with 0.35 w/c ratio. At 3.4 years, the half-cell potentials for Panel 7 all fall into the 10% corrosion probability range, indicating superior performance compared with Panel 1. Panel 7 has a lower water/cement ratio of 0.35 which provides better corrosion resistance compared the 0.40 w/c ratio of Panel 1. The data at the early age test all fall into the 50% probability range, and are larger than for Panel 1. The reason is not clear. It might be due to the measuring errors in the first measurement.

Control 7: Half-Cell Potentials for each location at the age of 3.4 years

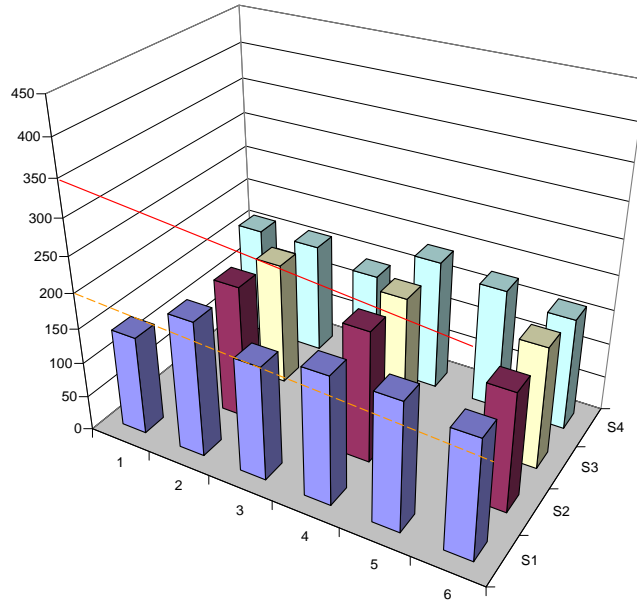


Figure 5-35 3D Presentation for each half cell potential of Panel 7 at the age of 3.4 years

Panel 7(Con 7) - Kapa - Control - 0.35w/c

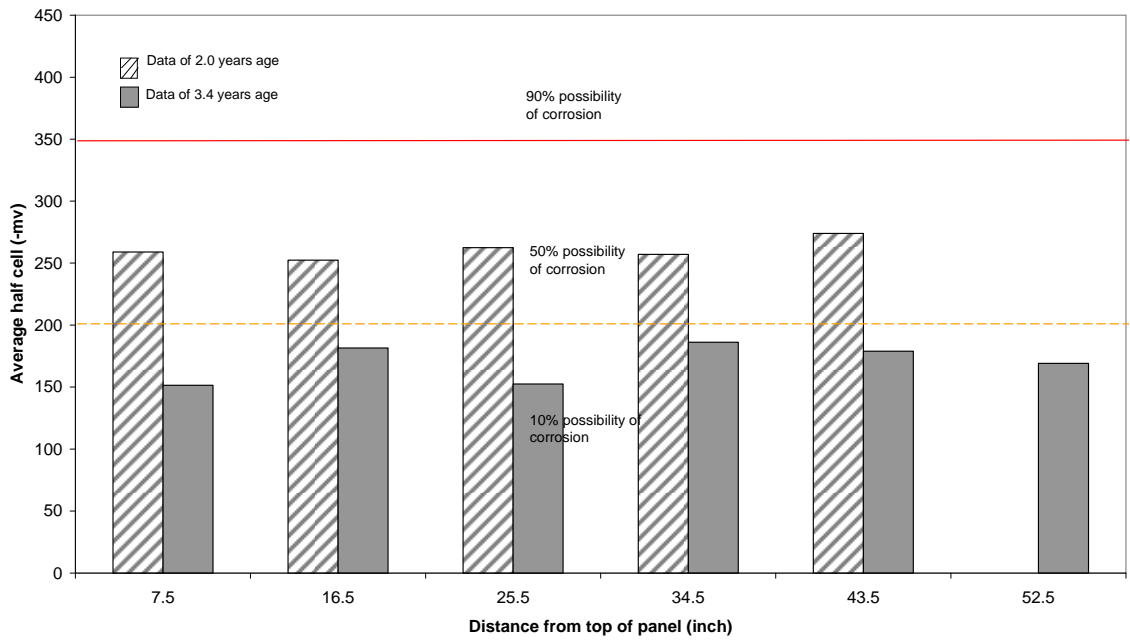


Figure 5-36 Comparison of the average half-cell at the different ages for Panel 7 (Con 7)

Figure 5-37 and Figure 5-38 present Panel 2, the Halawa control panel with 0.40 w/c ratio (HCon2). Compared with Panel 1, the half-cell potentials at 3.5 years for Panel 2 are collectively lower than Panel 1. They increase with distance from the top of the panel, reaching the 90% probability range for the bottom two rows. The superior performance of Panel 2 with Halawa aggregates agrees with the lower chloride concentrations measured in Panel 2 compared with Panel 1 (Figure 5-1 and Figure 5-3).

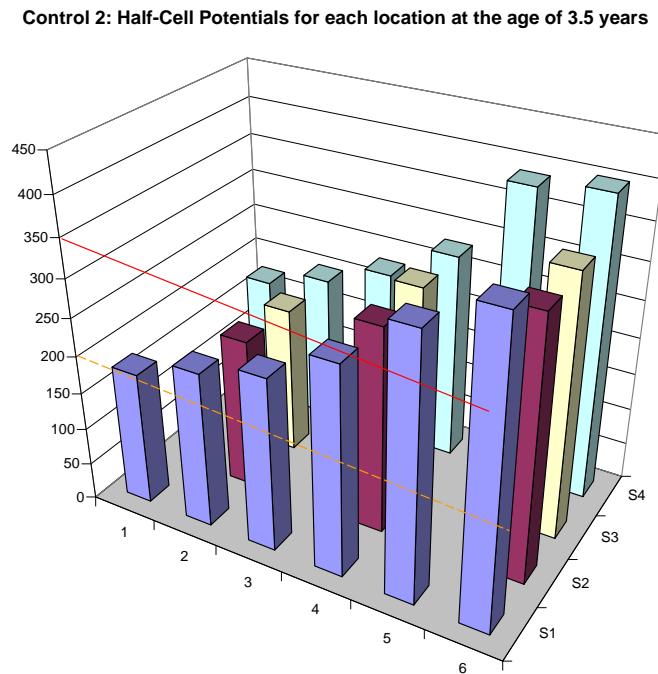


Figure 5-37 3D Presentation for each half cell potential of Panel 2 at the age of 3.4 years

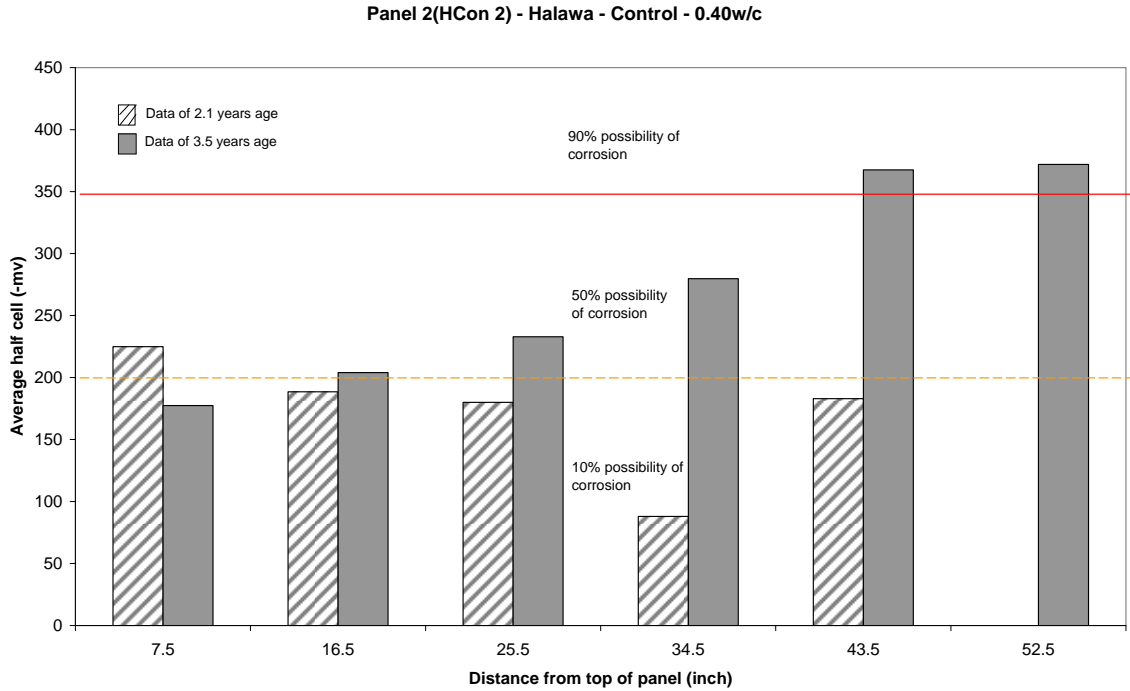


Figure 5-38 Comparison of the average half-cell at the different ages for Panel 2 (HCon 2)

Because the Half-cell readings are fairly consistent across the width of each panel, the 3-D plots for the remaining panels are not shown here but are included in Appendix B.

Only the 2-D plots of the remaining panels are included in the following sections.

5.3.2 DCI mixtures

Figure 5-39 and Figure 5-40 present Panel 3 (DCI 3) and Panel 3A (DCI3A). All readings fall in the 10% probability range. No conclusion can be made as to the DCI dosage since both panels show no signs of corrosion. However, the half-cell readings are significantly lower than from the corresponding control panel without DCI (Con 1).

Panel 3(DCI 3) - Kapa - DCI (2 gals./cu. yd.)

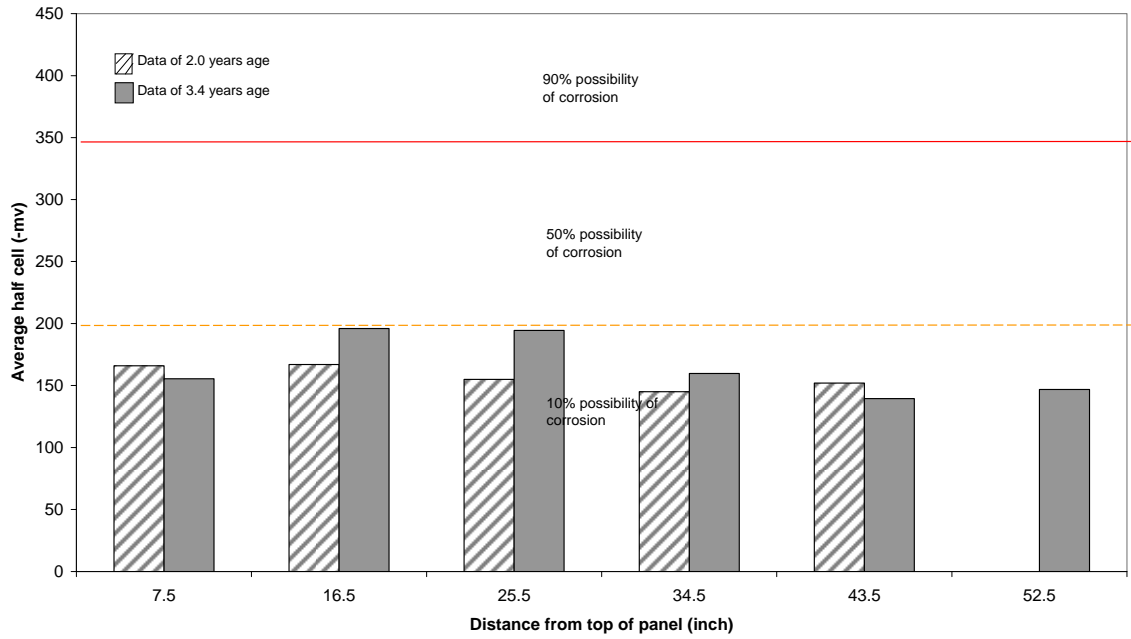


Figure 5-39 Comparison of the average half-cell at the different ages for Panel 3 (DCI3)

Panel 3A(DCI 3A) - Kapaa - DCI (4 gals./cu. yd.)

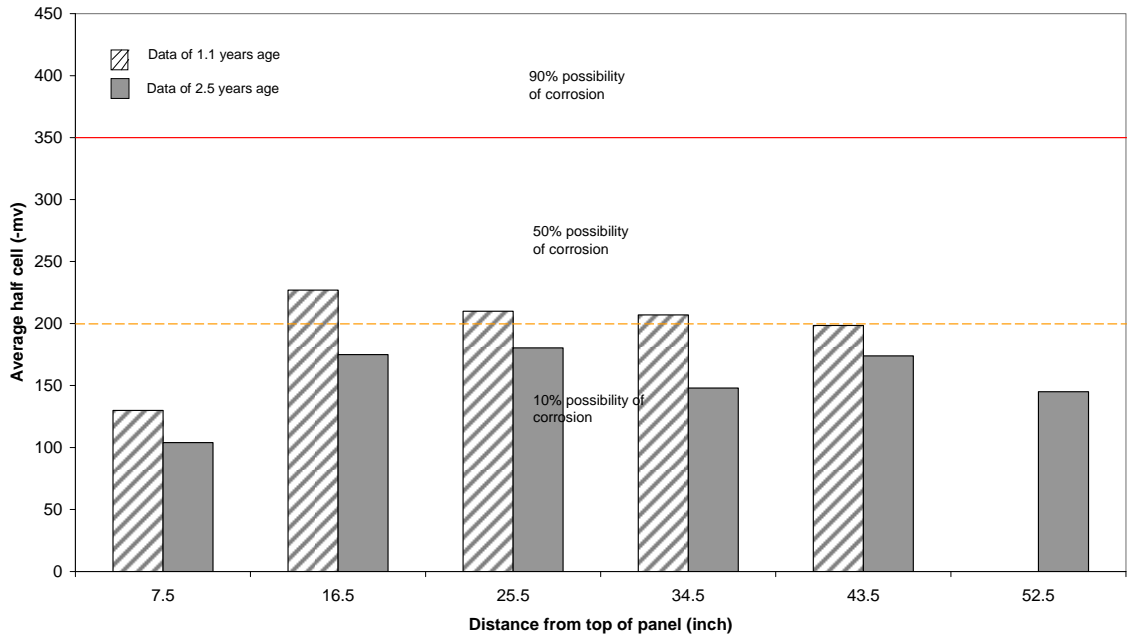


Figure 5-40 Comparison of the average half-cell at the different ages for Panel 3A (DCI3A)

Figure 5-41 presents half-cell readings for Panel 4 (HDCI 4). When compared with the corresponding control panel (HCon2, Figure 5-38), the half-cell readings are very similar, indicating that the low DCI dosage of 2 gal/cu. yd may not be effective at preventing corrosion.

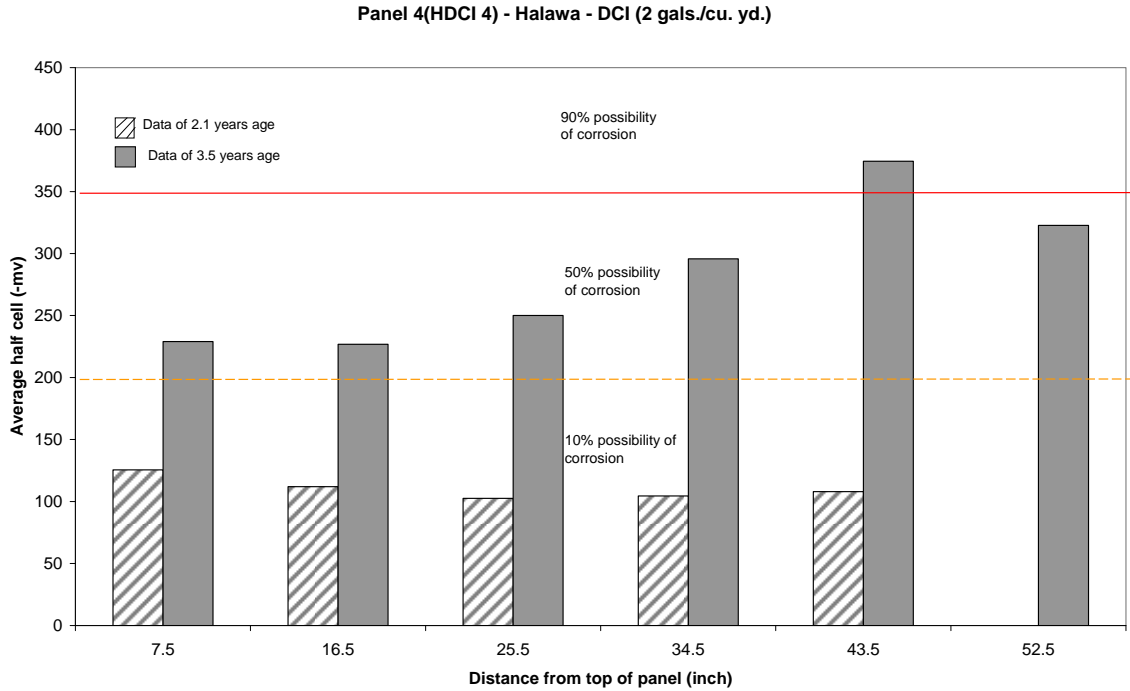


Figure 5-41 Comparison of the average half-cell at the different ages for Panel 4 (HDCI4)

5.3.3 CNI admixtures

Figure 5-42 and Figure 5-43 show half-cell readings for two nominally identical panels (Panel 5 and Panel 6) with kapaa aggregates and 2 gal/ cu. yd CNI admixture. It is not known why the half-cell readings for Panel 5 are significantly higher, however it appears that the 2 gal/cu. yd dosage does not reduce the probability of corrosion when compared with the corresponding control panel (Con 1, Figure 5-34).

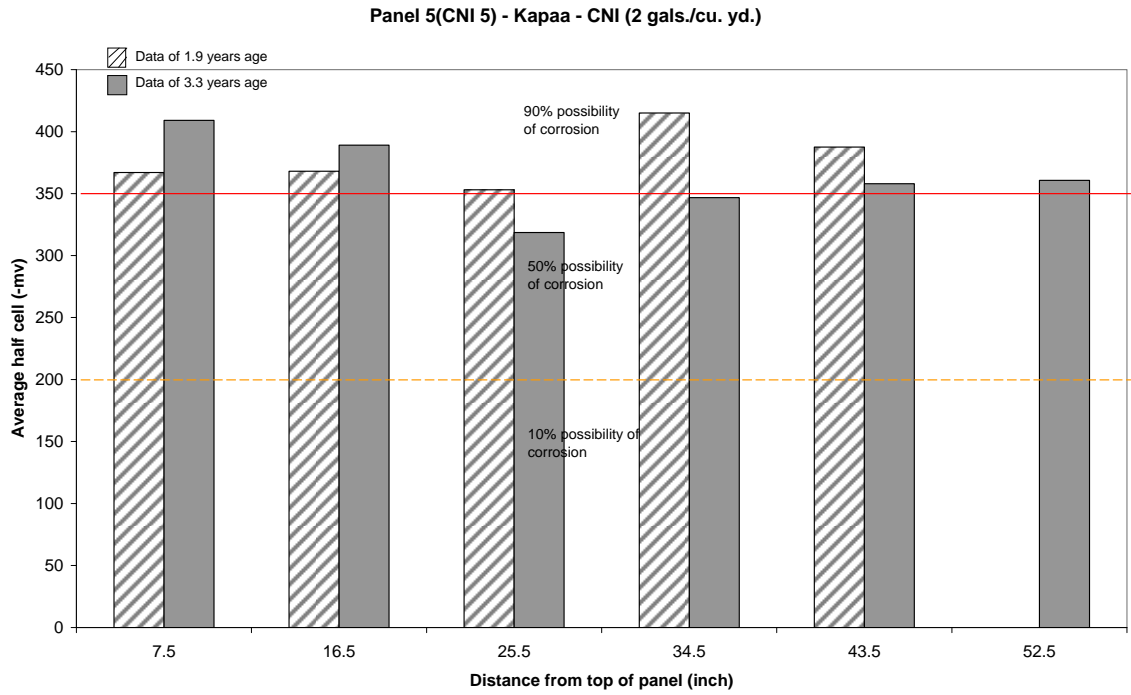


Figure 5-42 Comparison of the average half-cell at the different ages for Panel 5 (CNI5)

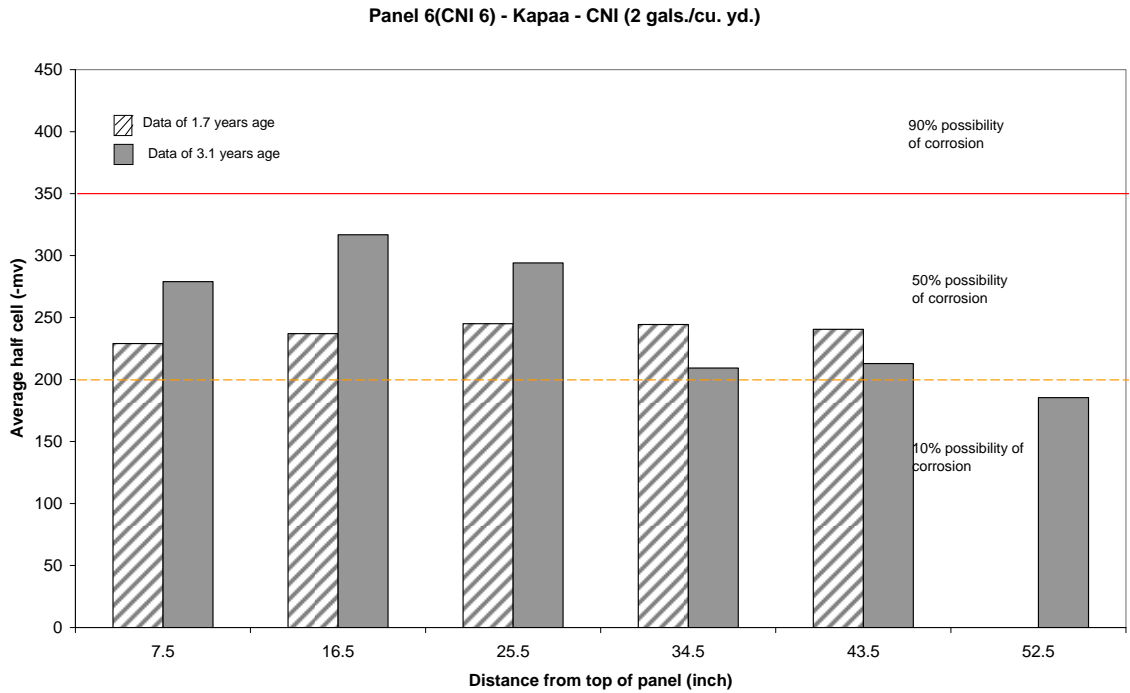


Figure 5-43 Comparison of the average half-cell at the different ages for Panel 6 (CNI6)

Figure 5-44 shows the half-cell readings for Panel 5A (CNI 5A) with 4 gal/cu. yd of CNI. As with the DCI admixture, there is now a significant reduction in corrosion probability compared with the corresponding control panel (Con 1) and the 2 gal/cu. yd panels (CNI 5 and CNI 6).

Panel 5A(CNI 5A) - Kapaa - CNI (4 gals./cu. yd.)

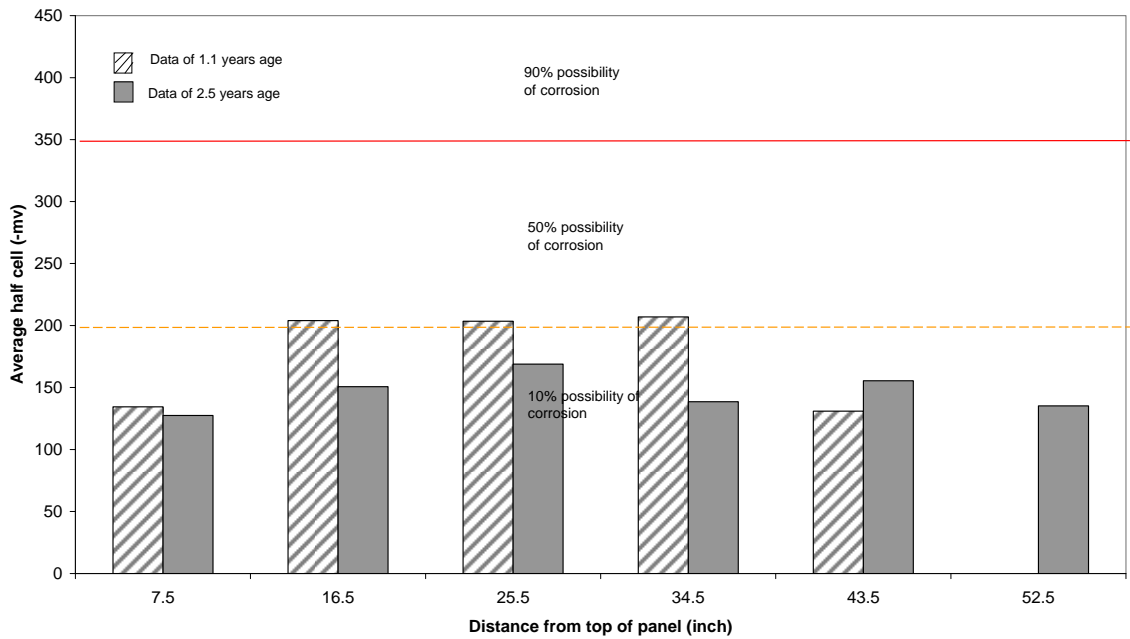


Figure 5-44 Comparison of the average half-cell at the different ages for Panel 5A (CNI5A)

5.3.4 Rheocrete 222+ admixtures

Panels 15 and 16 were nominally the same design but the results are significantly different (Figure 5-45 and Figure 5-46). The same behavior was noted for panels 17 and 17A (Figure 5-47 and Figure 5-48), nominally the same as Panel 15 and 16, but using halawa aggregates.

Panel 17 showed unexpectedly low concrete compressive strength of 1576 psi (Uno, Robertson 2005). Therefore the second panel (17A) was constructed to replace Panel 17, which had a compressive strength of 2010 psi. Similarly, Panel 16 had a compressive strength of 3148 psi, which is much lower than that of Panel 15 with 4218 psi compressive strength. The performance of Panel 15 and 17A (Figure 5-45 and Figure 5-48) indicate that Rheocrete 222+ can be effective at reducing corrosion compared with

corresponding control panels, however care must be taken during concrete mixing and panel fabrication.

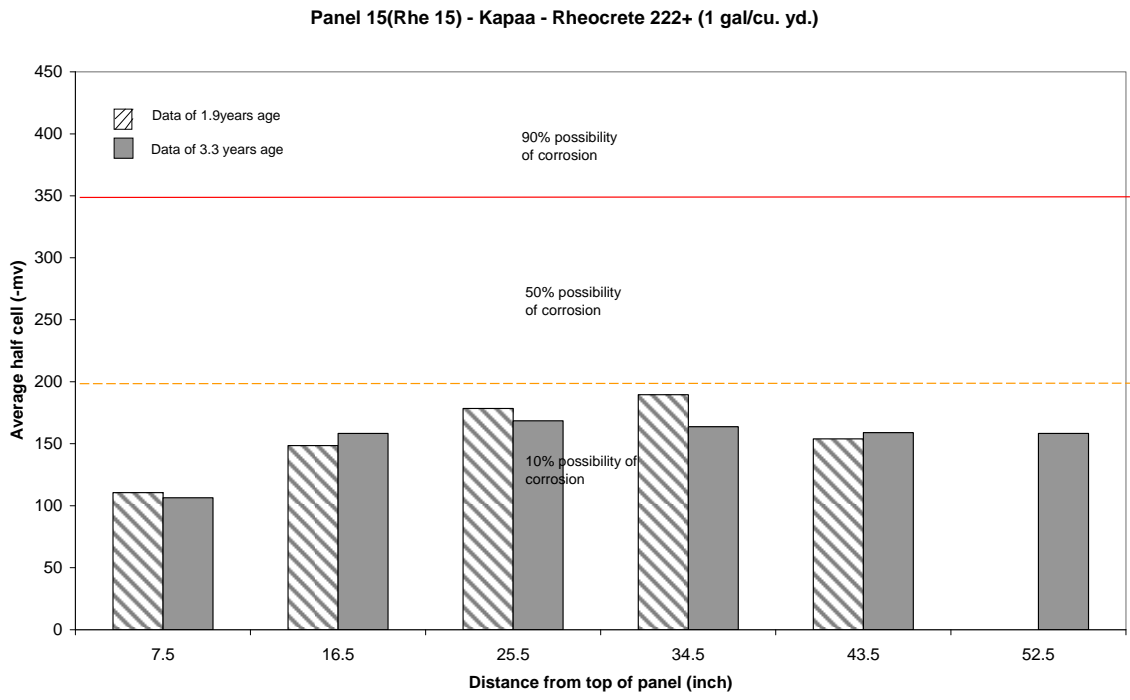


Figure 5-45 Comparison of the average half-cell at the different ages for Panel 15 (Rhe 15)

Panel 16(Rhe 16) - Kapaa - Rheocrete 222+ (1 gal/cu. yd.)

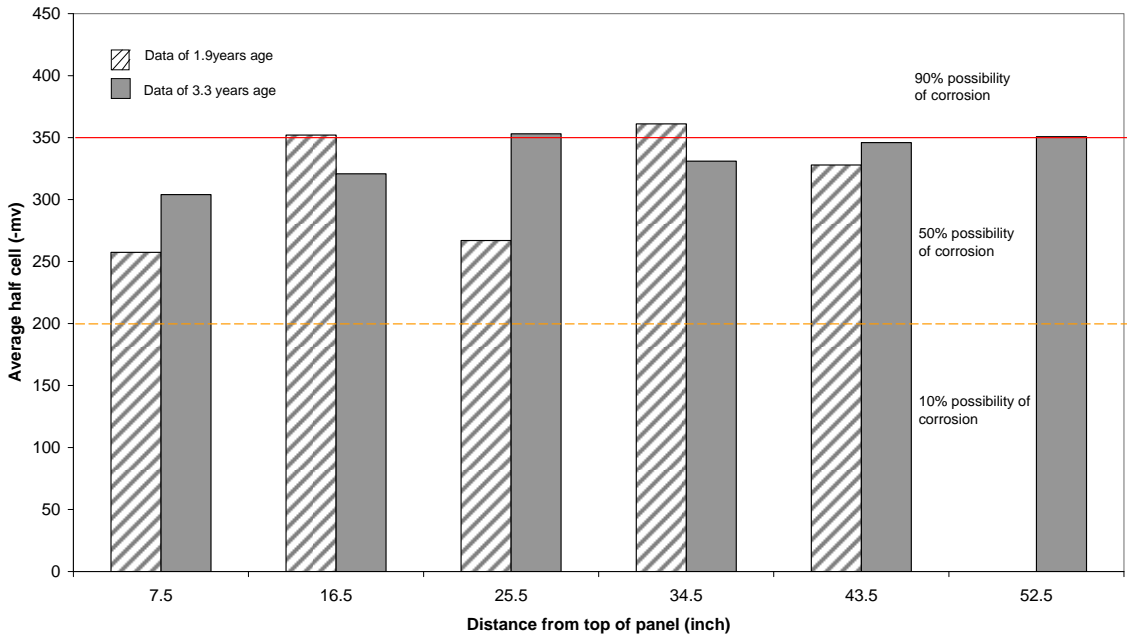


Figure 5-46 Comparison of the average half-cell at the different ages for Panel 16 (Rhe 16)

Panel 17(HRhe 17) - Halawa - Rheocrete 222+ (1 gal/cu. yd.)

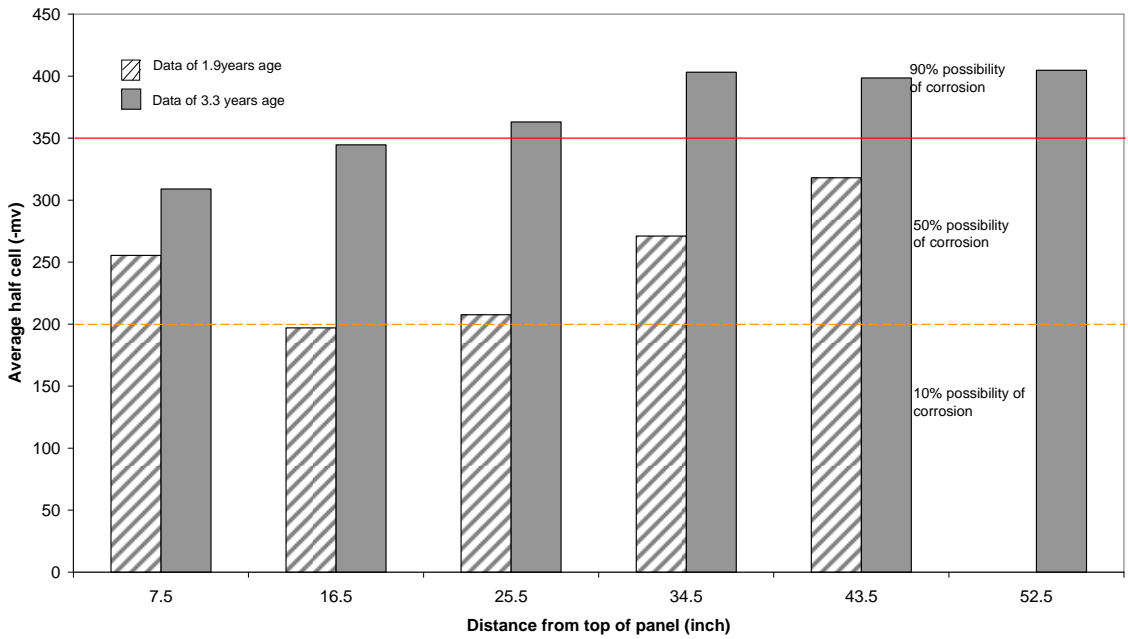


Figure 5-47 Comparison of the average half-cell at the different ages for Panel 17 (Rhe 17)

Panel 17A(HRhe 17A) - Halawa - Rheocrete 222+ (1 gal/cu. yd.)

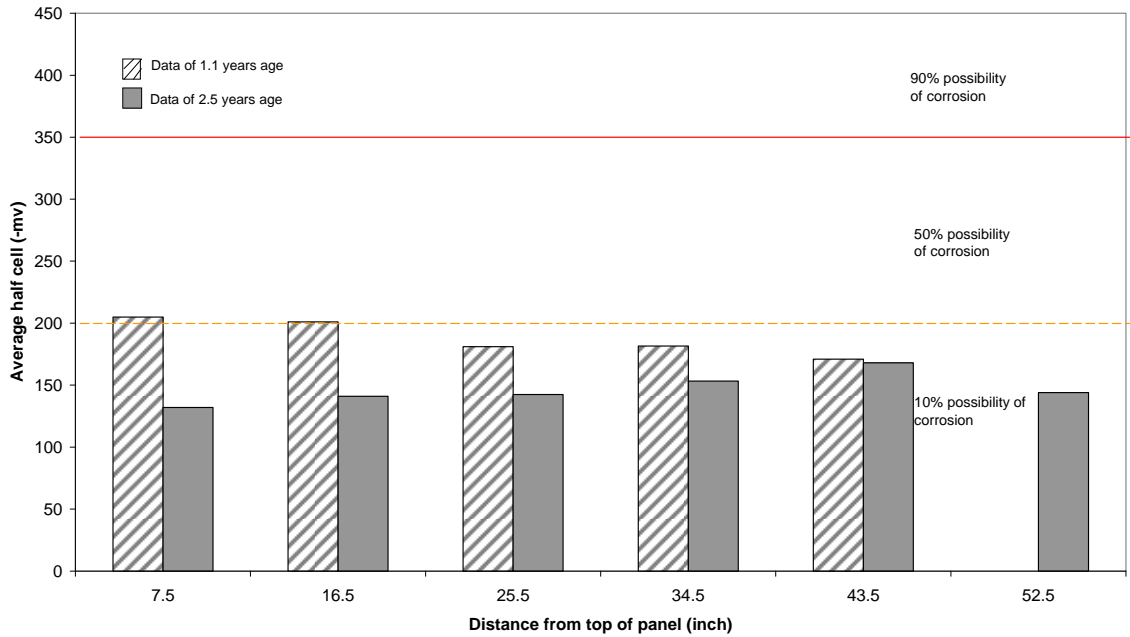


Figure 5-48 Comparison of the average half-cell at the different ages for Panel 17A (Rhe 17A)

5.3.5 FerroGard 901 admixtures

Half-cell readings for the three panels with FerroGard 901 (Panel 18, 19 and 20) are shown in Figure 5-49 to Figure 5-51. None of these readings exceed the -350mv level, showing improved performance compared with the corresponding control panels. The half-cell readings at the earlier age for Panel 20 were not included here since there was some error during the measurement.

Panel 18(HFer 18) - Halawa - FerroGard 901 (3 gals/cu. yd.)

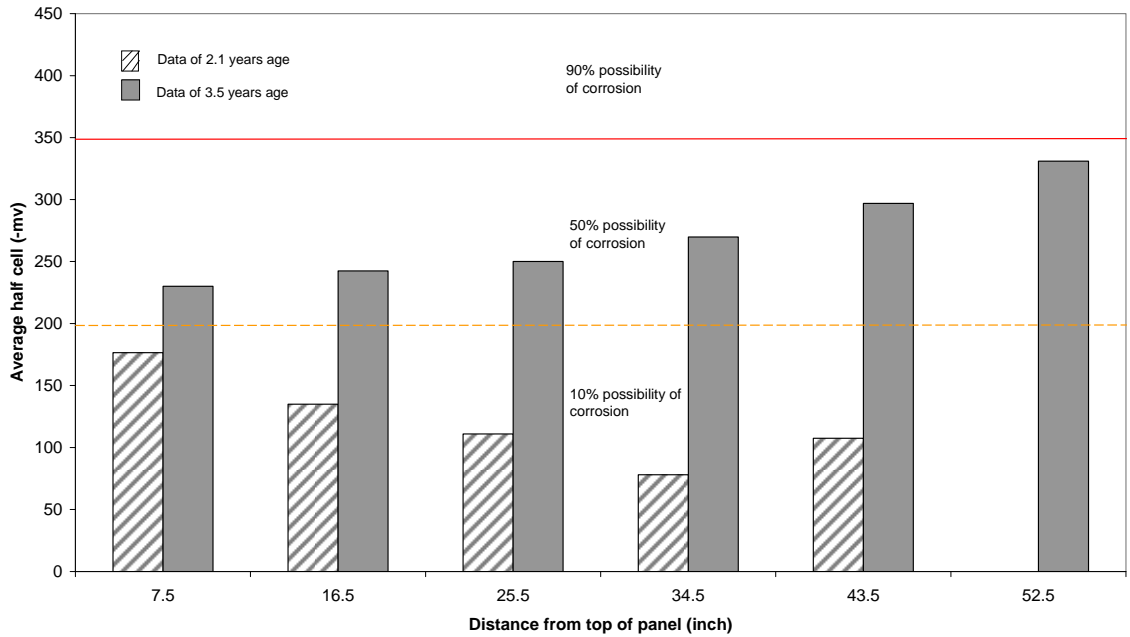


Figure 5-49 Comparison of the average half-cell at the different ages for Panel 18 (HFer 18)

Panel 19(HFer 19) - Halawa - FerroGard 901 (3 gals/cu. yd.)

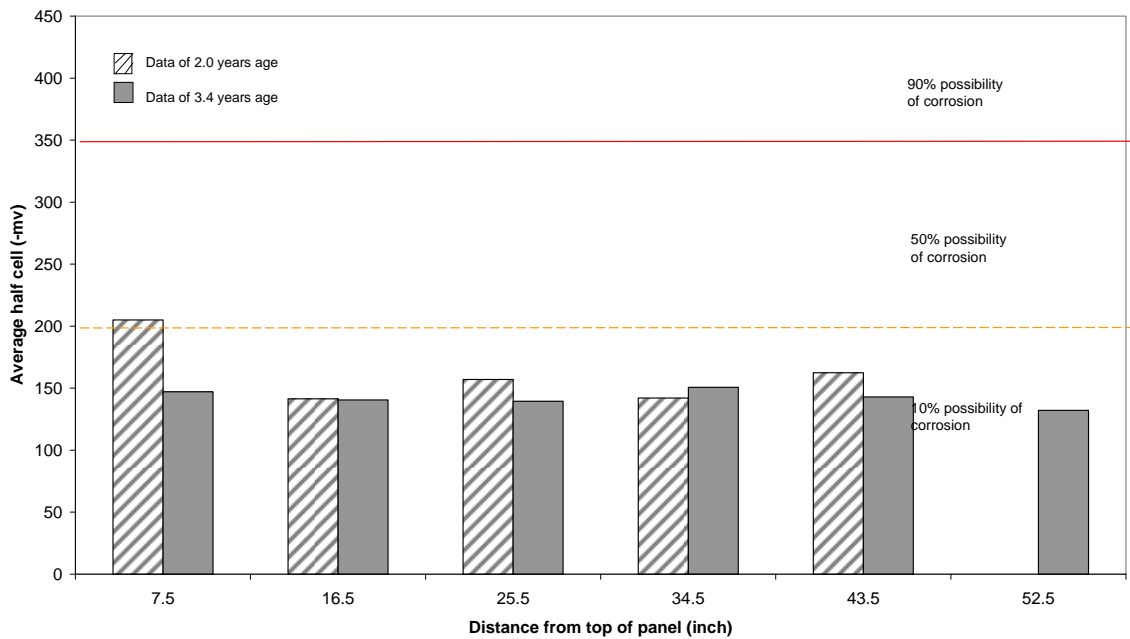


Figure 5-50 Comparison of the average half-cell at the different ages for Panel 19 (HFer 19)

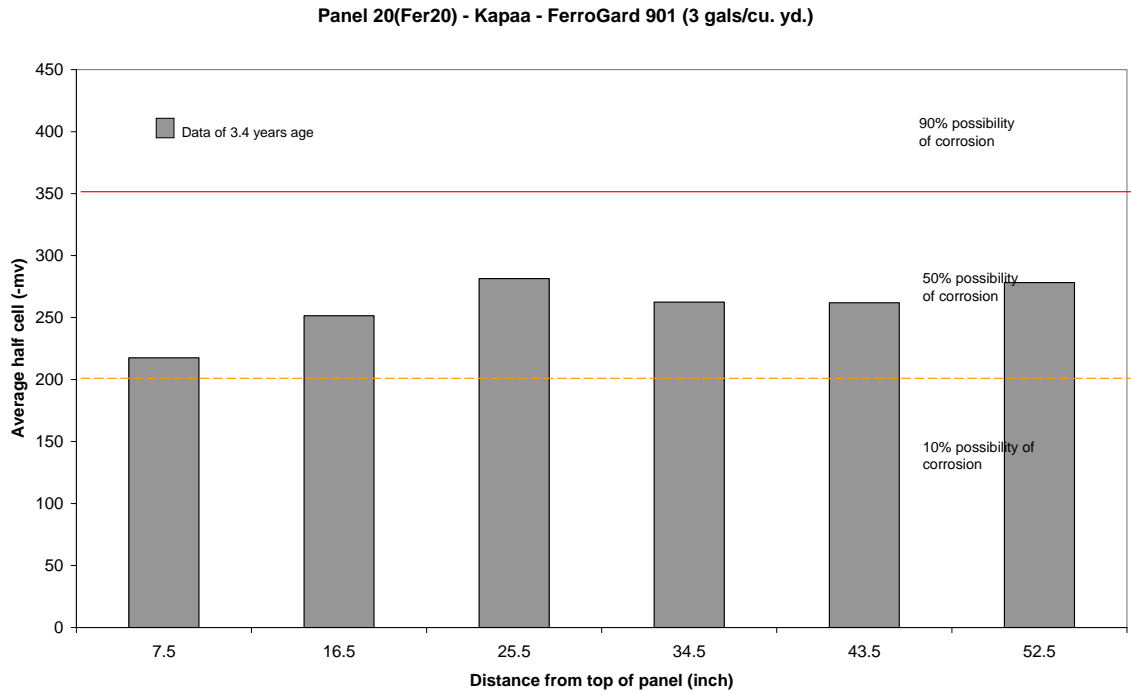


Figure 5-51 Half-cell at 3.4 years for Panel 20 (Fer 20)

5.3.6 Xypex admixtures

Figure 5-52 shows the half-cell readings for Panel 21 with Xypex admixture. The chloride concentrations in this panel are lower than for the control specimens (Figure 5-26 to Figure 5-28), however, the half-cell readings are nearing the -350 mv level, similar to the corresponding control panel (Con 1, Figure 5-34).

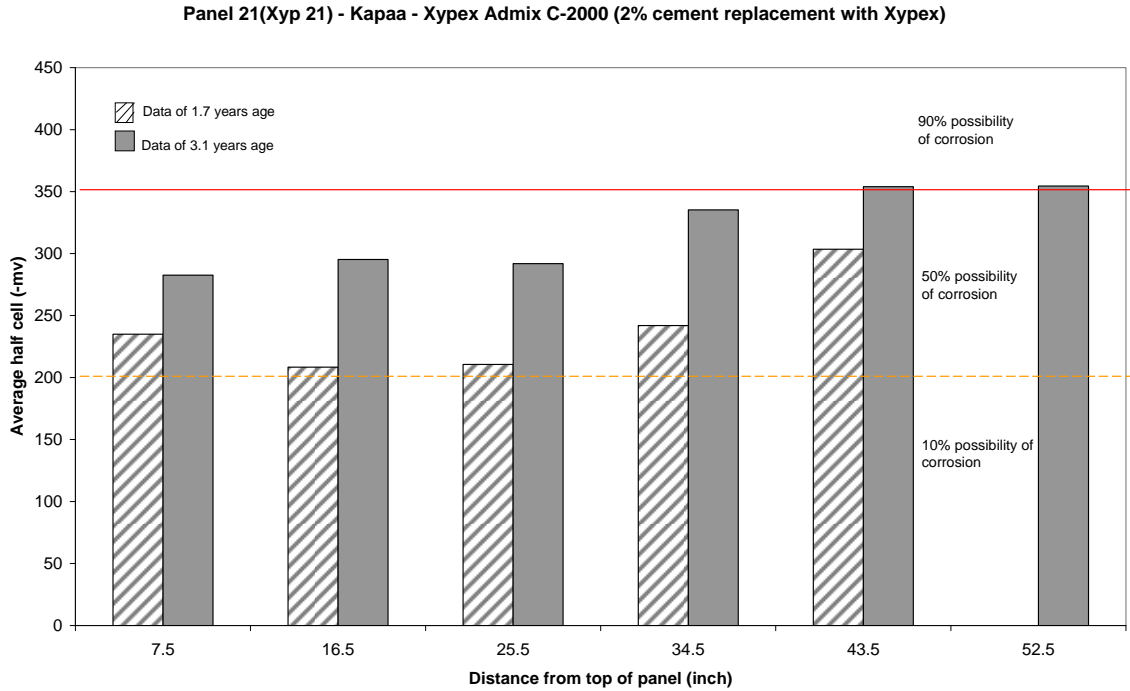


Figure 5-52 Comparison of the average half-cell at the different ages for Panel 21 (Xyp 21)

5.3.7 Latex admixtures

The half-cell readings for Panel 14 with Latex admixture was shown in Figure 5-53. The chloride concentrations in this panel are lower than for the control panel (Figure 5-26 to Figure 5-28). The half-cell readings are all in the 10% probability range, which is a significant improvement over the control panel (Con 7, Figure 5-36).

Panel 14(LA 14) - Kapa - 0.35 w/c - Latex (5% cement replacement with LA)

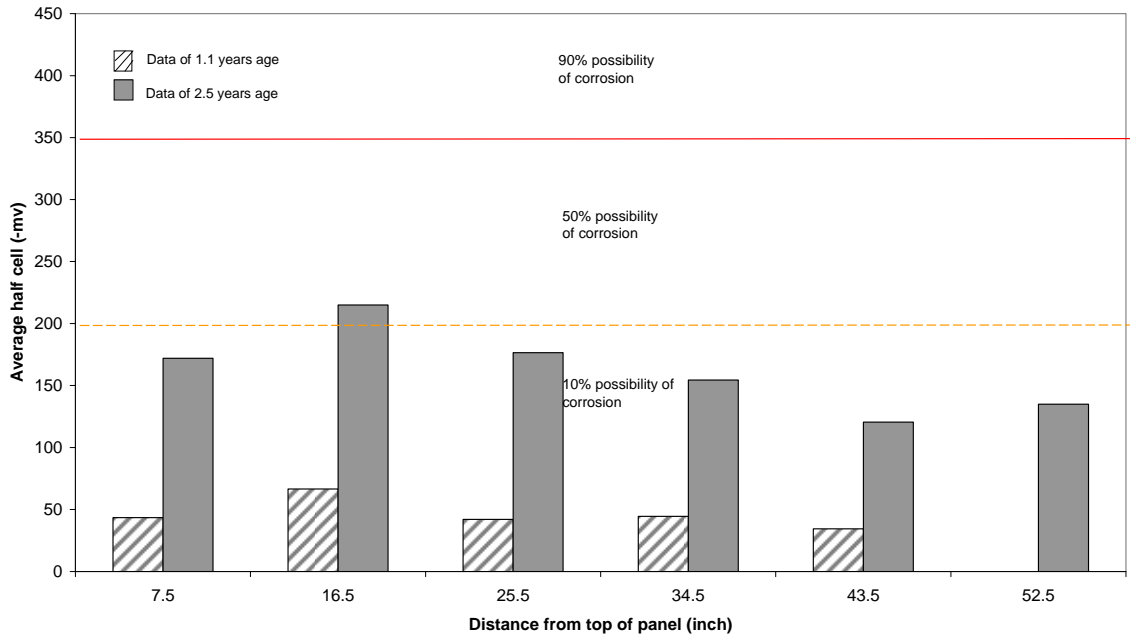


Figure 5-53 Comparison of the average half-cell at the different ages for Panel 14 (LA 14)

5.3.8 Fly Ash admixtures

Figure 5-54 to Figure 5-56 show the half-cell readings for Panel 11, 12 and 13 with 15% cement replacement using Fly Ash. All readings are in the 10% or 50% probability range. This is a significant improvement over the corresponding control panels.

Panel 11(FA 11) - Kapa'a - Fly Ash (15% cement replacement with FA)

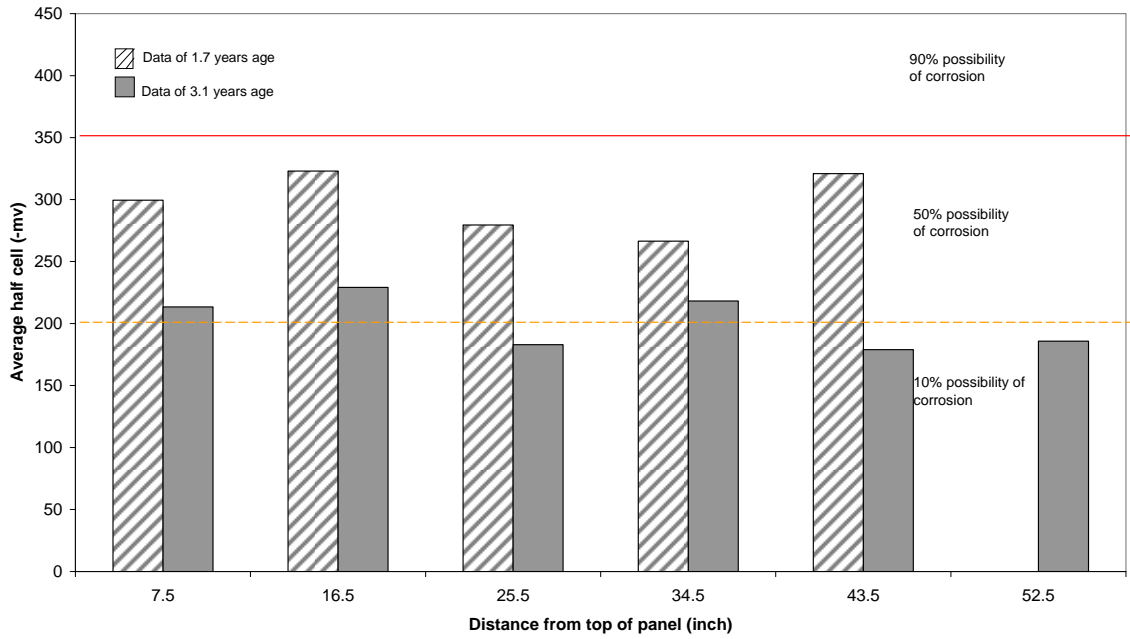


Figure 5-54 Comparison of the average half-cell at the different ages for Panel 11 (FA11)

Panel 12(HFA 12) - Halawa - Fly Ash (15% cement replacement with FA)

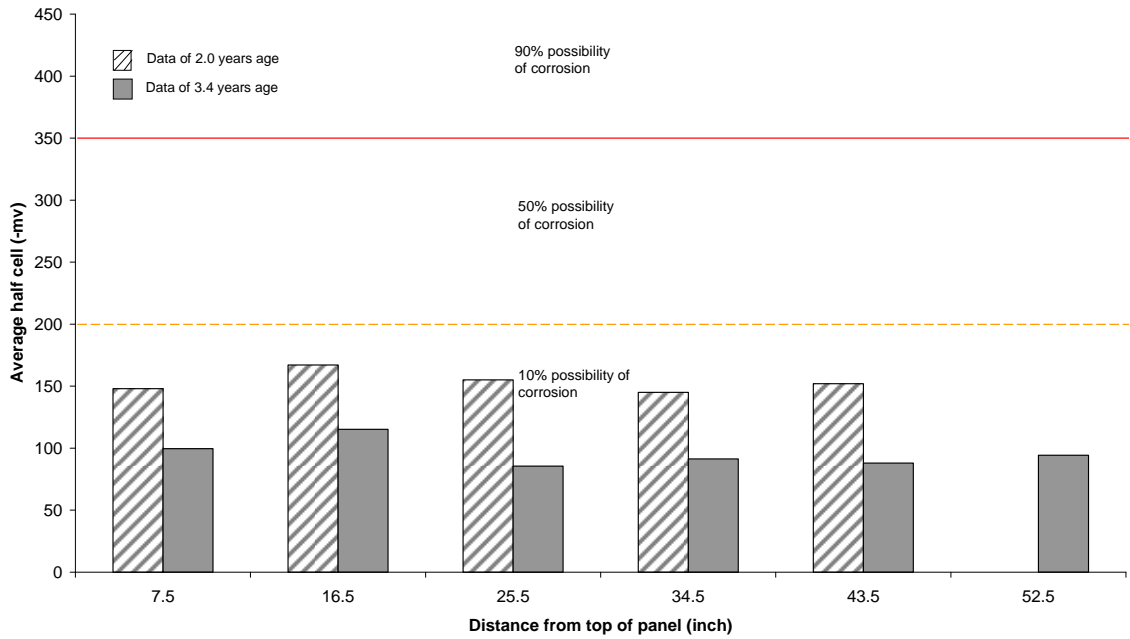


Figure 5-55 Comparison of the average half-cell at the different ages for Panel 12 (HFA12)

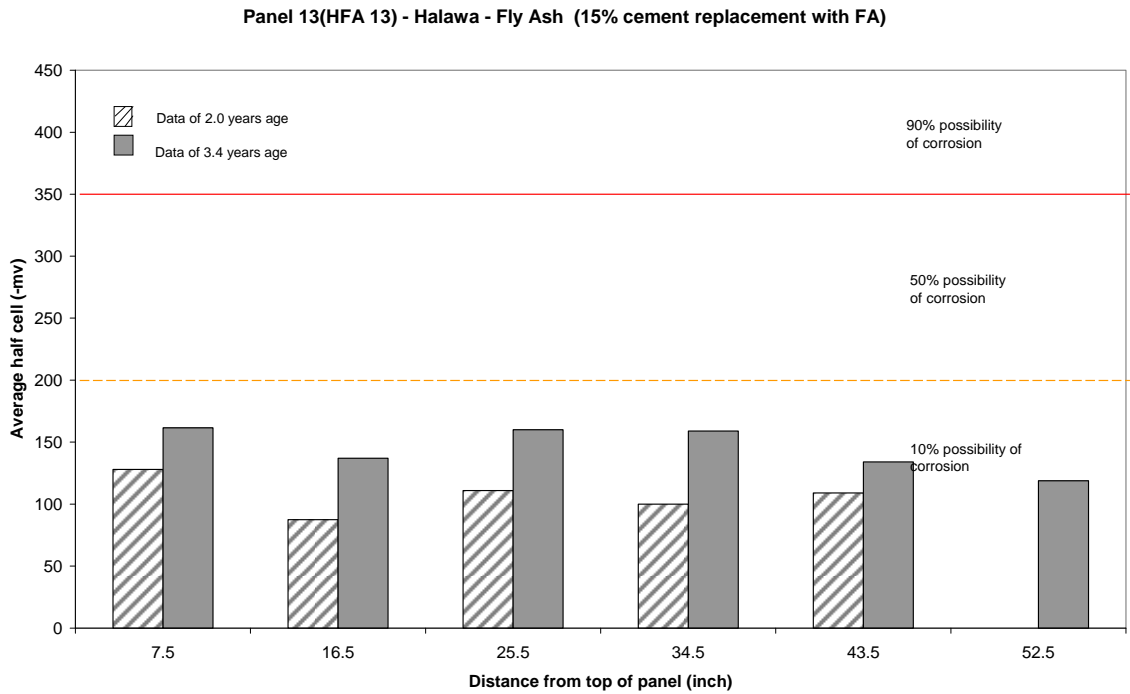


Figure 5-56 Comparison of the average half-cell at the different ages for Panel 13 (HFA 13)

5.3.9 Silica Fume admixtures

Figure 5-57 and Figure 5-58 show half-cell readings for Panel 8 and 9 using 5% cement replacement by Master Builder silica fume (Rheomac SF100). The 3.4 years readings are at the -200mv level. Figure 5-59 shows results for Panel 10 with 5% cement replacement by W.R. Grace silica fume (Force 10,000D). The readings are all in the 10% probability range. All SF panels perform significantly better than the corresponding control panels.

Panel 8(SF-Rh 8) - Kapaa - Rheomac SF100/M.B. (5% cement replacement with SF)

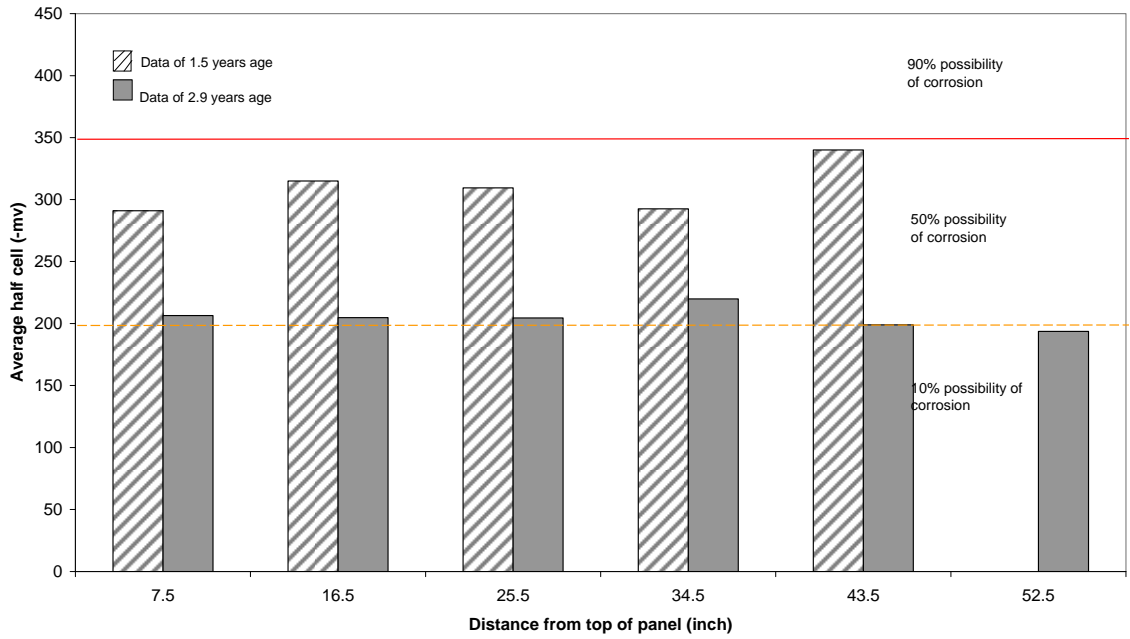


Figure 5-57 Comparison of the average half-cell at the different ages for Panel 8 (SF-Rh8)

Panel 9(SF-Rh 9) - Kapaa - Rheomac SF100/M.B. (5% cement replacement with SF)

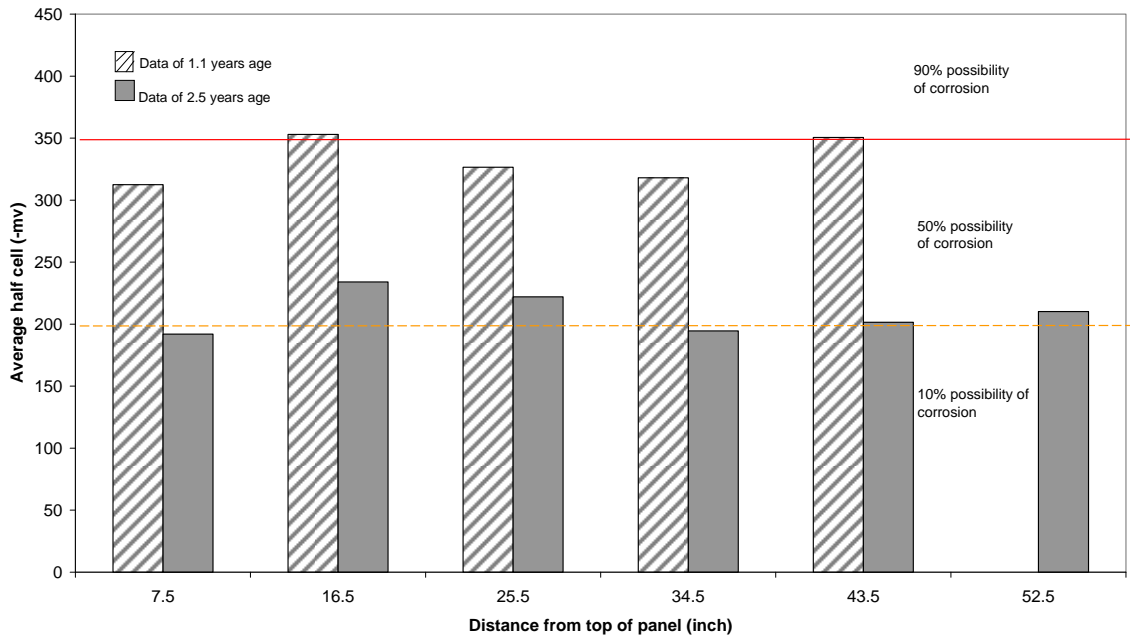


Figure 5-58 Comparison of the average half-cell at the different ages for Panel 9 (SF-Rh9)

Panel 10(SF 10) - Kapaa - Force 10,000D SF/W.R.Grace (5% cement replacement with SF)

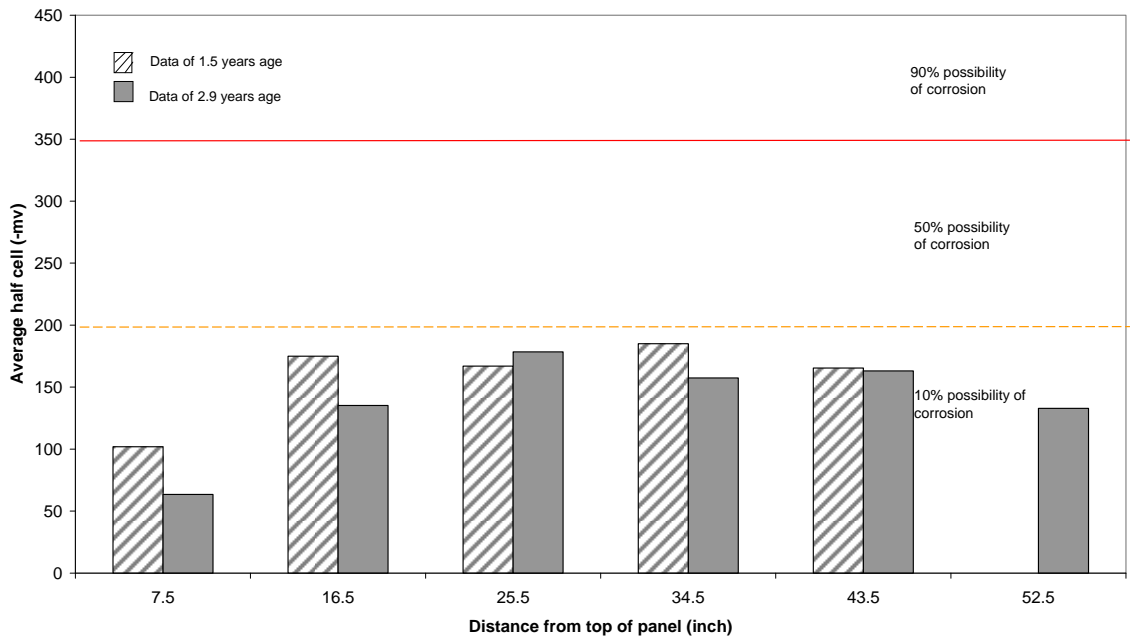


Figure 5-59 Comparison of the average half-cell at the different ages for Panel 10 (SF10)

5.3.10 Kryton admixtures

Figure 5-60 shows the half-cell readings for Panel 22 with Kryton admixture. It performs better than the corresponding control panel (Con 1, Figure 5-34).

Panel 22(Kry 22) - Kapaa - 0.40 w/c - Kryton KIM (13.5 lbs/cu. yd.)

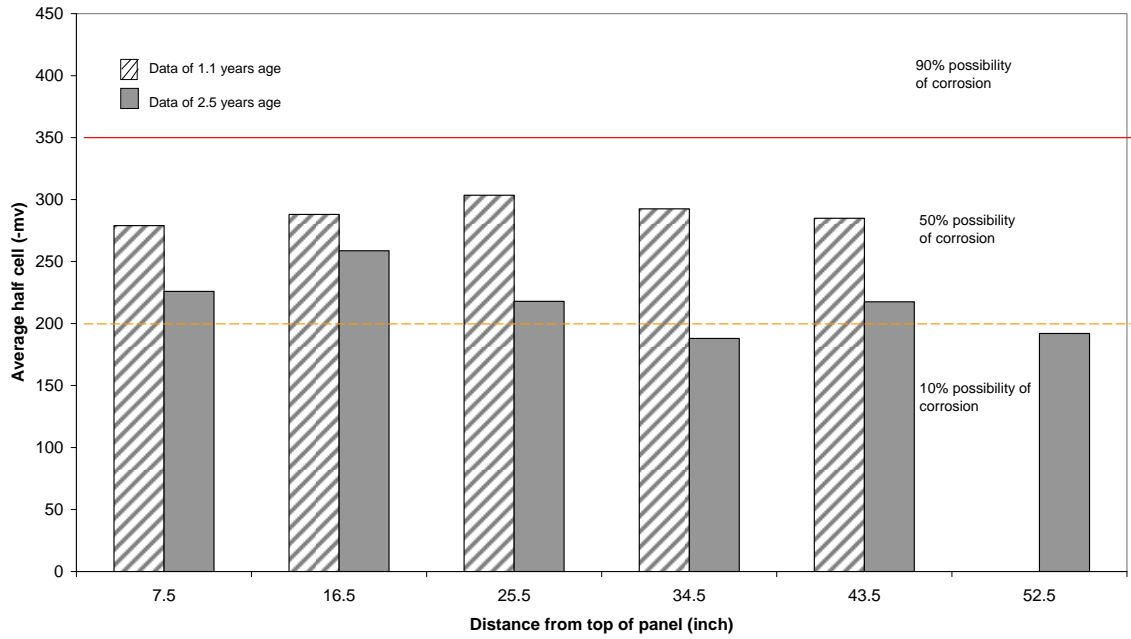


Figure 5-60 Comparison of the average half-cell at the different ages for Panel 22 (Kry22)

CHAPTER 6 CONCLUSIONS

Based on the results of this study, the following conclusions were drawn.

- The control panel using Kapaa aggregates with water/cement ratio of 0.35 had chloride concentration levels that were significantly lower than the control panel with 0.40 water/cement ratio.
- All panels using Type 1 corrosion inhibiting admixtures, which are intended to reduce the chloride permeability of the cover concrete, show lower chloride concentrations at the level of the reinforcing steel. These panels also have lower chloride migration rates than the corresponding control panels.
- Panels using Type 2 corrosion inhibiting admixtures, which are intended to raise the chloride threshold at the reinforcing steel, but not affect permeability of the concrete, show similar chloride concentrations and migration rates as the corresponding control panels.
- Half cell readings on the Kapaa control panel with 0.35 water/cement ratio show a low probability of corrosion. Half cell readings on the Kapaa control panel with 0.40 water/cement ratio are significantly higher indicating a 90% probability of corrosion after 3.4 years field exposure.
- All panels using Type 1 admixtures recorded half-cell readings predominantly in the 10% to 50% probability range. Some panels with Type 2 admixtures recorded half-cell readings in the 90% probability range indicating that corrosion has probably initiated in these panels.

REFERENCES

ACI Committee 318 (1999), *Building code Requirements for Reinforced Concrete*.

ASTM (1997), *1997 Annual book of ASTM Standards*, Easton, Maryland.

Berke, Neal S., Shen, Ding Feng., and Sundberg, Kathleen M. (1990), "Comparison of the Polarization Resistance Technique to the Macrocell Corrosion Technique," *Corrosion Rates of Steel in Concrete*, STP 1065, pp. 38-51.

Bola, M. M. B., and Newton, C. M. (2000). "Field Evaluation of Corrosion in Reinforced Concrete Structures in Marine Environment," Department of Civil Engineering Research Report, UHM/CE/00-01.

Civjan, Scott A., laFave, James M., Lovett, Daniel, Sund, Daneil J., Trybulski, Joanna (2003), *Performance Evaluation and Economic Analysis of Combinations of Durability Enhancing Admixtures (Mineral and Chemical) in Structural Concrete for the Northeast U.S.A.*, Research Report prepared for The New England Transportation Consortium, NETCR36 Project No. 97-2.

James Instruments Inc. www.ndtjames.com

Kakuda, D., Robertson, I. N. and Newton, C. M. (2005). "Evaluation of Non-Destructive Techniques for Corrosion Detection in Concrete Exposed to a Marine Environment," Department of Civil and Environmental Engineering Research Report, UHM/CEE/05-04.

Okunaga, G. J., Robertson, I. N., and Newton, C. M. (2005). "Laboratory Study of Concrete Produced with Admixtures Intended to Inhibit Corrosion," Department of Civil and Environmental Engineering Research Report, UHM/CE/05-05.

Pham, P.A., and Newton, C. M. (2000). “*Properties of Concrete Produced with Admixtures Intended to Inhibit Corrosion*,” Department of Civil Engineering Research Report, UHM/CE/01-01.

Sharp, J.V. Figg, J.W., and Leeming, M.B., (1988), “The Assessment of Corrosion of The Reinforcement in marine Concrete by Electrochemical and Other Methods,” *Proceedings, Second International conference on Concrete in Marine Environment*. SP-109-5, pp. 105-125.

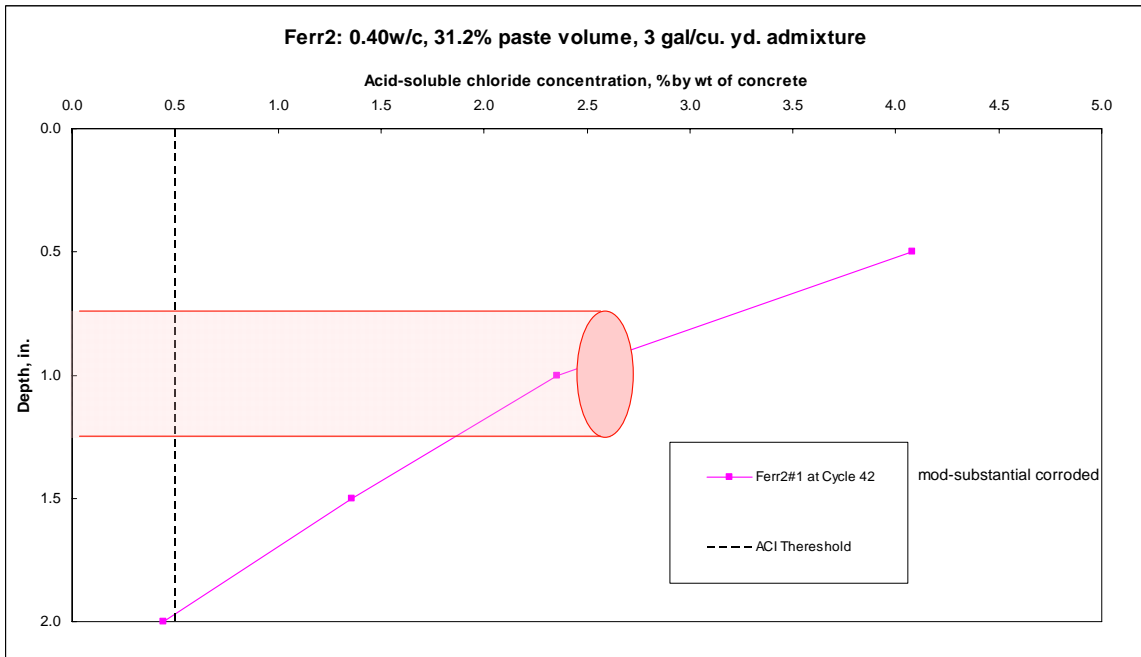
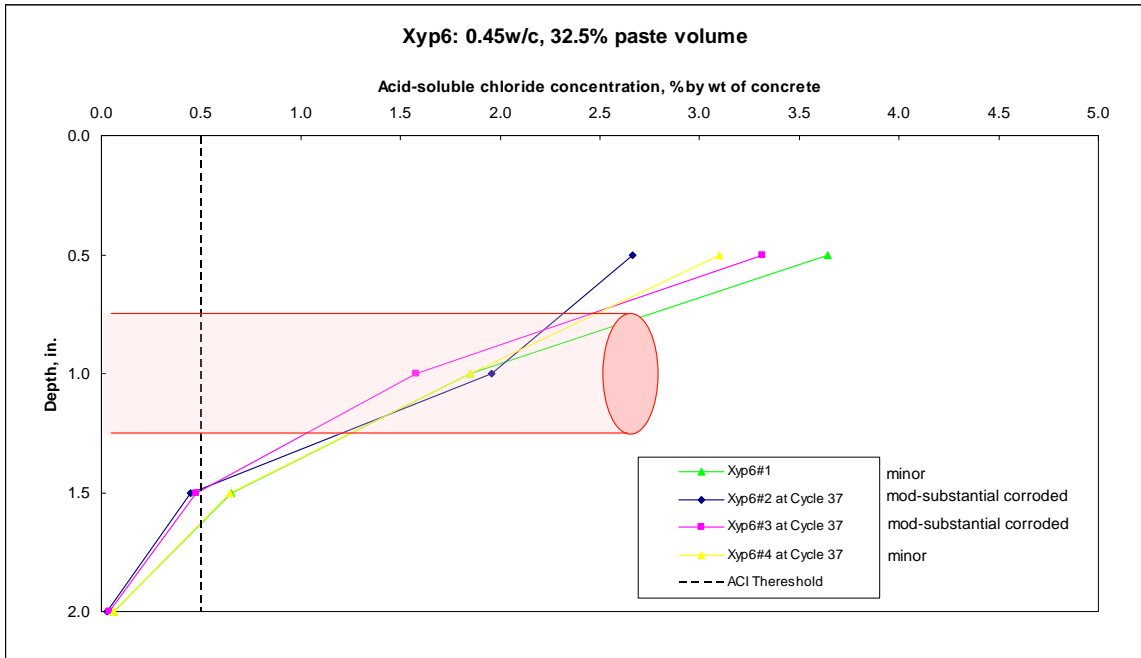
Srinivasan, S., Rengaswamy, N.S., and Pranesh, M.R., (1994), “Corrosion Monitoring of Marine Concrete Structures – An Appraisal.” *The Indian concrete Journal*, Vol. 68, No. 1, pp.13-19.

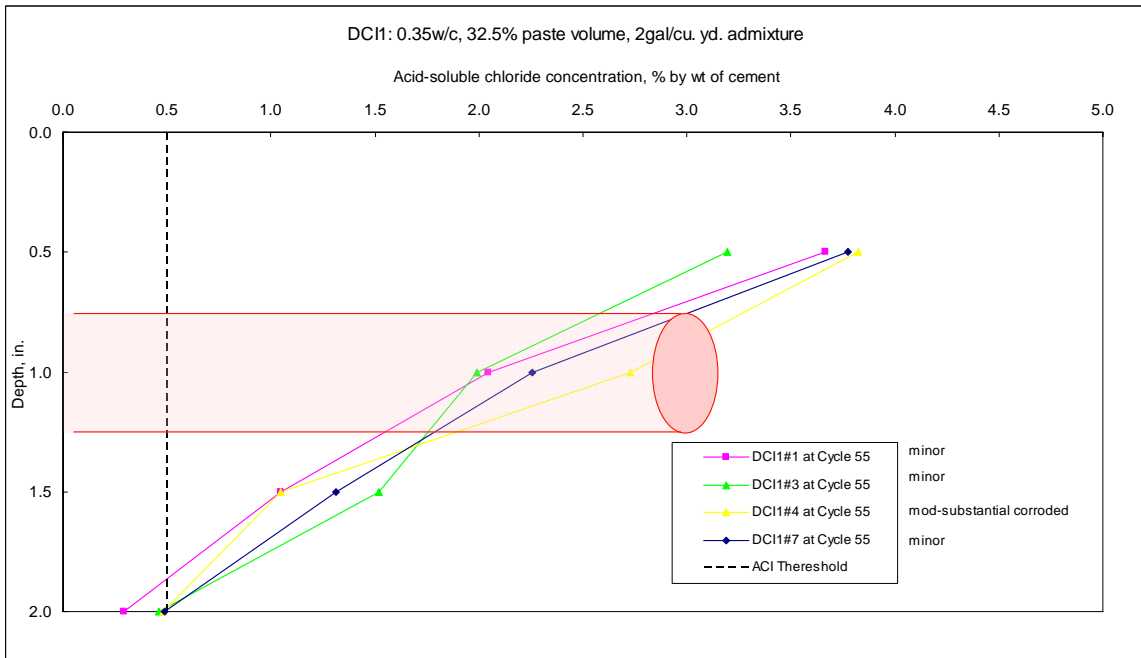
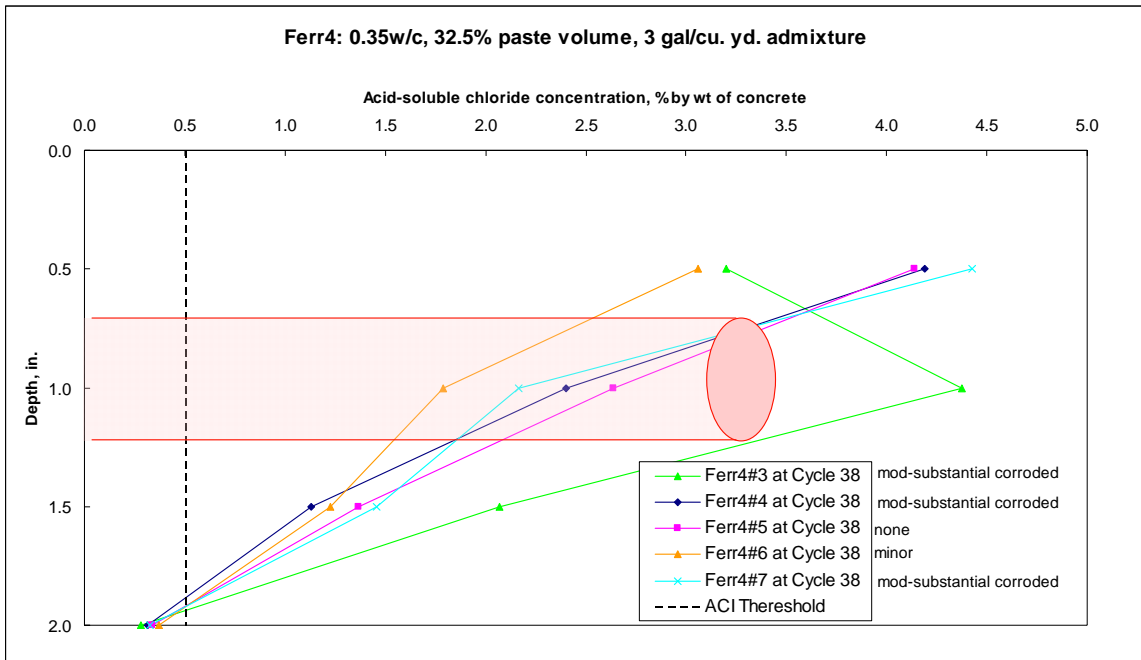
Uno, J., Robertson, I. N., and Newton, C. M. (2004). “*Corrosion Susceptibility of Concrete Exposed to a Marine Environment*,” Department of Civil and Environmental Engineering Research Report, UHM/CEE/04-09.

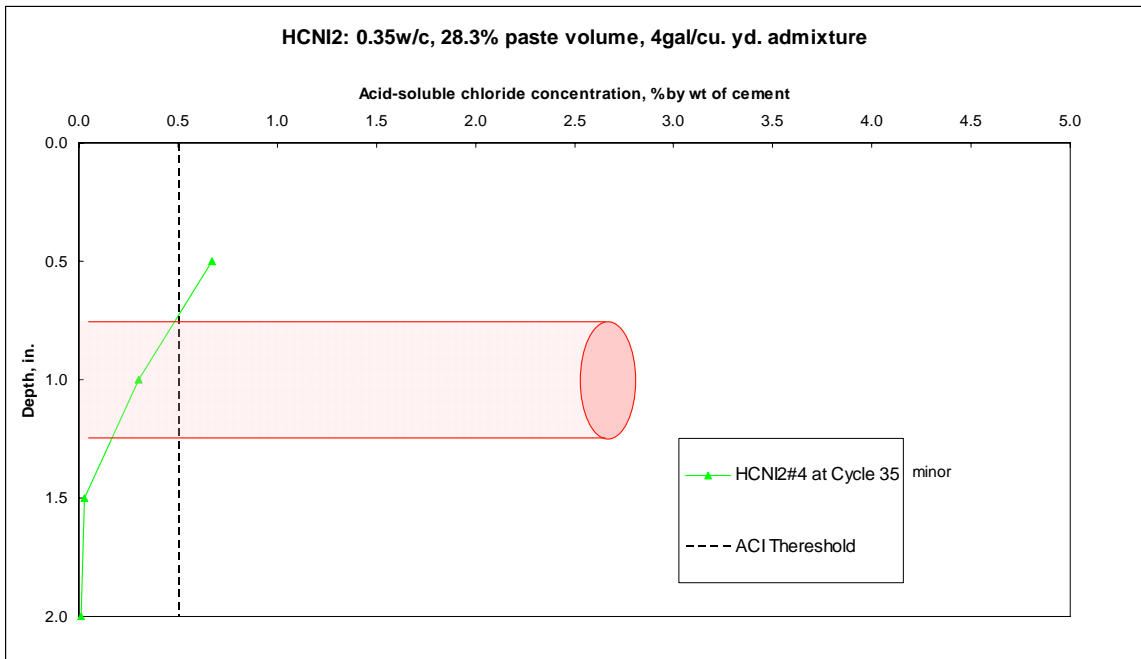
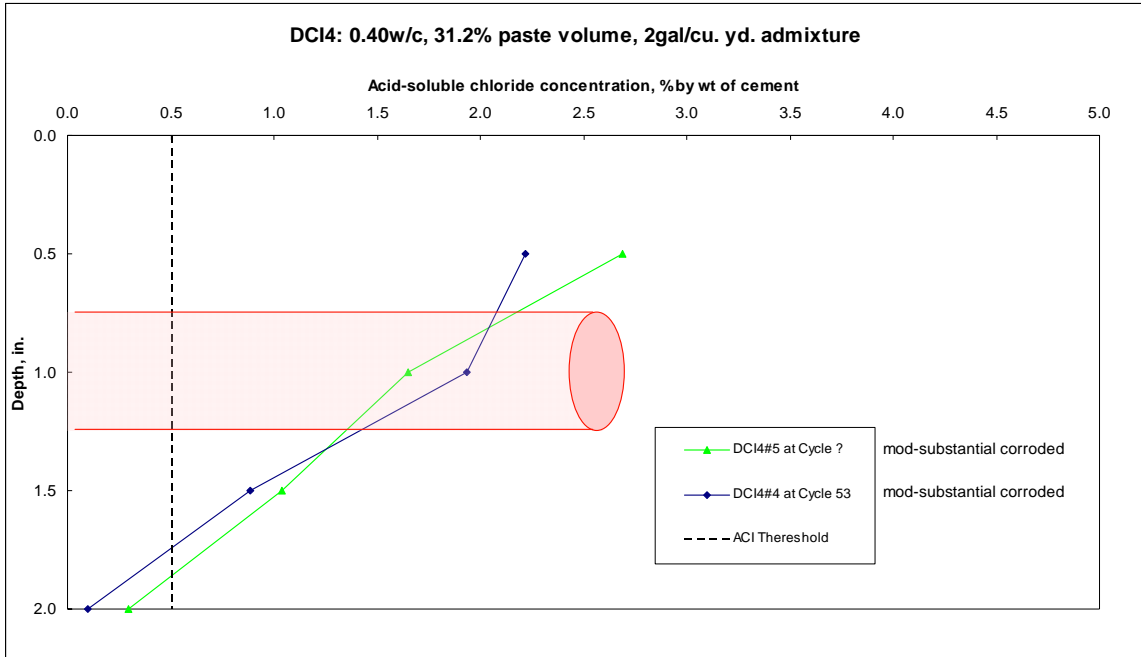
W.R. Grace & Co., www.graceconstruction.com

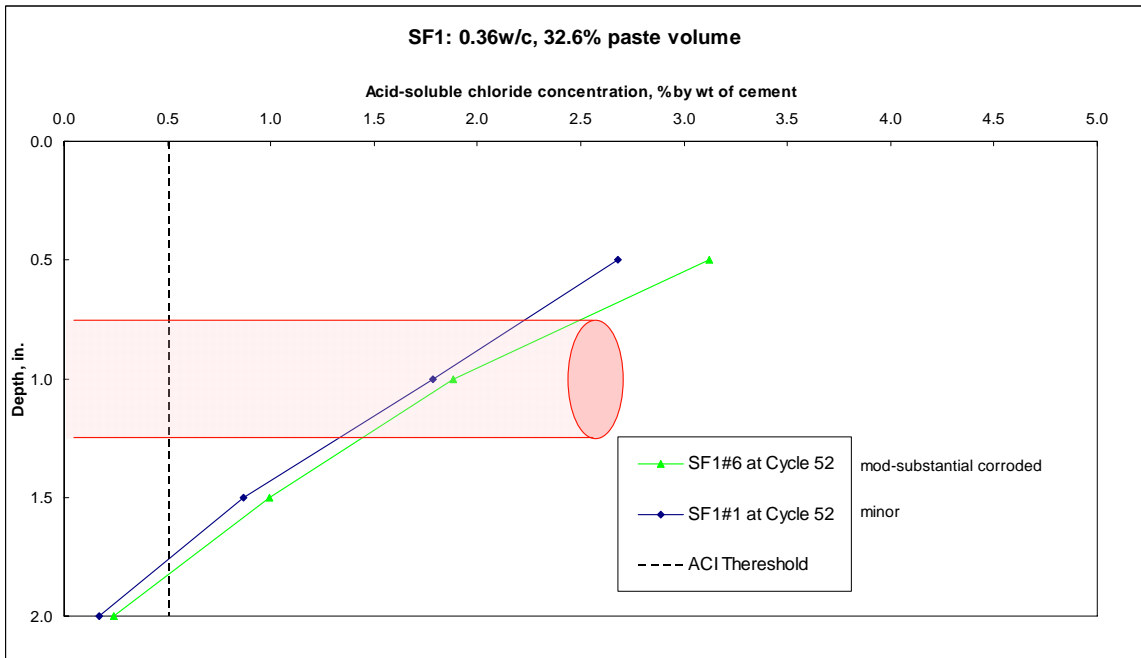
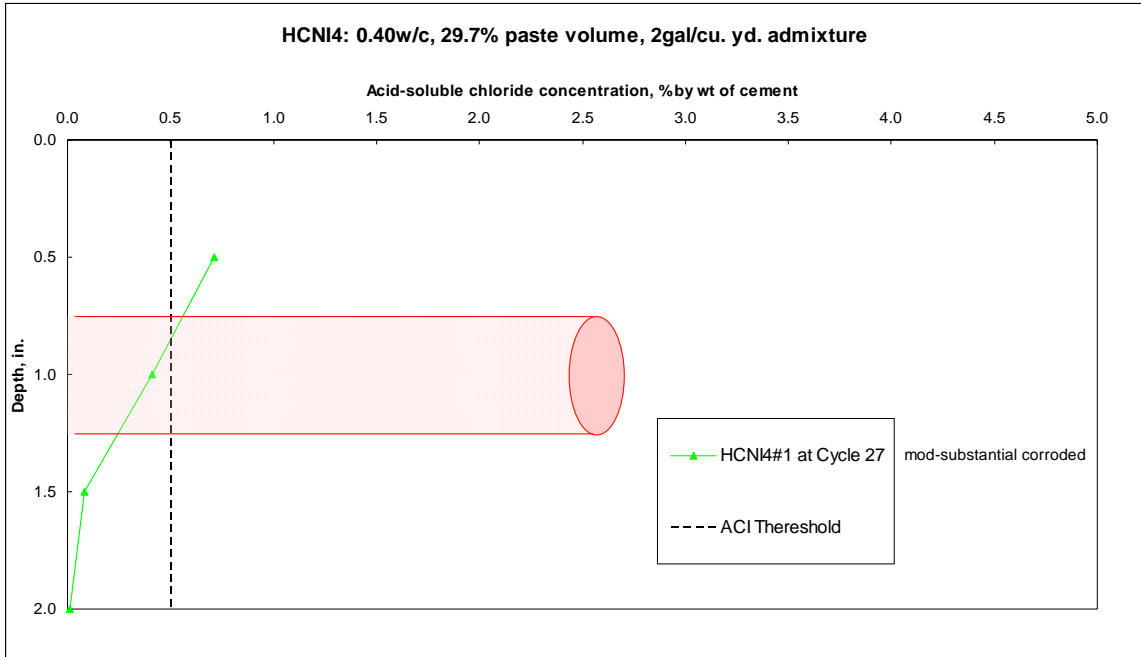
APPENDIX A

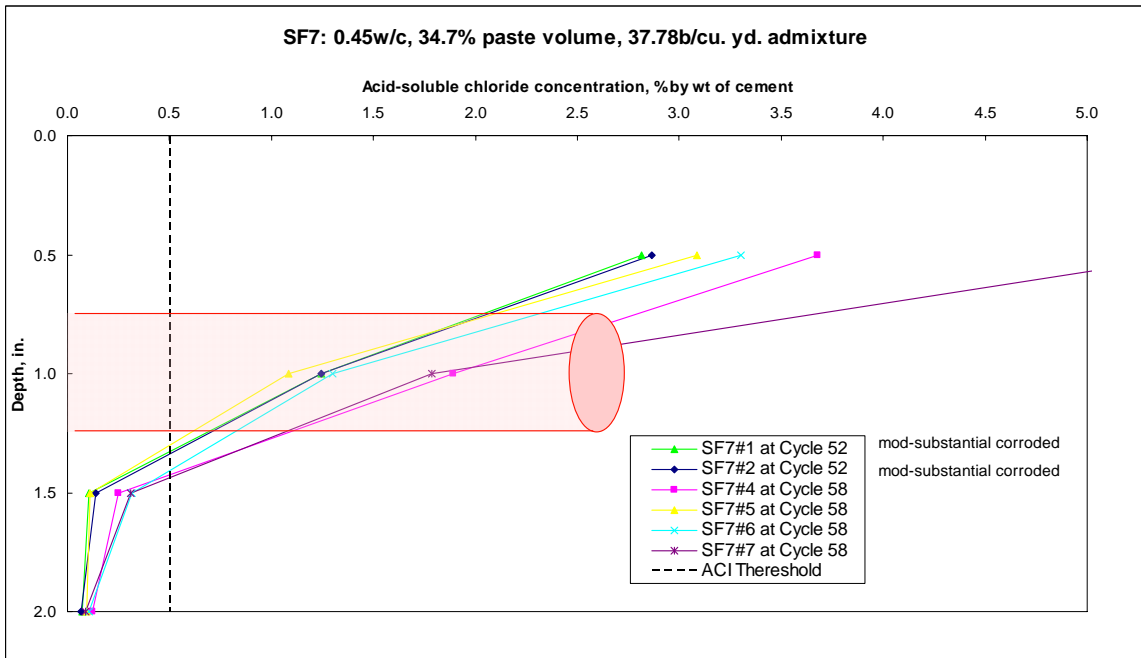
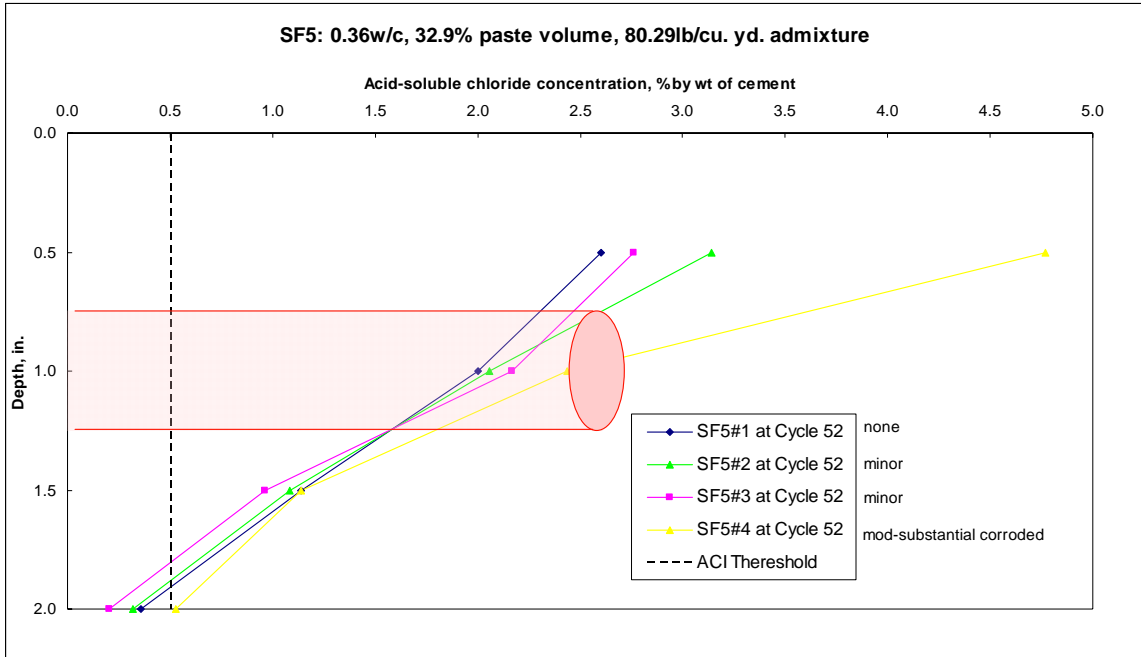
Lab Specimens' chloride concentration with the visible observation after splitting

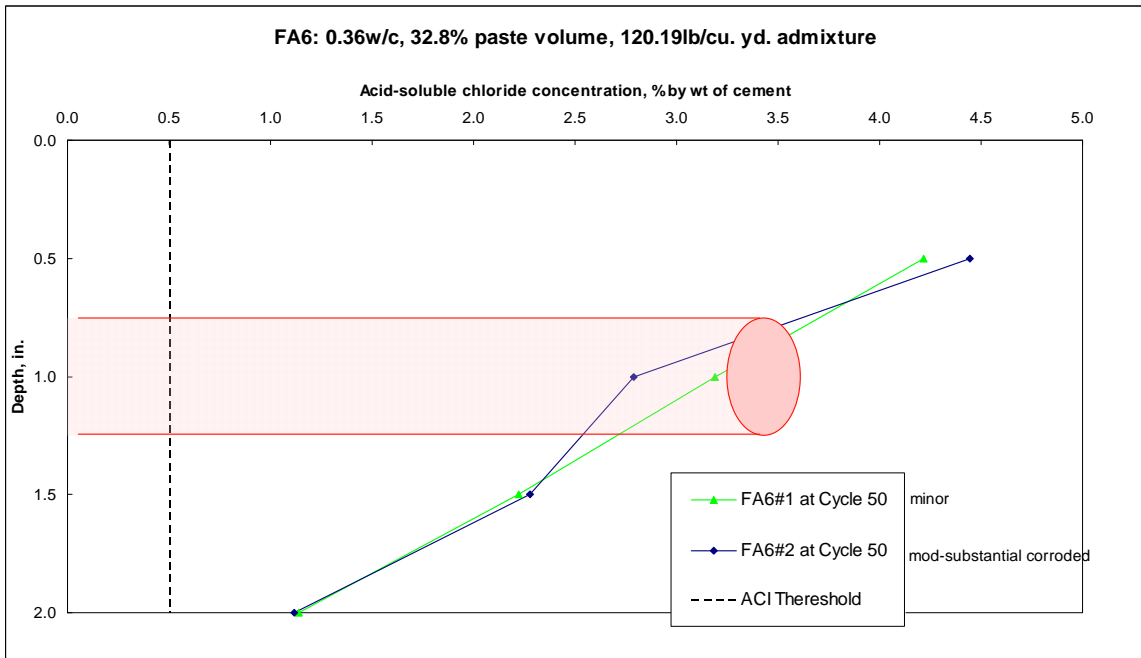
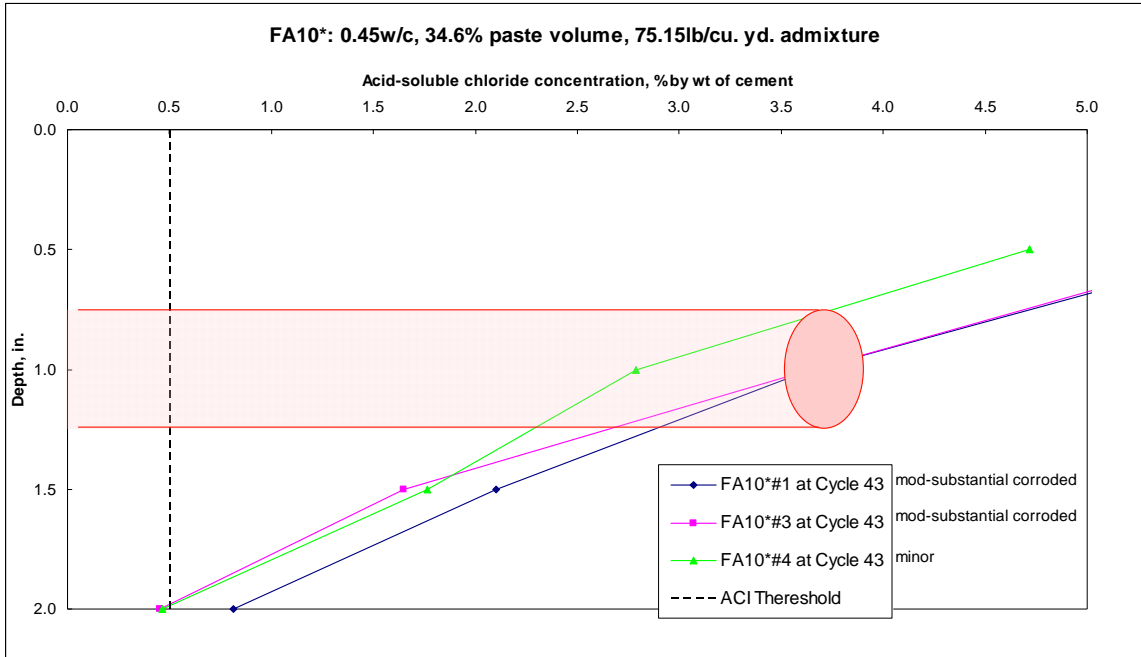


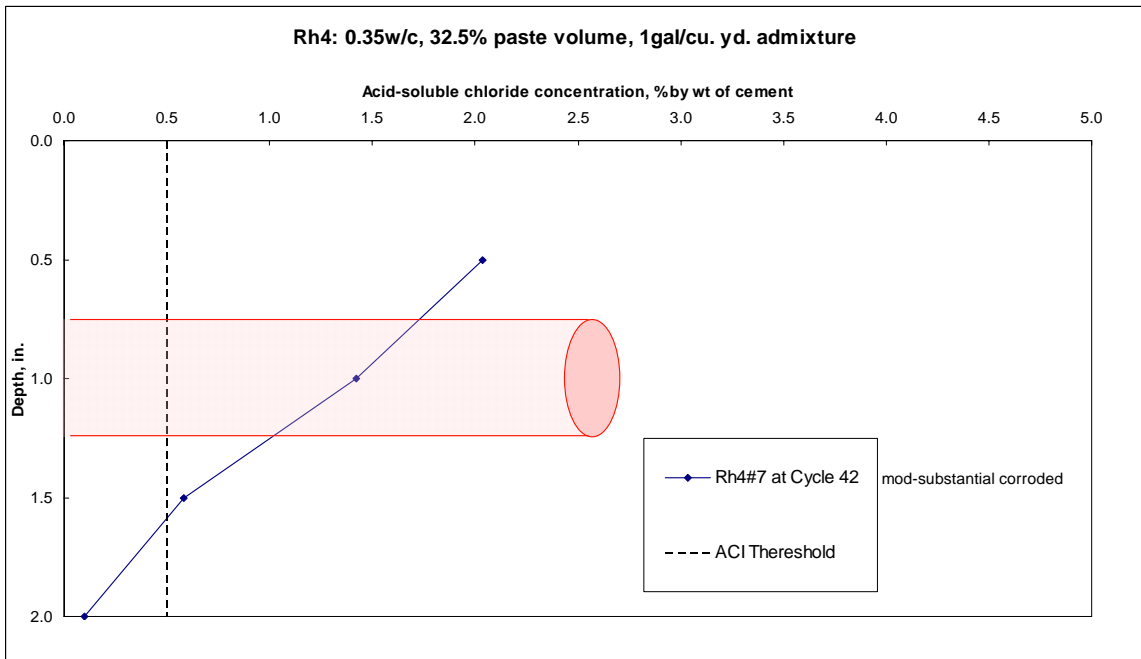
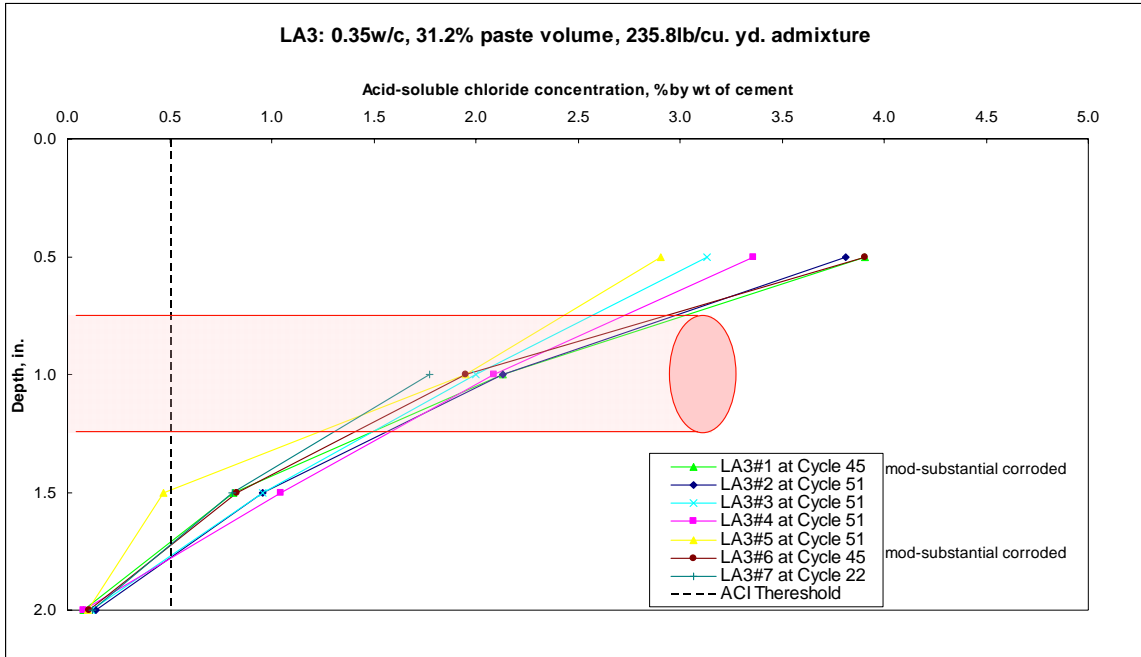






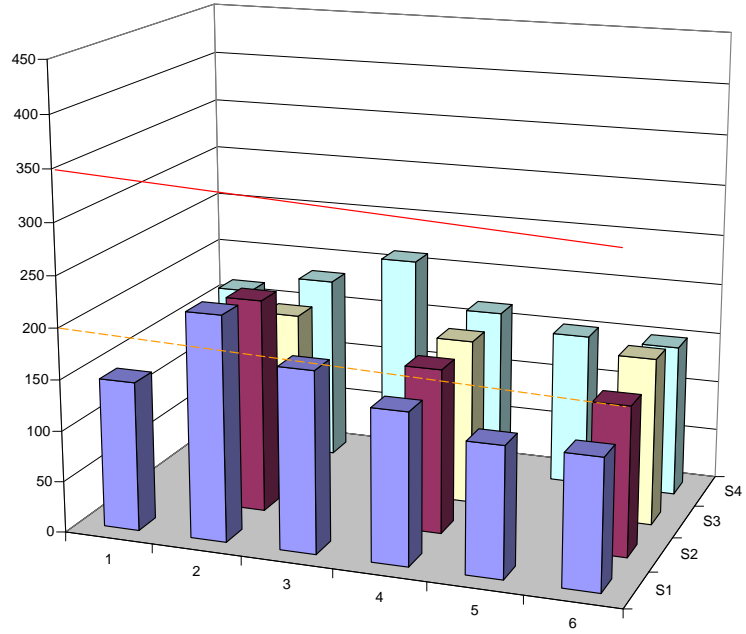




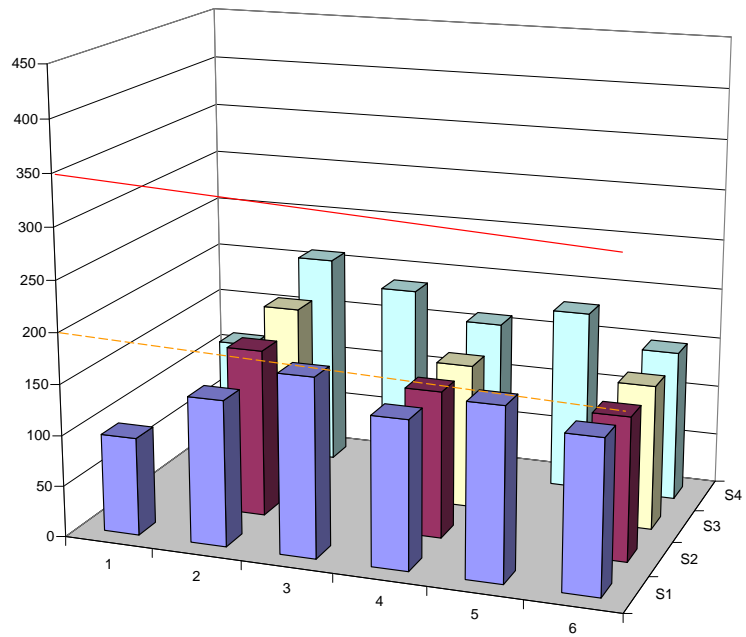


APPENDIX B

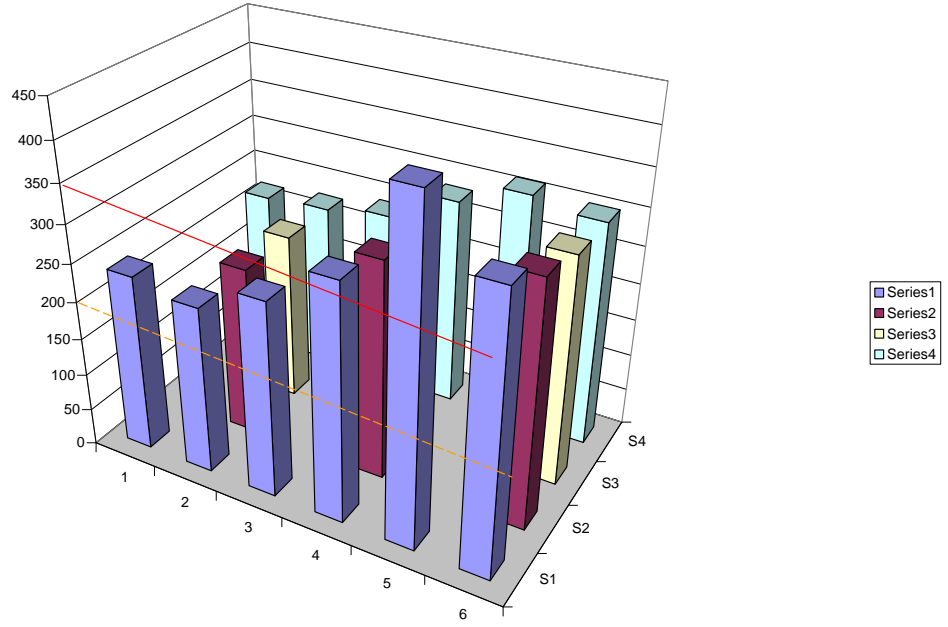
DCI 3: Half-Cell Potentials for each location at the age of 3.4 years



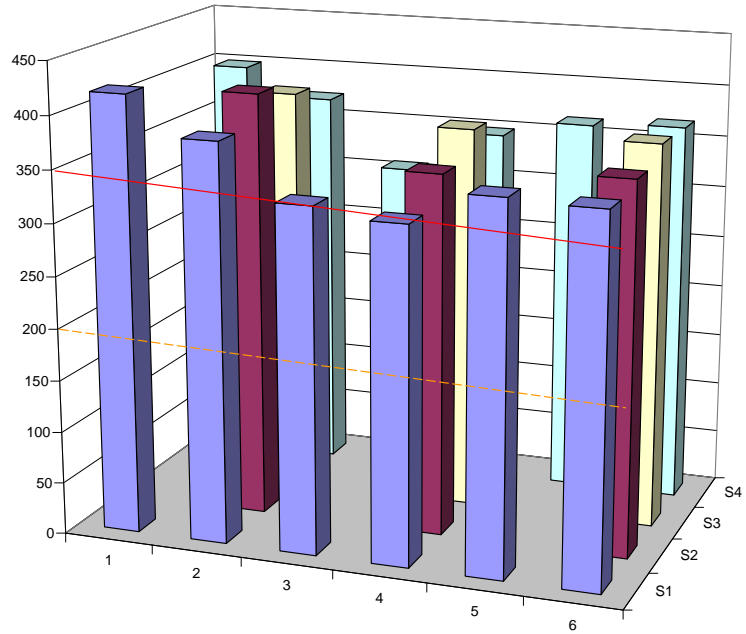
DCI 3A: Half-Cell Potentials for each location at the age of 2.5 years



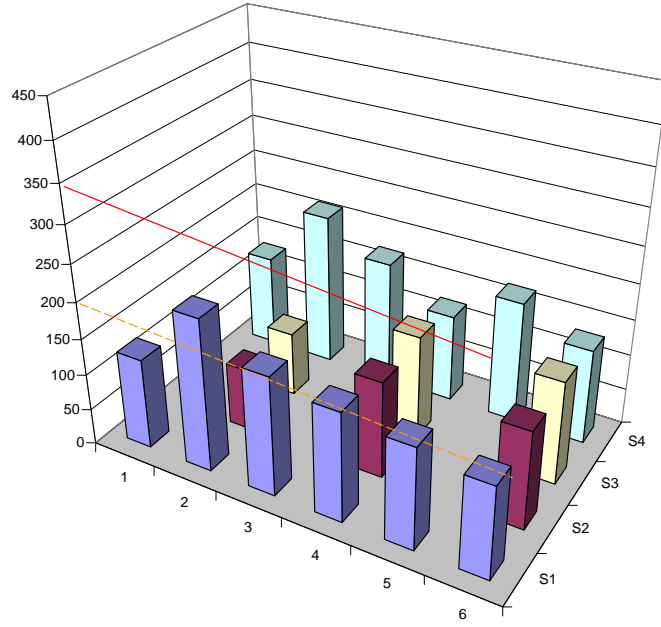
DCI 4: Half-Cell Potentials for each location at the age of 3.5 years



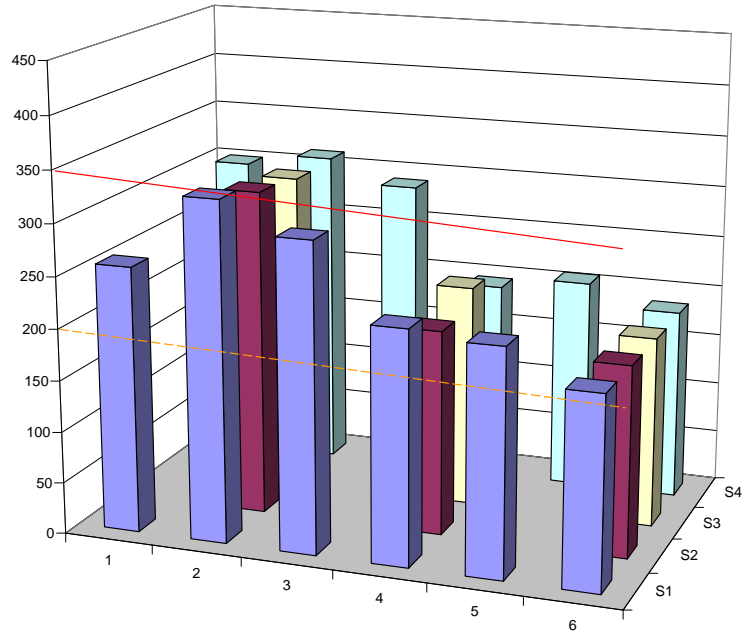
Rh CNI 5: Half-Cell Potentials for each location at the age of 3.3 years



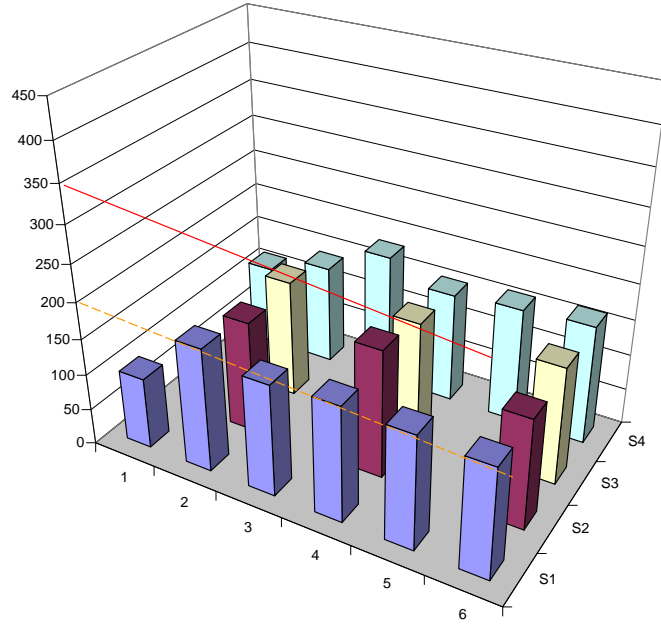
Rh CNI 5A: Half-Cell Potentials for each location at the age of 2.5 years



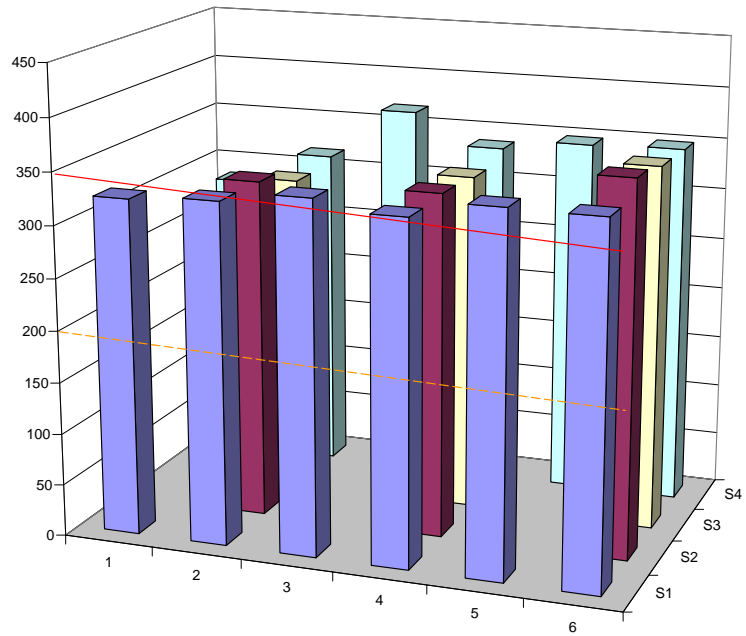
Rh CNI 6: Half-Cell Potentials for each location at the age of 3.1 years



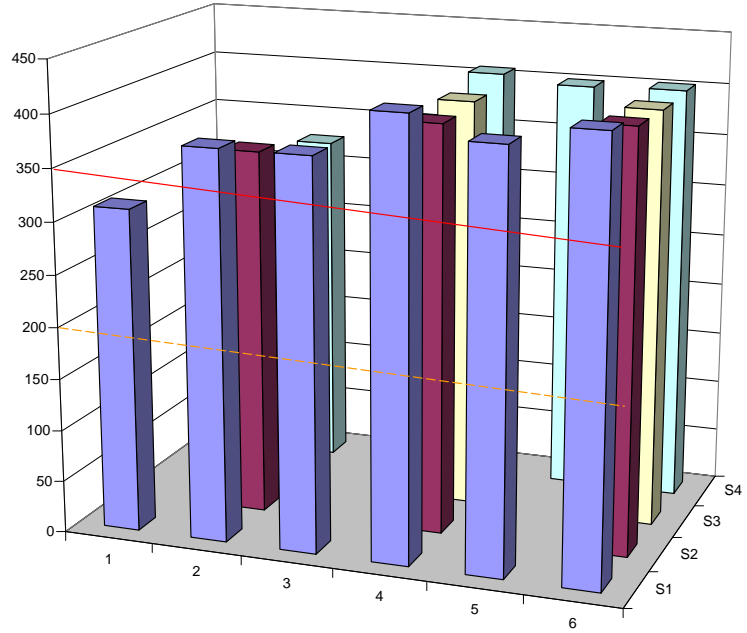
Rh 222+ 15: Half-Cell Potentials for each location at the age of 3.3 years



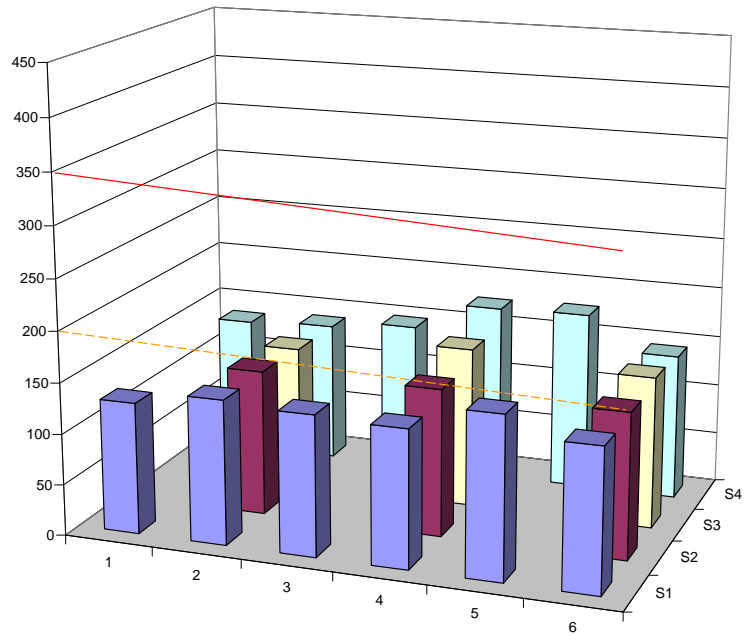
Rh 222+ 16: Half-Cell Potentials for each location at the age of 3.3 years



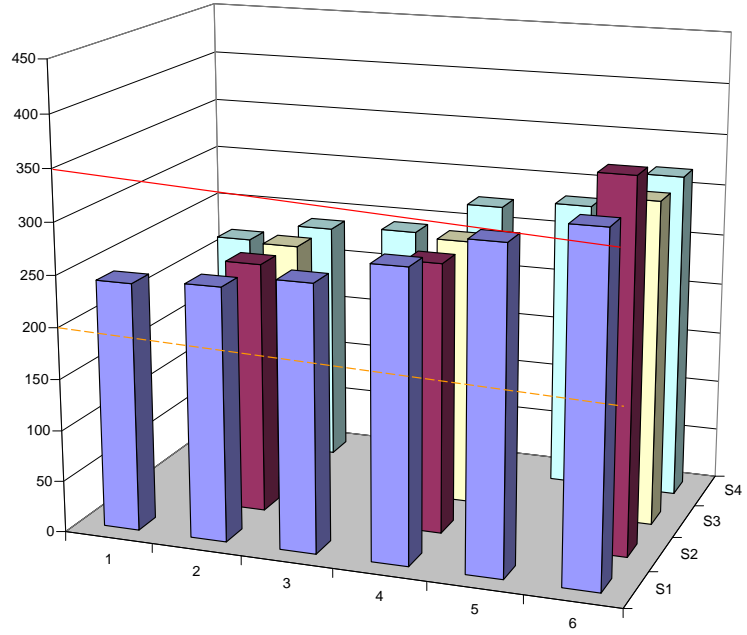
Rh 222+ 17: Half-Cell Potentials for each location at the age of 3.3 years



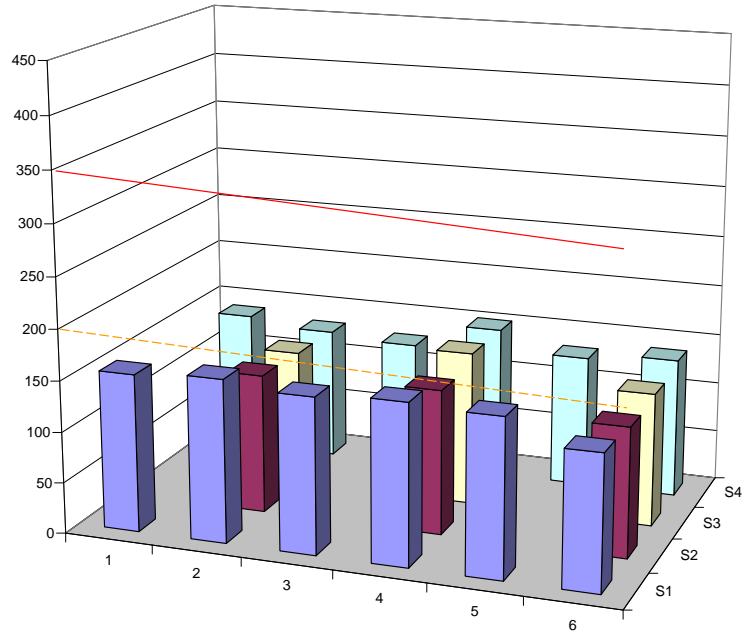
Rh 222+ 17A: Half-Cell Potentials for each location at the age of 2.5 years



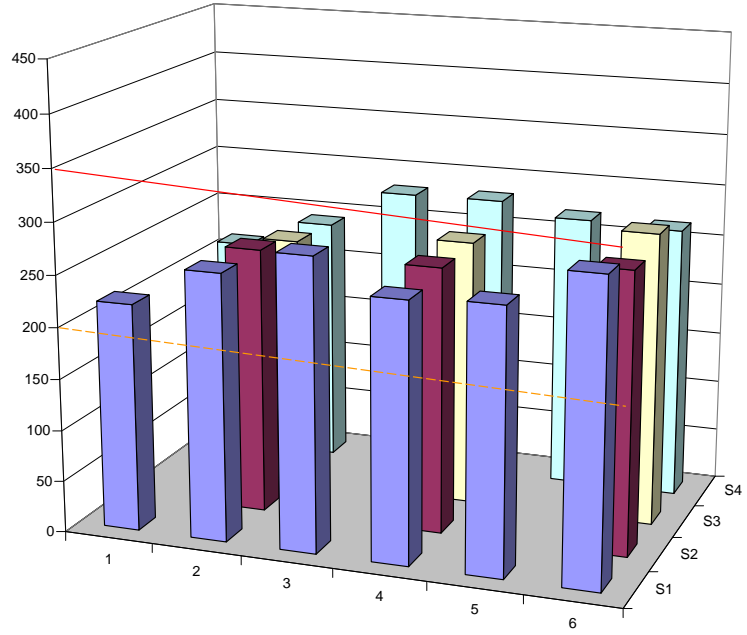
Ferr 18: Half-Cell Potentials for each location at the age of 3.5 years



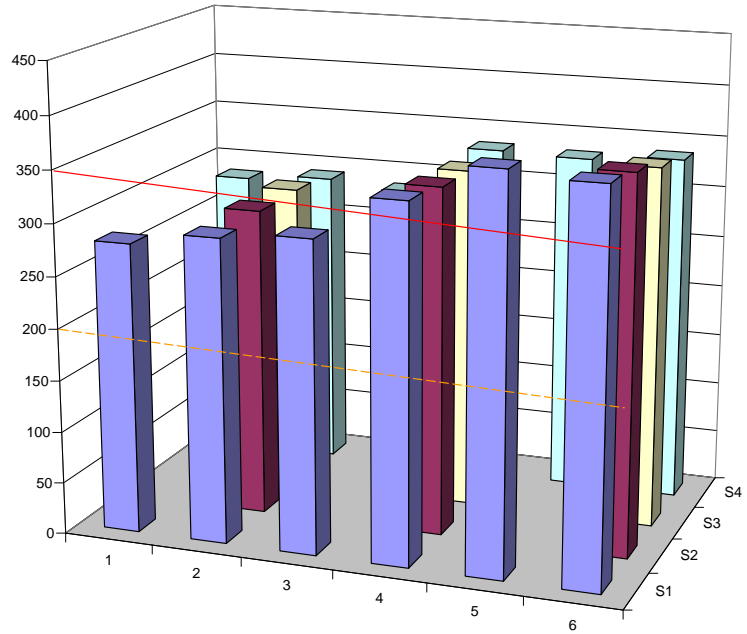
Ferr 19: Half-Cell Potentials for each location at the age of 3.4 years



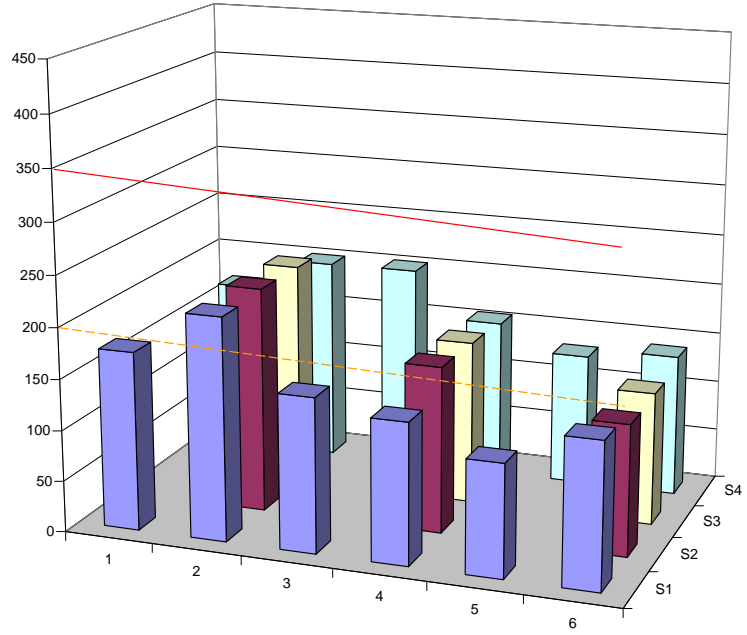
Ferr 20: Half-Cell Potentials for each location at the age of 3.4 years



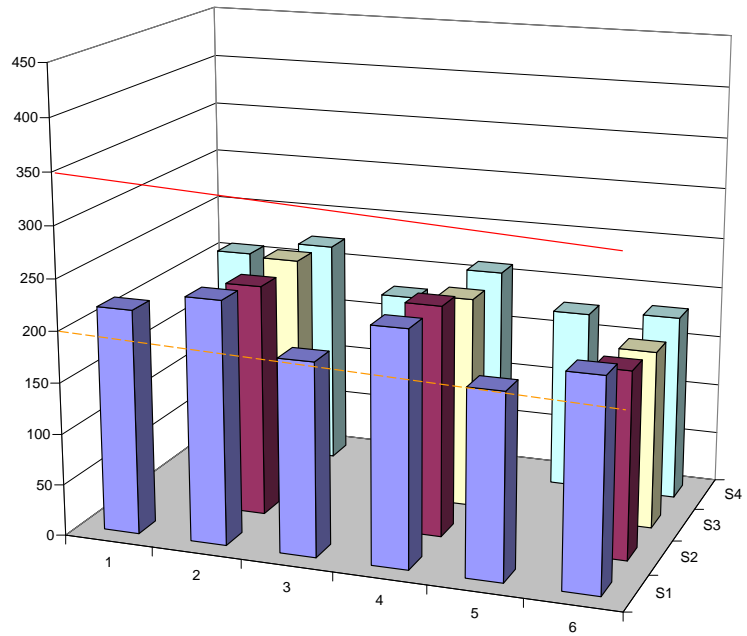
Xyp 21: Half-Cell Potentials for each location at the age of 3.1 years



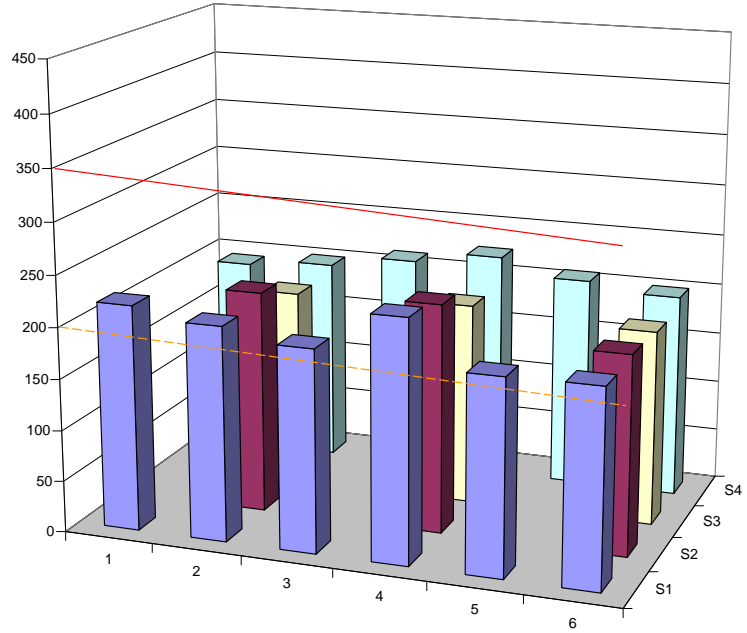
Latex 14: Half-Cell Potentials for each location at the age of 2.5 years



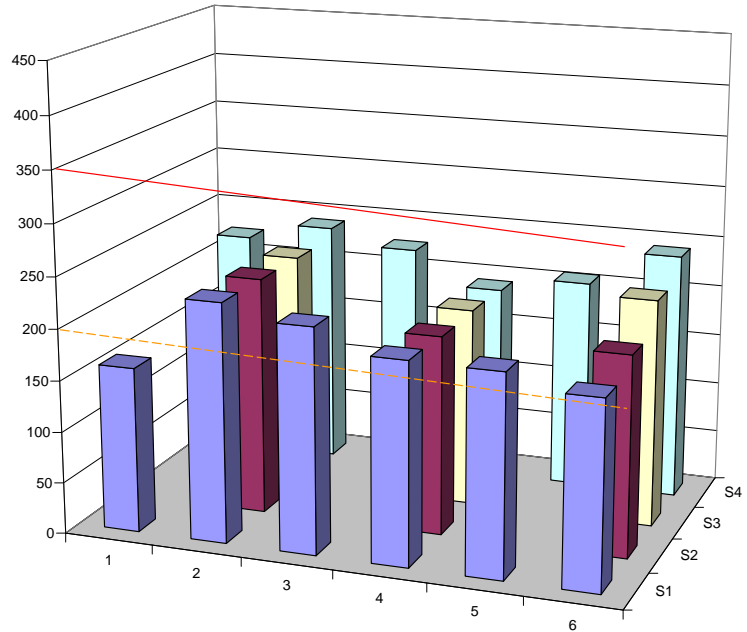
FA 11: Half-Cell Potentials for each location at the age of 3.1 years



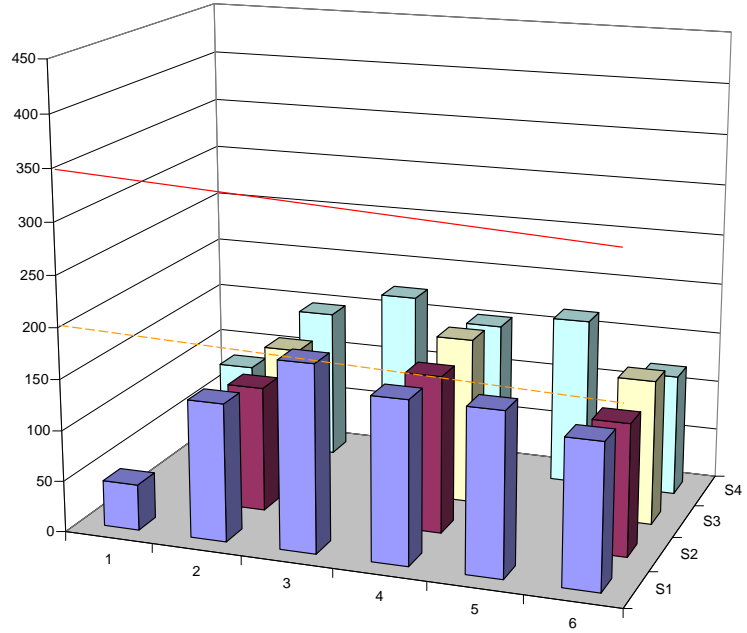
SF 8: Half-Cell Potentials for each location at the age of 2.9 years



SF 9: Half-Cell Potentials for each location at the age of 2.5 years



SF 10: Half-Cell Potentials for each location at the age of 2.9 years



Krypton 22: Half-Cell Potentials for each location at the age of 2.5 years

